

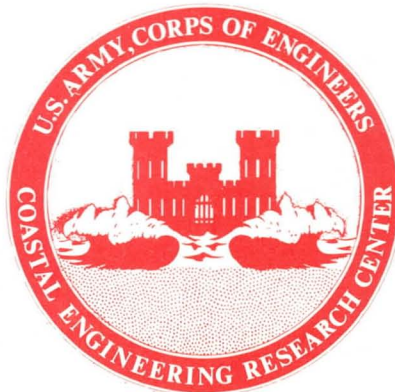
ward
Property of
Flood Control District of ADC Library
Please Return to
2801 W. Durango **T.M. 37**
Phoenix, AZ 85009

Riprap Stability on Earth Embankments Tested in Large— and Small-Scale Wave Tanks

by
Arvid L. Thomsen, Paul E. Wohlt
and
Alfred S. Harrison

TECHNICAL MEMORANDUM NO. 37
JUNE 1972

LIBRARY



U. S. ARMY, CORPS OF ENGINEERS
COASTAL ENGINEERING
RESEARCH CENTER
AND
MISSOURI RIVER DIVISION

Approved for public release; distribution unlimited.

101.110

Reprint or republication of any of this material shall give appropriate credit to the U. S. Army Coastal Engineering Research Center.

Limited free distribution within the United States of single copies of this publication is made by:

*Coastal Engineering Research Center
5201 Little Falls Road, N.W.
Washington, D. C. 20016*

Contents of this report are not to be used for advertising, publication, or promotional purposes. Citation of trade names does not constitute an official endorsement or approval of the use of such commercial products.

The findings in this report are not to be construed as an official Department of the Army position unless so designated by other authorized documents.

Riprap Stability on Earth Embankments Tested in Large— and Small-Scale Wave Tanks

by

**Arvid L. Thomsen, Paul E. Wohlt
and**

Alfred S. Harrison

TECHNICAL MEMORANDUM NO. 37

JUNE 1972



**U. S. ARMY, CORPS OF ENGINEERS
COASTAL ENGINEERING
RESEARCH CENTER
AND
MISSOURI RIVER DIVISION**

Approved for public release; distribution unlimited.

ABSTRACT

Tests of models in wave tanks were made to determine the effectiveness of several riprap designs in protecting embankment slopes from wave action.

Models ranging from about 1:20 scale to almost full scale were tested with waves up to about 6 feet high. A range of wave periods were tested, embankment slopes varied from 1 on 2 to 1 on 5, and armor layers were composed of quarried stone, glacial boulders and tribars.

Relationships that define the effect of wave height, wave period, embankment slopes and Reynolds number on size of stable armor units were experimentally determined and are given in graphs and tables.

Significant conclusions are:

1. The median weight of graded armor material is a satisfactory "effective size" with respect to stability.
2. Small-scale models are less stable than larger scale models. The difference in stability is a function of Reynolds number apparently caused by viscous effects. Consequently, there is a "scale effect" that produces conservative results when the stability determined in a small model is scaled up to prototype size on the basis of Froude number alone when equivalent viscous fluids exist in both prototype and model.
3. Stability is a function of wave period. For longer periods that produced wave steepness less than 0.03, stability is little affected by period. For wave steepness greater than 0.03, stability increases with shorter period.

Section VI of this report presents a detailed summary and conclusions.

FOREWORD

Although this work was pointed primarily at protection for earth dams and embankments in reservoirs, it applies also to stability of riprap seawalls and other coastal protection. Application is strongest to areas of limited fetch, such as large bays and estuaries (e.g., San Francisco and Chesapeake Bays and the Great Lakes); the general data, however, also apply to ocean coasts. Because of this greater applicability, and because of the great interest of coastal engineers in this subject, the report is being published by the Coastal Engineering Research Center for distribution to coastal engineers.

Work reported on was carried out for the Missouri River Division (MRD), U. S. Army Corps of Engineers, under authorization from the Office, Chief of Engineers (OCE), Department of the Army in the 1st Indorsement dated 16 June 1965 to a letter from the Missouri River Division dated 23 April 1965 entitled "Wave Model Investigation of Riprap Rehabilitation". The Coastal Engineering Research Center agreed to

perform the model tests in Comment 2 dated 18 May 1965 to the 23 April 1965 letter. Additional funding was provided by the Coastal Engineering Research Center to extend the testing range in some instances to a longer period to increase the applicability to ocean coastal works.

In addition, data from 10 large-scale tests (SPL Series) included in this report are part of data currently being collected by Mr. John Ahrens, Oceanographer, CERC, in a further CERC-sponsored study of rip-rap stability having a more generalized purpose.

This report was prepared by Arvid L. Thomsen, Hydraulic Engineer, Planning and Reports Branch, Engineering Division, Omaha District; Paul E. Wohlt, Geology, Soils and Materials Branch, Engineering Division, Missouri River Division; and Alfred S. Harrison, Chief, Hydraulics and Hydrology Section, Technical Engineering Branch, Engineering Division, Missouri River Division.

Comments on the preliminary draft from the Office, Chief of Engineers, the Waterways Experiment Station, and the Coastal Engineering Research Center were of great help in the preparation of this report.

Director of the Coastal Engineering Research Center during the model testing was Colonel F. O. Diercks; Technical Director was Joseph M. Caldwell; Chief of the Research Division was Thorndike Saville, Jr.

At the time of publication, Brigadier General Edwin T. O'Donnell was the Missouri River Division Engineer; L. A. Duscha was Chief of the Engineering Division, Missouri River Division. Lieutenant Colonel Don S. McCoy was Director of CERC; Thorndike Saville, Jr. was Technical Director.

Views and conclusions in this report are those of the authors, and do not necessarily represent those of the Office, Chief of Engineers, nor do they promulgate official policy or guidance by CERC, MRD, or OCE.

NOTE: Comments on this publication are invited. Discussion will be published in the next CERC Bulletin.

This report is published under authority of Public Law 166, 79th Congress, approved July 31, 1945, as supplemented by Public Law 172, 88th Congress, approved November 7, 1963.

CONTENTS

	<u>Page</u>
Section I. INTRODUCTION	1
Section II. ANALYTICAL CONSIDERATIONS	4
Section III. LABORATORY APPARATUS	10
1. Wave Tanks and Generators	10
2. Tank Calibration	10
3. Survey Equipment	12
a. Large Tank	12
b. Medium Tank	12
c. Small Tank	12
Section IV. DESCRIPTION OF TESTS	14
1. Model Construction	14
a. Core	14
b. Bedding and Spalls	14
c. Armor	15
2. Test Materials	18
a. Core	18
b. Bedding and Spalls	18
c. Armor	18
3. Testing the Models	22
a. Description of Test Waves	22
b. Wave Damage on Models	27
c. Determination of Zero-Damage and Limited-Damage Wave Heights	30
d. Photography	30
e. Other Measurements	32
Section V. TEST RESULTS	32
1. General	32
2. Effect of Underlayers on Zero-Damage Stability	33
3. Effect of Water Depth on Zero-Damage Stability	34
4. Effect of Armor Gradation Uniformity on Zero-Damage Stability	35
5. Effect of Model Size on Zero-Damage Stability	40
6. Effect of Wave Period on Zero-Damage Stability	42
7. Effect of Armor Shape and Placement on Zero-Damage Stability	49

CONTENTS (Continued)

	<u>Page</u>
8. Effect of Embankment Slope on Zero-Damage Stability	49
9. Effect of Armor Thickness on Zero-Damage Stability	51
10. Stability Equation	52
11. Data Scatter	52
12. Reserve Stability	52
13. Comparison of Results with Those of Other Investigators . .	56
Section VI. SUMMARY AND CONCLUSIONS	67
Section VII. RECOMMENDATIONS FOR ADDITIONAL TESTS OF RIPRAP STABILITY	70
LITERATURE CITED	71
BIBLIOGRAPHY	72
Appendix A. MODEL DESCRIPTIONS	73
Appendix B. GRADATION CURVES	81
Appendix C. DAMAGE CURVES	89
Appendix D. TABLE OF MODEL TEST CONDITIONS AND RESULTS.	105
Appendix E. TABLE OF MODEL TEST CONDITIONS AND RESULTS IN DIMENSIONLESS FORM.	111

ILLUSTRATIONS

Table

1. Variables and Corresponding Dimensionless Parameters	6
2. Dimensionless Parameters Used in Data Analysis	8
3. Variables Represented by Dimensionless Parameters	32
4. Effect of Underlayer Thickness	34
5. Stability as Limited by Wave Period	46
6. Zero-Damage Stability Numbers	53
7. Reserve Stability of Tribars and Stone	56
8. Model Descriptions	74
9. Model Test Conditions and Results	106
10. Model Test Conditions and Results in Dimensionless Form . . .	112

ILLUSTRATIONS (Continued)

<u>Figure</u>	<u>Page</u>
Frontispiece	xii
1. Photographs of Wave Tanks	11
2. Photographs of Survey Equipment	13
3. Photographs of Dumped Stone Armor Layer Construction	16
4. Skip Loads of 81.3 and 0.43-pound Tribars	17
5. Placed Tribar Construction in the Large Tank	17
6. Photographs of Rounded Boulders Used in Model Tests	19
7. Photographs of Kimmswick Limestone Used in Model Tests	20
8. Photographs of Sioux Quartzite Used in Model Tests	21
9. Shape and Dimensions of Tribars Tested	23
10. Wave Height Frequency Distributions	24
11. Sample Wave Gage Records	26
12. Damage Profile	28
13. Typical Damage Development	31
14. Determination of Best Representative Size of Graded Armor on a 1 on 3 Embankment Slope with Large-Scale Models	36
15. Determination of Best Representative Size of Graded Armor on a 1 on 3 Embankment Slope with Small-Scale Models	37
16. Determination of Best Representative Size of Graded Armor on a 1 on 5 Embankment Slope with Large-Scale Models	38
17. Determination of Best Representative Size of Graded Armor on a 1 on 5 Embankment Slope with Small-Scale Models	39
18. Effect of Reynolds Number on Zero-Damage Stability	41
19. Stability Correction for Scale Effect as a Function of Reynolds Number	43
20. Effect of Wave Period on Zero-Damage Stability of Dumped Stone	44

ILLUSTRATIONS (Continued)

<u>Figure</u>	<u>Page</u>
21. Effect of Wave Period on Zero-Damage Stability of Tribars and Placed Stone	45
22. Effect of Wave Period on Zero-Damage Stability of Dumped Stone with Respect to Deepwater Wave Steepness	47
23. Effect of Wave Period on Zero-Damage Stability of Dumped Stone on Flat Embankment Slopes	48
24. Effect of Embankment Slope on Zero-Damage Stability of Dumped Stone	50
25. Zero-Damage Stability Curves for Stone and Tribars	54
26. A Comparison of the Hindcast Zero-Damage Wave Height and the Actual Zero-Damage Wave Height for each Model Test	55
27. Determination of Reserve Stability of Stone on an Embankment Slope of 1 on 2	57
28. Determination of Reserve Stability of Dumped Stone on Embankment Slopes of 1 on 3 and 1 on 5	58
29. Determination of Reserve Stability of Tribars on an Embankment Slope of 1 on 2	59
30. Photographs Showing Equilibrium Stages of Damage of Test L-1.2	60
31. Photographs Showing Equilibrium Stages of Damage of Test L-7.1	61
32. Photographs Showing Equilibrium Stages of Damage of Test L-13.1	62
33. Photographs Showing Equilibrium Stages of Damage of Test L-17.1	63
34. Photographs Showing Equilibrium Stages of Damage of Test L-2.2	64
35. Photographs Showing Equilibrium Stages of Damage of Test L-5.1	65
36. A Comparison of Zero-Damage Model Test Results of Dumped Stone Armor of Various Investigations	66
37. Model Layer Configuration and Nomenclature	73

ILLUSTRATIONS (Continued)

<u>Figure</u>	<u>Page</u>
38. Gradation Curves	82
39. Gradation Curves	83
40. Gradation Curves	84
41. Gradation Curves	85
42. Gradation Curves	86
43. Gradation Curves	87
44. Gradation Curves	88
45. Damage Curves of Dumped Kimmswick Limestone Tests, $\cot \alpha = 2$.	90
46. Damage Curves of Dumped Kimmswick Limestone Tests, $\cot \alpha = 2$.	91
47. Damage Curves of Dumped Sioux Quartzite Tests, $\cot \alpha = 2$. . .	92
48. Damage Curves of Dumped Boulder Tests, $\cot \alpha = 2$	93
49. Damage Curves of Placed Sioux Quartzite Tests, $\cot \alpha = 2$. . .	94
50. Damage Curves of Dumped Occoquan Granite Tests, $\cot \alpha = 2\frac{1}{2}$. .	95
51. Damage Curves of Dumped Kimmswick Limestone Tests, $\cot \alpha = 3$.	96
52. Damage Curves of Dumped Kimmswick Limestone Tests, $\cot \alpha = 3$.	97
53. Damage Curves of Dumped Kimmswick Limestone Tests, $\cot \alpha = 5$.	98
54. Damage Curves of Dumped Kimmswick Limestone Tests, $\cot \alpha = 5$.	99
55. Damage Curves of Dumped Kimmswick Limestone Tests, $\cot \alpha = 7$ and 10	100
56. Damage Curves of Placed Tribar Tests, $\cot \alpha = 2$	101
57. Damage Curves of Placed Tribar Tests, $\cot \alpha = 2$	102
58. Damage Curves of Dumped Tribar Tests, $\cot \alpha = 2$	103

CONVERSION FACTORS, BRITISH TO METRIC UNITS OF MEASUREMENT

British units of measurement used in this report can be converted to metric units as follows:

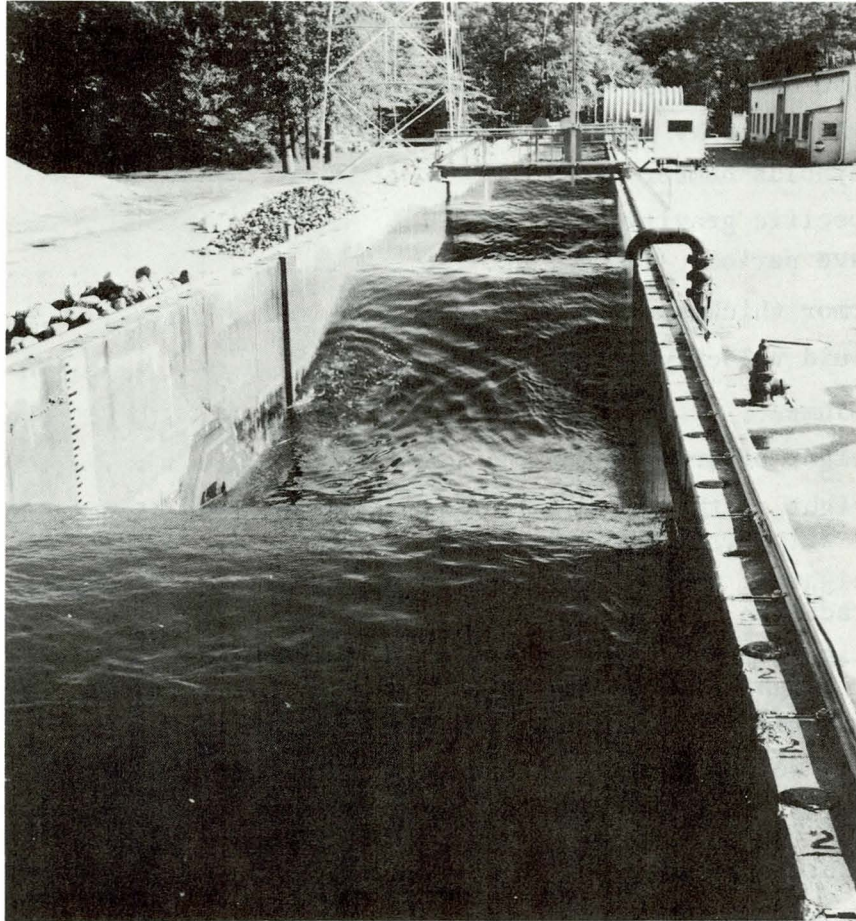
<u>Multiply</u>	<u>by</u>	<u>to Obtain</u>
inch	2.54	centimeter
foot	30.48	centimeter
square foot	929.0	square centimeter
cubic foot	2.832×10^4	cubic centimeter
foot per second	30.48	centimeter per second
foot per second ²	30.48	centimeter per second ²
pounds	453.6	grams (Force)
foot-pounds per foot	44.49×10^4	ergs per centimeter
foot pounds per foot-second	44.49×10^4	ergs per centimeter-second
pounds-second per square foot	0.4883	grams (Force) - second per square centimeter
pounds per cubic foot	0.01602	grams (Force)per cubic centimeter

LIST OF SYMBOLS AND UNITS OF MEASUREMENT IN BRITISH SYSTEM

A	Cross-section area of damage	sq ft
A'	Cross-section area of accretion	sq ft
b	Wave tank width	ft
B	Dimensionless damage	
B _A	Dimensionless damage computed from cross-section area of damage	
B _J	Dimensionless damage computed from number of armor units eroded	
c	Armor coverage	lbs/sq ft
d	Water depth	ft
D	Representative linear dimension of armor unit	ft
D ₅₀	Representative linear dimension of median weight armor unit	ft
E	Specific wave energy	ft-lbs/ft
F _R	Stability correction for scale effect (viscous effects)	
g	Gravitational acceleration	ft/sec ²
h	Actual zero-damage wave height from test observations	ft
H _O	Deepwater wave height	ft
H _M	Modal wave height	ft
H _S	Significant wave height	ft
H _{LD}	Limited-damage, deepwater wave height	ft
H _{ZD}	Zero-damage, deepwater wave height	ft
J	Number of armor units eroded	
K	Constant	
L _O	Deepwater wave length	ft

LIST OF SYMBOLS AND UNITS OF MEASUREMENT IN BRITISH SYSTEM (Continued)

n	Porosity of Armor layer	
N	Froude number or stability number	
N_{ZD}	Zero-damage stability number	
N'_{ZD}	Zero-damage stability number for large scale with no viscous effects	
N''_{ZD}	Zero-damage stability number for large scale, no viscous effects, and for most destructive wave periods	
P	Specific wave power	ft-lb/ft-sec
R_N	Reynolds number	
S	Specific gravity	
T	Wave period	sec
T_h	Armor thickness	in
v	Fluid velocity.	ft/sec
V	Volume.	cu ft
W	Weight of armor unit.	lbs
W_{15}	Weight of the armor unit that is larger than 15 percent, by weight, of the gradation	lbs
W_{50}	Weight of median size armor unit, by weight, in the gradation	lbs
W_{85}	Weight of the armor unit that is larger than 85 percent, by weight, of the gradation	lbs
α	Embankment slope angle from the horizontal	
γ	Unit weight of armor material	lbs/cu ft
γ_f	Unit weight of fluid.	lbs/cu ft
μ	Absolute viscosity.	lb-sec/sq ft
ρ_f	Density of fluid.	slug/cu ft



RIPRAP STABILITY ON EARTH EMBANKMENTS TESTED IN
LARGE- AND SMALL-SCALE WAVE TANKS

by

Arvid L. Thomsen
Paul E. Wohlt, and
Alfred S. Harrison

Section I. INTRODUCTION

In many areas within the Missouri River Division (MRD) suitable riprap stone for protecting earth embankments from wave action is not available. Stone must often be transported hundreds of miles from a suitable source to the area where the stone is needed with the result that slope protection becomes a significant proportion of the total embankment cost.

During the planning stage of this study, the Snake Creek embankment in the Garrison Reservoir in North Dakota was of particular concern. The reservoir was in the initial filling stage and the riprap was protected by offshore islands and a reduced fetch, but damage caused by storms during this stage made it apparent that the existing riprap would be inadequate when the pool rose to higher levels. Overlaying of the existing riprap was among the solutions under consideration, but there was uncertainty as to the size of stone required, and doubt about the feasibility of an overlay of the existing glacial boulder riprap on a 1 on 2 slope.

As a result of the high cost of providing riprap protection and the problems which had developed at several projects, this study was initiated. Its purpose was to provide information for design of new construction and improvement to existing riprap by overlays. The models were designed to simulate representative existing structures. Figure 37 on page 73 in Appendix A is a schematic drawing showing the model layer configuration and nomenclature. However, early in the investigation, questions arose concerning such effects as model scale and wave period and the investigation became more generalized.

The results of the Snake Creek overlay models were used in the design of upgrading of the riprap, and the field construction has been completed.

It was found in the models that the overlay construction (A layer of larger stones on top of an original armor layer) did not have a significantly different stability from conventional armor layers. Therefore, the results of the overlay models are not segregated from the remainder of the models.

The slopes of all models were constructed with an impervious core representing an earth embankment and successive layers of bedding, spalls and armor similar to conventional prototype designs. See Model S-13 on page 74 in Appendix A for the layer construction of a typical model, and Figure 39, Appendix B, for the gradations showing the relative size of the stone in the layers in Model S-13. Care was taken during construction of all slopes to avoid artificial placement of armor units not representative of practical field construction. Armor stones were shipped to CERC from sources in the Missouri River Division to ensure that model armor was similar to the armor material used in prototype MRD structures.

As a general study of riprap stability, this investigation includes consideration of the effects of:

1. Underlayers
2. Water depth
3. Armor gradation
4. Viscosity
5. Wave period
6. Armor placement
7. Armor unit shape
8. Embankment slope
9. Armor layer thickness

Underlayers in most models were conventionally constructed of layers of bedding and spalls. Some models were constructed as overlays, and a few were constructed to test the effects of the thickness of spall layers.

Water depth was generally the same for all models in each tank. However, there was some incidental variation in the relative water depth (water depth with respect to the size of the armor on the model).

Armor gradations were tested ranging from nearly uniform to the least uniform expected for field use ("quarry run").

Model scales varied from about 1:20 to almost full scale. In terms of median weight of the armor, this is a range of from about 0.03 pound

to 400 pounds, and in terms of wave height, from 0.1 foot to 6 feet. Testing each model at both small and large scales provided information concerning scale effect on stability.

Although most models were tested at a wave period that provided wave steepness similar to that observed in wind-generated wave systems in reservoirs, some models were tested at other wave periods in an effort to determine if wave period affects stability.

Three distinctly different shapes were tested as model armor; these included glacial boulders, quarried stone, and tribars. Some of the stone shapes were tested both in an individually placed armor layer, and in an armor layer simply dumped onto the model slope. Tribars were tested both as placed and dumped armor.

Tribars and placed-stone armor were tested on models with an embankment slope of 1 on 2 (1 vertical to 2 horizontal). Dumped stone armor was tested on models with embankment slopes of 1 on 2, 1 on 3, 1 on 5, 1 on 7, and 1 on 10; 1 on 7 and 1 on 10 data are from small-scale tests only.

Placed armor layers were constructed about one armor unit thick. Dumped armor layer thicknesses were generally about 1.5 times the median dimension of the median sized stone of the gradation.

Because of the great number of variables involved, each variable could not be as systematically and exhaustively studied as desired. Instead, the heterogeneous data collected from the models were used to evaluate the effects of the variables with the aid of dimensionless parameters developed for the analysis of this data.

Additional studies of the effects of armor thickness and scale effect on steep slopes ($\cot \alpha < 5$) and of the effects of all variables on flat slopes ($\cot \alpha > 5$) would be useful.

Recommendations for design criteria have not been included in this report because in addition to determination of the relationship of wave properties to the stability of stone, establishment of criteria is inseparably tied to determination of design wave conditions, field construction and risk involved in failure of the structure. It is expected that the Chief of Engineers (OCE) will establish design criteria using these and other data. This study is, therefore, limited to the presentation of the results of model tests and a generalized analysis to determine the effects of the important variables. However, the information given in Figure 27 and Tables 6 and 7 is suitable for design use after the designer has adjusted the wave height or chosen a "safety factor" to take account of the uncertainties and risks.

Section II. ANALYTICAL CONSIDERATIONS

Stability of riprap on earth embankments subjected to wave action depends on many variables. The most significant are listed below along with their dimension, where L, F and T represent length, force and time respectively:

<u>Variables that describe the waves</u>	<u>Dimension</u>
Wave height H_0	L
Wave period T	T
Wave length L_0	L
Wave depth d	L
Specific wave energy E	$L \cdot F/L$
Specific wave power P	$L \cdot F/T/L$
Wave height distribution	-----
Wave length spectrum	-----
Duration of attack	T
Angle of wave attack	-----
Type of breaking wave	-----
 <u>Variables that describe the individual armor unit</u>	
Weight of armor unit W	F
Shape of armor unit	-----
Unit weight of armor unit γ	-----
 <u>Variables that describe the riprap layer system</u>	
Armor gradation uniformity	-----
Method of placement	-----
Underlayers	-----
Armor layer thickness T_h	L
Armor layer coverage c	F/L^2
Porosity n	-----

<u>Variables that describe the embankment geometry</u>		Dimension
Embankment slope in wave zone	α	-----
Embankment profile above and below wave zone		-----
<u>Variables that describe the fluid</u>		
Unit weight of fluid	γ_f	F/FL ³
Absolute viscosity	μ	F·T/L ²
Fluid temperature		-----
<u>Other variables</u>		
Gravitational acceleration	g	L/T ²
Damage	J/b	1/L

Some of the variables are interdependent. L_0 , E and P can be described in terms of H_0 , T, d, γ_f and g (U.S. Army Corps of Engineers, 1966). Th depends on W, c, γ , and armor shape, gradation, and placement. The porosity, n, is a function of armor shape, gradation, and placement. Absolute viscosity, μ , is a function of fluid temperature and it is assumed that fluid temperature is significant only in its effect on viscosity. Therefore, L_0 , E, P, Th, n, and fluid temperature can be eliminated as variables because the values of these variables are implicit in the remaining variables.

Some of the variables listed were not studied in this investigation:

Wave height distribution - Wave height distributions were incidental because of the method of operating the wave generators. Selection of the representative wave of these distributions is discussed in Section IV.

Wave length spectrum - Each model was tested with waves of uniform length.

Duration of attack - Each wave attack was continued until the model approached a state of equilibrium.

Angle of wave attack - All models were two-dimensional, i.e., the waves approached perpendicular to the embankment.

Type of breaking wave - Waves were not classified with respect to their breaking characteristics.

Porosity - Porosity was not systematically varied, and only the porosity of the armor layer was measured.

Embankment profile above and below wave zone - All models had uniform embankment slopes.

After elimination of the interdependent variables and the variables that were not studied, the following remain: H_0 , T , d , W , Shape of Armor unit, γ , Armor gradation uniformity, Method of placement, Underlayers, Layer thickness, α , γ_f , μ , g and B .

Dimensional analysis using the Pi Theorem provides many different sets of dimensionless parameters depending upon the combination of repeating variables selected. Since W , γ and g are easy to measure accurately, they were chosen as repeating variables for this analysis. H_0 was not selected as a repeating variable because it is difficult to define and measure accurately; however, isolating it in one parameter confines the scatter due to its uncertainties. H_0 is the dependent variable in this study, therefore, it should not be included in more than one dimensionless parameter. Dimensionless parameters derived for the analysis of the data using W , γ and g as repeating variables are shown in Table 1. Dimensionless parameters for armor gradation uniformity and embankment slope (α) were arbitrarily assigned. B represents cross-section damage in dimensionless terms; computation of B is explained in Section IV.

TABLE 1

Variables and Corresponding Dimensionless Parameters

<u>Variable</u>	<u>Dimensionless Parameter</u>
H_0	$H_0 / (W/\gamma)^{1/3}$
γ_f	γ / γ_f
Underlayers	----
d	$d / (W/\gamma)^{1/3}$
Armor Gradation Uniformity	
μ	$\mu g^{1/2} / (W/\gamma)^{1/2}$
T	$gT^2 / (W/\gamma)^{1/3}$
Armor Unit Shape and Placement	----
α	$\cot \alpha$
C	$c / (W/\gamma)^{1/3} \gamma$
J/b	$J (W/\gamma)^{1/3} / b$

The term $(W/\gamma)^{1/3}$ is the representative length of an armor unit; therefore, it is the normalizing term for obtaining geometric similarity between model and prototype. When a particular length in different sized systems measures the same number of $(W/\gamma)^{1/3}$ units in each system, geometric similarity exists.

Dynamic similarity can also be demonstrated. If various size models and model and prototype are dynamically similar, corresponding forces of fluid viscosity, inertia and gravity are in the same ratio in each. Ratios of these forces provide the Froude number,

$$N = \frac{\text{inertial forces}}{\text{gravity forces}} = \frac{\rho_f D^2 V^2}{(\gamma - \gamma_f) D^3}$$

and the Reynolds number,

$$R_N = \frac{\text{inertial forces}}{\text{friction forces}} = \frac{\rho_f D^2 V^2}{\mu D V}$$

into which the following substitutions are made:

$$\rho_f = \gamma_f / g$$

$$D = (W/\gamma)^{1/3} \quad (\text{a representative length in the system})$$

$$v = (gH_0)^{1/2} \quad (\text{a representative velocity in the system})$$

$$S = \gamma/\gamma_f \quad (\text{specific gravity of the armor unit})$$

When these substitutions are made, we have for the Froude number,

$$N = \frac{H_0}{(W/\gamma)^{1/3} (S-1)}$$

The first dimensionless parameter in Table 1 can be transformed into this same Froude number by dividing by a function of the second parameter, γ/γ_f .

When the above substitutions are made for the Reynolds number,

$$R_N = \frac{\gamma_f}{\mu} \left(\frac{W}{\gamma}\right)^{1/3} \left(\frac{H_0}{g}\right)^{1/2}$$

The sixth dimensionless parameter in Table 1 can be transformed into this Reynolds number by combining with the first and second parameters.

The armor specific gravity $S = \gamma/\gamma_f$ was not varied significantly in this investigation. It is assumed, however, that its effect is accounted for in the Froude number N . It will, therefore, be omitted as an independent variable. Armor gradation uniformity will be represented by the parameter $(W_{85}/W_{15})^{1/3}$. The slope angle will be represented by $\cot \alpha$.

After making the above transformations, elimination, and substitutions, we have the set of dimensionless parameters listed in Table 2.

TABLE 2

Dimensionless Parameters Used in Data Analysis

<u>Variable</u>	<u>Dimensionless Parameter</u>
H_0	$N = H_0 \gamma^{1/3} / W^{1/3} (S-1)$
Underlayers	----
d	$d / (W/\gamma)^{1/3}$
Armor gradation uniformity	$(W_{85}/W_{15})^{1/3}$
Viscosity	$R_n = (\gamma_f/\mu) (W/\gamma)^{1/3} (H_0/g)^{1/2}$
T	$gT^2 / (W/\gamma)^{1/3}$
Armor unit shape and placement	----
α	$\cot \alpha$
C	$c / (W/\gamma)^{1/3} \gamma$
J/b	$J(W/\gamma)^{1/3} / b$

Treating N as the dependent variable, the following equation can be written:

$$\begin{aligned}
 N &= \frac{H_0}{(W/\gamma)^{1/3} (S-1)} \\
 &= f [\text{underlayer, } d/(W/\gamma)^{1/3}, (W_{85} W_{15})^{1/3}, \\
 &\quad R_n, gT^2/(W/\gamma)^{1/3}, \text{ armor shape and placement,} \\
 &\quad \cot \alpha, c/(W/\gamma)^{1/3} \gamma, J(W/\gamma)^{1/3}/b] \tag{2.1}
 \end{aligned}$$

The Froude number N has been used as the dependent variable in many other studies of wave riprap. N has commonly been referred to as the "Stability Number" and will be referred to as such in the remainder of this report. Model test results that demonstrate the influence on the stability number of each variable in Equation (2.1) are discussed in Section V.

Section III. LABORATORY APPARATUS

1. Wave Tanks and Wave Generators

Model slopes were tested in three wave tanks that differ principally in size. The tanks are designated as:

Large tank - generates waves from 0.5 to 6.0 feet in height.

Medium tank - generates waves from 0.1 to 0.8 feet in height.

Small tank - generates waves from 0.1 to 0.5 feet in height.

Each tank is equipped with a piston-type wave generator. A flap-type generator can be installed in the large tank to generate waves smaller than 2 feet in height. The frontispiece shows the large tank with waves 5 feet high and 69 feet long. Figure 1 shows the medium and small tanks.

a. Large Tank. CERC's tank for large waves is an outdoor, reinforced concrete flume 635 feet long, 15 feet wide and 20 feet deep. Model slopes were built against a bulkhead inserted 504 feet from the wave generator. The wave generator is a movable bulkhead driven by an 800-horsepower electric motor through dual flywheels and reciprocating arms. Wave height is primarily a function of the bulkhead displacement. This displacement is determined by the position of the reciprocating arms on the flywheels. Wave period is determined by the speed of the motor.

b. Medium Tank. CERC's 85-foot tank is an indoor, reinforced concrete flume 14 feet wide and 4 feet deep. Model slopes were constructed with the toe positioned 53.5 feet from the generator blade. A 7.5-horsepower electric motor drives the wave generator through eccentric arms. Wave height is determined by the eccentricity of the arms and the wave period is determined by the motor speed.

c. Small Tank. CERC's 72-foot tank is a glass-walled flume 1.5 feet wide and 2 feet deep. Model slopes were constructed with the toe positioned 45 feet from the generator blade. The wave generator is powered by an electronically controlled hydraulic pump.

2. Tank Calibration

Each tank was calibrated to establish the relationships between generator-blade displacement, wave height, wave period, and water depth. These relationships were determined by measuring the wave heights at the location of the toe of the model slope at various magnitudes of wave period, blade displacement and water depth *without* the model slope in place. It is necessary to remove the slope during calibration because the measured wave heights with the slope in place were affected by the reflections from the slope, making it difficult to define the approaching

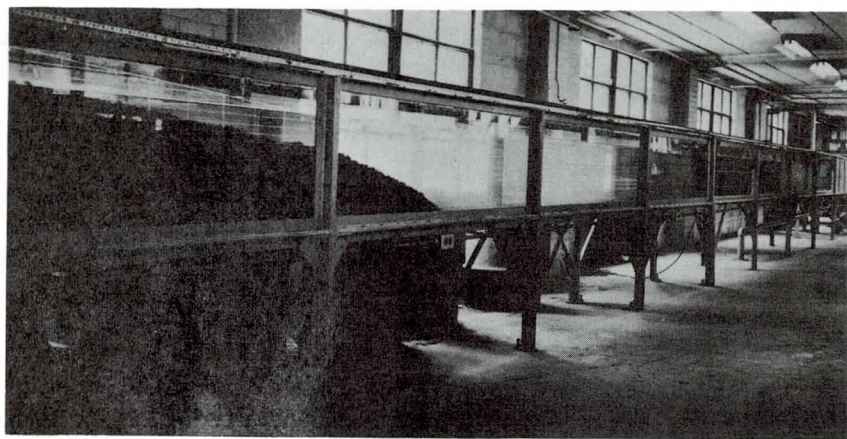
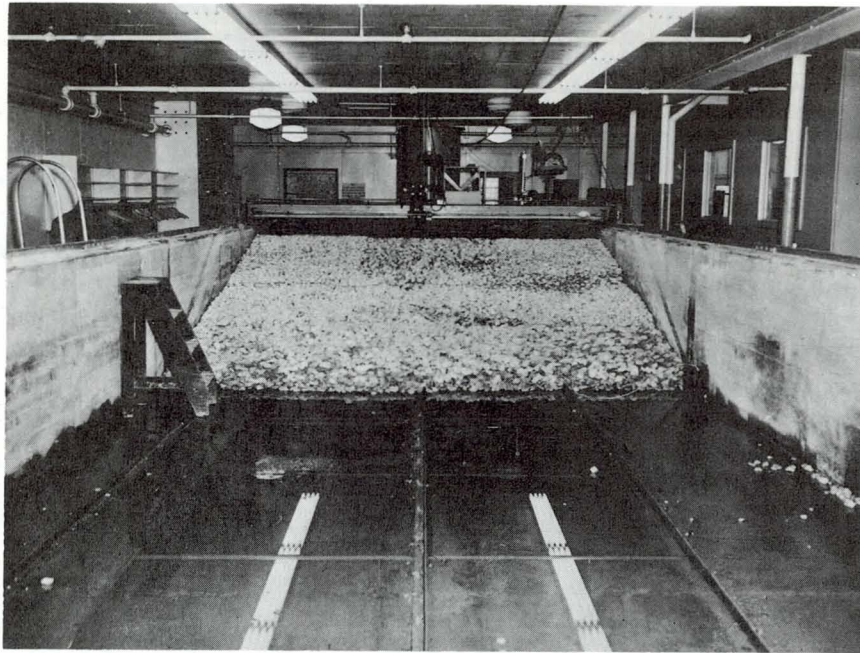


Figure 1. Photographs of Medium and Small Tanks

wave train. Wave reflection was reduced during calibration with an absorbing structure placed in the far end of the tank from the wave generator. During calibration, the wave generator was operated precisely as it was during the tests.

Parallel-wire resistance gages were used to measure the wave height in the small and medium tanks; and a step-resistance gage with 0.1 foot resolution was used in the large tank. Gage output was recorded on a strip chart.

3. Survey Equipment

Each tank was equipped with a surveying device for the purpose of establishing surface profiles of the models. Figure 2 shows photographs of the survey equipment in large and small tanks.

a. Large Tank. Surveying was done manually from a movable bridge mounted on rails atop the tank walls. A subcarriage that could be moved across the tank was attached to the movable bridge. Soundings were located with an accuracy of approximately 0.05 foot in a horizontal plane and to 0.01 foot in a vertical plane by vernier gages. A vertical sounding rod with a circular foot, mounted on the lower end with a ball joint, was attached to the subcarriage. The ball joint allowed rotation of the foot up to a maximum angle of 30 degrees on the uneven rock surface of the model. Model surface elevations were measured on a 2-foot horizontal grid with a 6.75-inch-diameter foot for large armor stones and with a 3-inch-diameter foot for the smaller armor stone of tests L-10 and L-12.

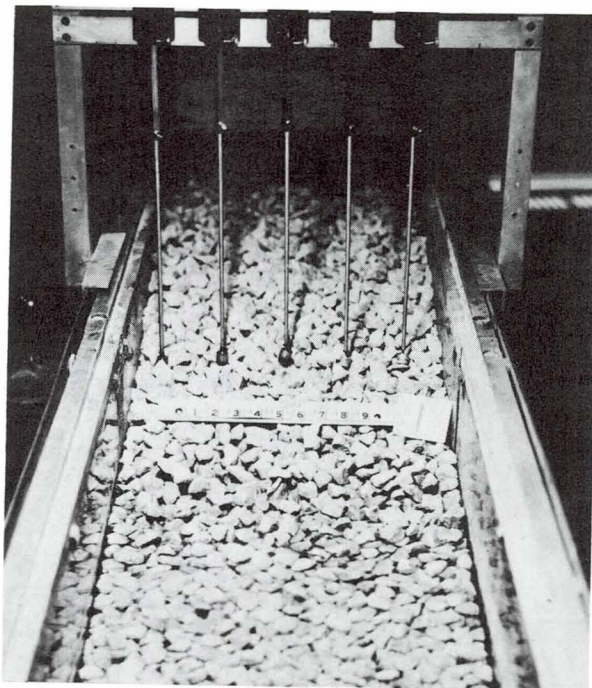
b. Small Tank. Model slopes in the small tank were surveyed with five vertical sounding rods mounted on a rack that could be moved along level rails mounted on the tank walls. A 5/8-inch-diameter foot was ball-joint mounted on the lower end of each rod. Model surface elevations were measured on a horizontal grid 0.3-foot across by 0.1-foot longitudinal.

c. Medium Tank. A sonic sounder was used to survey the models in the medium tank. The sonic device was previously developed and used to monitor stream bed profiles in hydraulic research (Karakı, Gray and Collins, 1961). Resolving power of this device was capable of detecting the outline of individual armor units.

The sounder transducer was mounted on a transverse moving subcarriage attached to a longitudinally moving carriage mounted on rails on the tank walls. The face of the transducer was positioned below the water surface. The sounder output is a d.c. voltage directly proportional to the distance from the transducer face to the armor surface. This output was used to drive the y-axis of an x-y recorder. A potentiometer attached to the moving subcarriage supplied a d.c. voltage directly proportional to the transverse distance between the subcarriage and the left tank wall. This voltage was used to drive the x-axis of the x-y plotter. A family of transverse profiles of the model was provided by this arrangement when the subcarriage was moved across the slope at various longitudinal tank locations.



Sounding Rod in Large Tank



Sounding Rods in Small Tank

Figure 2. Photographs of Survey Equipment

Section IV. DESCRIPTION OF TESTS

1. Model Construction

All models were constructed in a manner realistic and practical for prototype construction. Since the model results were intended to aid in the design of riprap on impervious earth embankments, impervious cores were constructed as the foundation of all models. Armor and underlayers were extended upslope beyond the zone of possible wave action in all models. Therefore, all wave energy was either reflected or dissipated by the armor and filter layers of the models.

Each model test is identified by a coded test number of the form L-2.3. The letter (L, M or S) designates the tank in which the model was tested (large, medium or small), the number following the dash identifies a particular model design and the number after the decimal indicates the particular test of the model design. For instance, test L-2.3 was conducted in the large tank and was the third test of model design number 2. The SPL series of tests are part of a separate study conducted by CERC for OCE. These models were constructed and tested in a manner similar to the models in this study.

In constructing models similar to prototype structures, the sequence of model construction was as follows:

- 1) Construction of a compacted, low porosity core simulating impervious prototype earth embankments.
- 2) Placement of bedding and spalls layers as a filter to prevent migration of material through the voids in the armor layer.
- 3) Construction of armor layer.

Where strengthening of existing riprap by overlaying with more stable armor was under study, placement of the overlay armor was the fourth step. When a model design was tested a number of times consecutively, disturbed portions of each layer were removed and replaced between tests, and generally the armor layer was completely removed and rebuilt. Detailed descriptions of all models are given in Appendixes A and D.

a. Core. In the large tank, the impervious core was placed and compacted in 6-inch lifts. In the small and medium tanks, the fine sand core was consolidated in a saturated condition with an internal concrete vibrator to ensure low permeability.

b. Bedding and Spalls. Bedding and spalls layers were designed to be sandwiched between the core and the armor so that the 15 percent size of the overlying material was smaller than 5 times the 85 percent size of the material in the underlying layer in accordance with the filter criteria in EM 1110-345-282 (U. S. Army Corps of Engineers, June 1955). These layers were constructed by simply dumping the material onto the embankment slope, and spreading to the desired thickness.

c. Armor. Both stone and tribars were tested as armor. Often the armor consisted of more than one layer, particularly when the slope was designed to test the effectiveness of overlaying existing armor with a layer of larger armor units. Examples of overlay models are Model Nos. L-6 and L-7, Table 1 and Figure 43. Two methods were used in constructing armor layers.

(1) Dumped Stone - Dumped stone armor layers were constructed by spreading the stone in a single lift from a skip with little or no rearranging of individual stones after dumping. This is the most common method of constructing armor layers in the Missouri River Division in accordance with Guide Specifications CE 1308 (U. S. Army Corps of Engineers, July 1958). In large-tank slope construction, the skip was operated with a crane. In construction of slopes in the small and medium tanks, the skip was operated by hand (Figure 3).

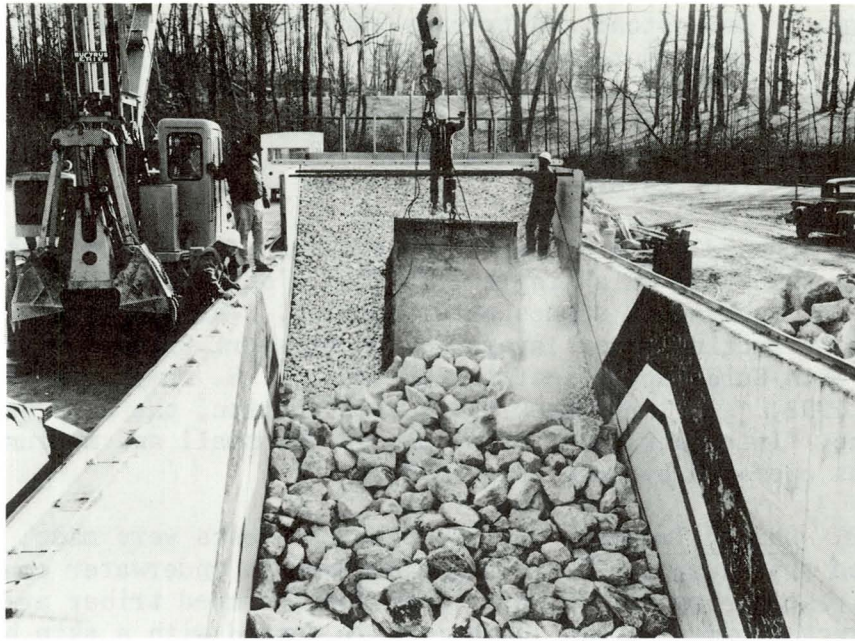
(2) Dumped Tribars - At the time the tests were made, it was contemplated that dumped tribars might be used in underwater construction to overlay glacial boulder riprap. Therefore, dumped tribar armor layers were constructed under water. Tribars were dumped with a skip because prototype tribars in the Missouri River Division were not expected to exceed 1,000 pounds each, and the skip method of construction would be economical and feasible in this case.

Twelve tribars were placed in the skip in two layers. Tribars in the lower layer were placed upright and in the upper layer they were placed on their side as shown in Figure 4. The skip was positioned over the water by reference marks on the tank walls, lowered to the armor layer and tilted downslope to slide the tribars into place. Dumping was completed in two lifts on offset grids to increase chances of complete coverage. After the armor layer was constructed, water was drained from the tank and the model was surveyed, examined and photographed. Individual tribars were not moved to provide a more uniform coverage once they had been dumped from the skip; however, this was generally accomplished naturally by the first few test waves.

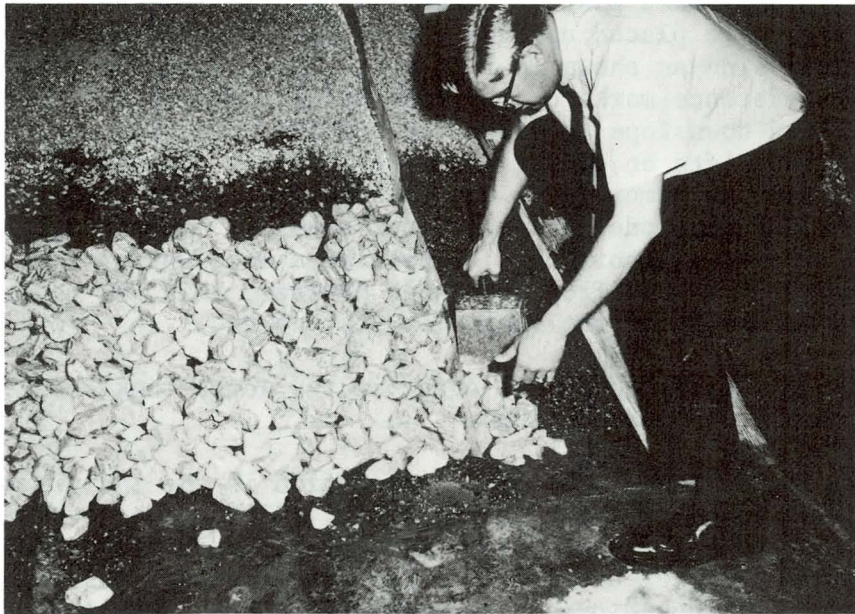
The skip was operated with a crane in the large tank model, and by hand in the small and medium tanks.

(3) Placed Stone - Placed construction is the individual placement of single stones of a narrow gradation. Although a pavement of carefully selected and fitted stones was not intended, some advantage from the interlocking of the individually placed stones was expected to the extent that seemed practical when placing the stones by crane. Stones were handled with a crane operated orange-peel in large-tank construction. Workmen on the slope directed the crane operator and guided the stones into place, but did not manually handle the stones. Generally, an attempt was made to orient the long axis of each stone parallel to the tank walls and the intermediate axis vertically.

In the small and medium tanks, the stones were individually placed by hand in an attempt to duplicate the placement in the large tank.



Large Tank



Medium Tank

Figure 3. Photographs of Dumped Stone Armor Layer Construction

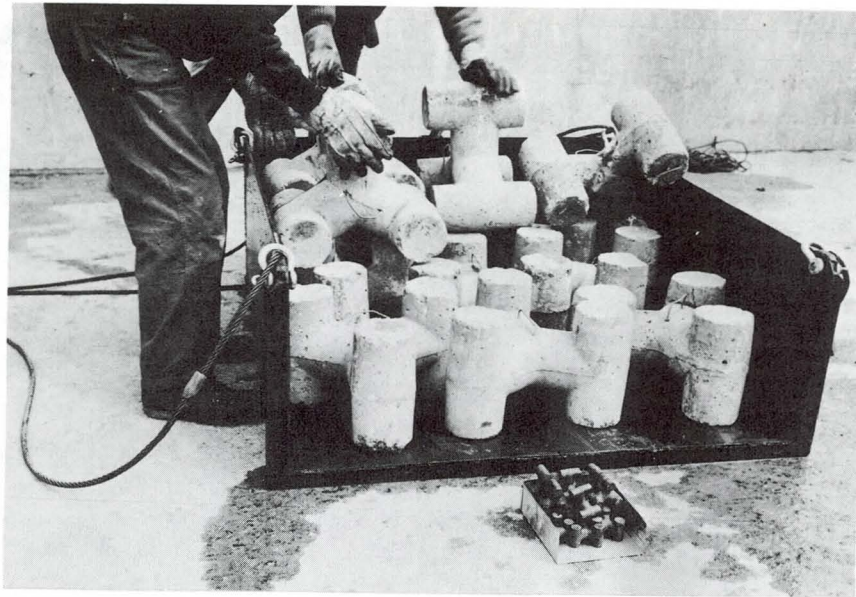


Figure 4. Skip Loads of 81.3 and 0.43-pound Tribars
(Small skip is in the foreground.)



Figure 5. Placed Tribar Construction in the Large Tank

(4) Placed Tribars - Tribars were individually placed with the legs normal to the slope. For the placed-tribar tests, three large-tank tribars were hoisted by the crane at one time but were individually placed on the slope as shown in Figure 5. In the small and medium tanks, tribars were placed individually by hand in an effort to duplicate placed-tribar construction in the large tank.

2. Test Materials

All armor stone was shipped to CERC from sources in the Missouri River Division to ensure similarity in model armor stone, and to obtain armor stone typical of that used in prototype structures.

Materials used in each test are listed in Table 8 in Appendix A; the gradation curves are given in Figures 38 through 44 in Appendix B. Figure 37 on page 73 of Appendix A is a cross section showing the general layer configuration and nomenclature. Every test did not include all the layers shown on the figure.

a. Core. Uniformly graded fine quartz sand was used for the cores in the small and medium tanks. Bank run gravel, inexpensive and locally available, was selected for the core in the large tank.

b. Bedding and Spalls. Quartz sand, crushed stone, and most of the rounded gravel were obtained near Washington, D. C. All other materials were shipped to CERC from sources in the Missouri River Division.

c. Armor. Four different armor shapes were tested: rounded boulders, Kimmswick limestone, Sioux quartzite and tribars. Boulders, limestone and quartzite represent a wide range in natural stone shapes - from rounded and smooth to angular and jagged. Figures 6, 7, and 8 illustrate the similarity of the shapes of small stones used in the small and medium tanks to the large stones used in the large tank. These figures also show the relative shapes of the three types of stone tested.

Occoquan granite, similar in shape to Sioux quartzite was used in the SPL tests at CERC. Unit weights of the armor materials were determined in accordance with CRD-C 107-60 (U. S. Army Corps of Engineers, 1960).

Rounded boulders and rounded gravel are granitic in composition and of glacial origin. The boulders came from Spencer, South Dakota, and the gravel from Hawardin, Iowa.

Kimmswick limestone is a mottled gray, fine to coarse crystalline, relatively soft limestone of middle Ordovician age. The tested limestone was quarried from the lower 40-foot face of a limestone ledge near Huntington, Missouri. The quarried limestone tended to be cubically shaped.

Sioux quartzite is of Precambrian age and is composed of pink, fine, rounded quartz grains cemented with secondary quartz with minor amounts

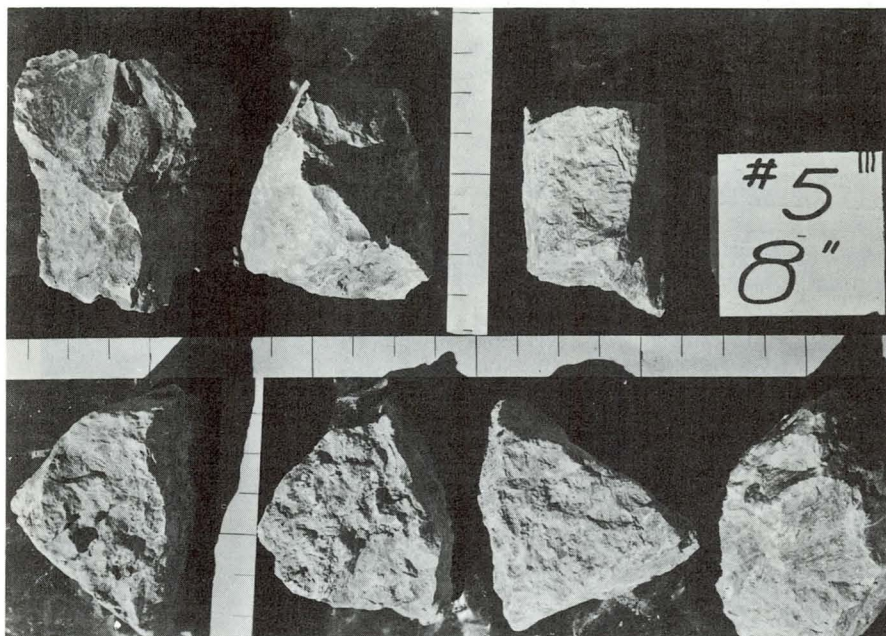


Median Dimension = 12 1/2 inches

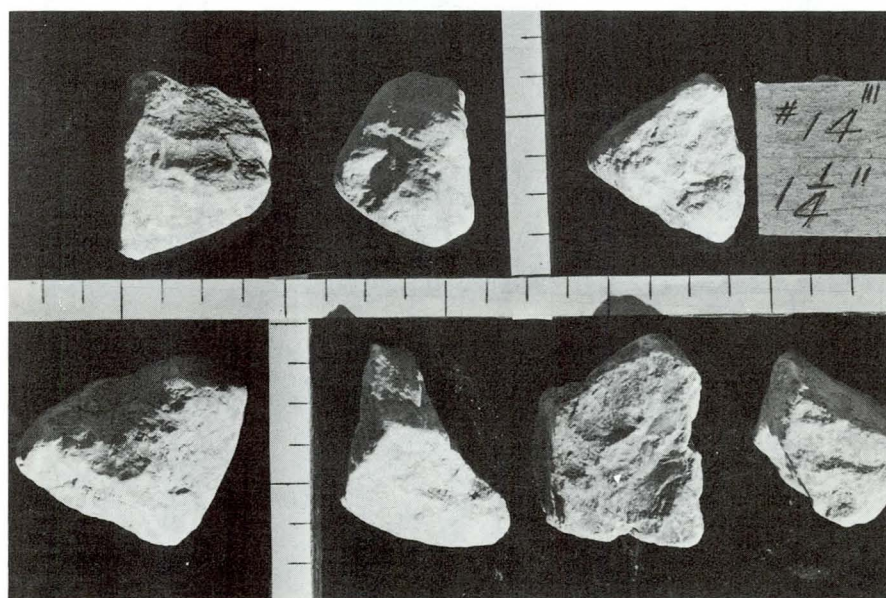


Median Dimension = 7/8 inch.

Figure 6. Photographs of Rounded Boulders used in Model Tests

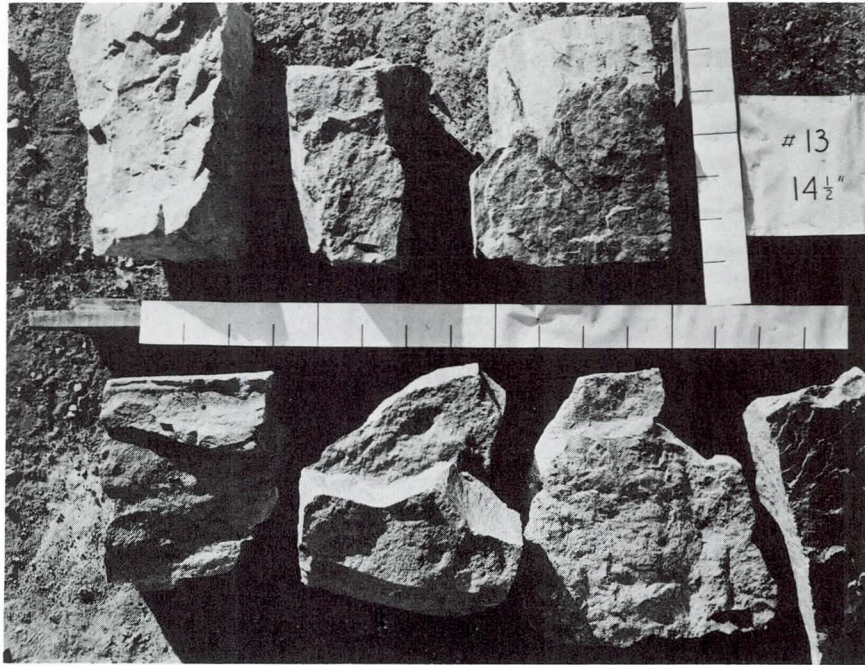


Median Dimension = 8 inches.

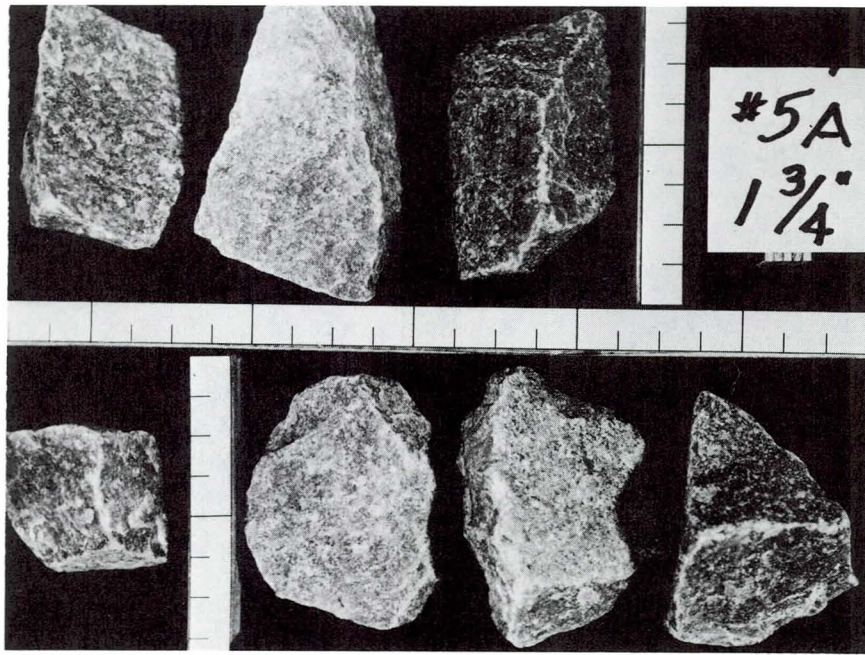


Median Dimension = 1 1/4 inches.

Figure 7. Photographs of Kimmswick Limestone used in Model Tests



Median Dimension = 14 1/2 inches



Median Dimension = 1 3/4 inches

Figure 8. Photographs of Sioux Quartzite used in Model Tests

of other materials. Quarried quartzite tends to be slabby; the test stones were selected to include only those stones having a longest dimension less than four times the shortest dimension. Large Sioux quartzite was quarried at Spencer, South Dakota; small sizes were quarried and crushed at Dell Rapids, South Dakota.

The tribar is a precast shape consisting of three bars tied together by three radial arms. Mr. Robert Q. Palmer, U. S. Army Engineer District, Honolulu, developed and patented the tribar. Shape and dimensions of the tribar are shown on Figure 9. The large tribars (81.3 pounds) were cast from concrete; the small tribars (0.12, 0.30 and 0.43 pounds) from leadite. Leadite is a trade name of a caulking compound that after melting and casting has a specific gravity nearly equal to, and a grain size finer than that of concrete.

3. Testing the Models

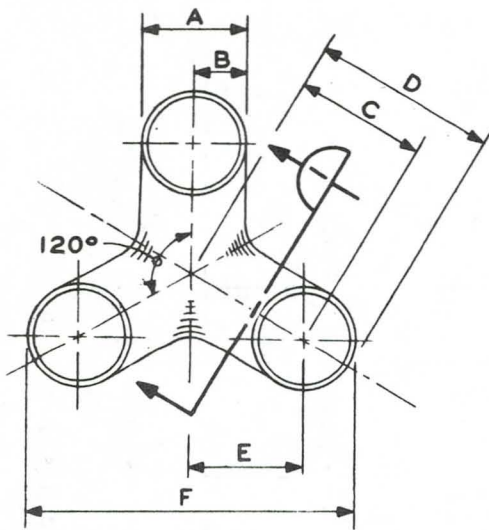
After completion of model slope construction, the armor surface was surveyed and photographed, the tank filled to the proper water depth, and the wave period and generator eccentricity adjusted. Testing began by applying "seasoning" waves, i.e., small waves that might cause some settlement and adjustment but no removal of armor units. If none of the armor was removed by about 1,200 of these waves, the armor surface was again surveyed and photographed and the wave height increased 5 to 10 percent and the process repeated.

Generally, the first wave heights that move armor units only reorient some of the least stable units. If, after some movement, the model withstood at least 300 waves without any further movement, the slope was considered to be stable for the particular wave height. Surveys and photographs were then taken, and the wave height was again increased 5 to 10 percent. This procedure was repeated until the waves removed armor units continuously. The condition of the model was continually documented with surveys and photographs.

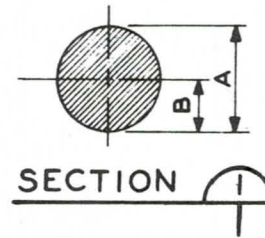
Judgment was required to decide when to change the wave height and to determine when the test should be terminated. Movies of earlier tests were frequently reviewed as an aid in maintaining consistent decisions.

In these models, progressively larger waves were applied without rebuilding or repairing the model between wave heights. This expedited the testing, and was not inconsistent with prototype wave action. It is unlikely that large waves of the "design" wave height will be experienced in the prototype before a number of smaller storms have occurred, or that the "design" storm will generate the "design" wave before many other smaller waves have reached the slope.

a. Description of Test Waves. Wind-generated waves in a reservoir can be represented by a unique frequency distribution (Saville, McClendon, and Cochran, May 1962). Waves generated in the tanks at CERC are more uniformly distributed as shown on Figure 10.

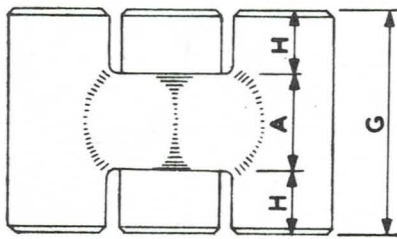


PLAN



SECTION

	WEIGHT (LBS)	81.3	0.43	0.30	0.12
	UNIT WEIGHT (PCF)	143	140	140	140
<u>SYMBOL</u>	<u>DIMENSION IN FEET</u>				



ELEVATION

A	0.477	0.077	0.069	0.051
B	0.239	0.039	0.035	0.026
C	0.573	0.093	0.083	0.061
D	0.811	0.131	0.117	0.087
E	0.489	0.079	0.071	0.052
F	1.458	0.235	0.211	0.156
G	0.954	0.154	0.138	0.102
H	0.239	0.039	0.035	0.026

Figure 9. Shape and Dimensions of Tribars Tested

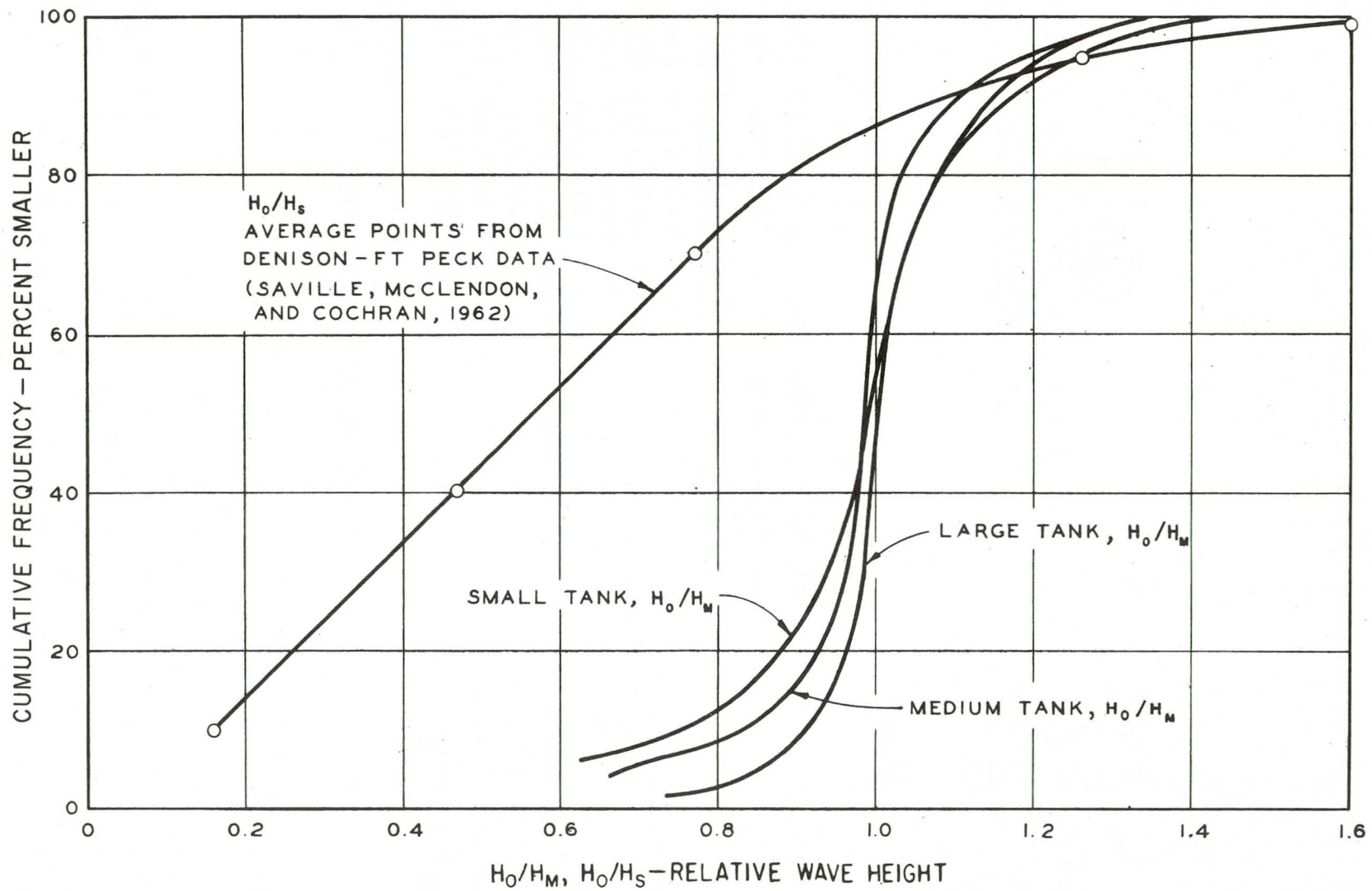


Figure 10. Wave Height Frequency Distributions

The distribution of wave heights in the tanks depends primarily upon the wave period and manner of operating the wave generator. Distributions shown on Figure 10 were measured while operating the generators intermittently at the wave period most often used in each tank. Longer wave periods provide more uniform wave-height distributions, and shorter wave periods generally provide slightly less uniform wave height distributions.

(1) Wave Generation - If the incident wave energy is completely absorbed by the slope, i.e., none is reflected, continuous operation of the wave generator will provide incident waves nearly uniform in height. Embankment slopes of 1 on 5 and flatter seemed to absorb enough of the incident wave energy to allow continuous operation of the wave generator. The average wave height during continuous operation was used in the analysis of the data collected in the small and medium tanks when the embankment slope was 1 on 5, 1 on 7 or 1 on 10.

Steeper slopes (1 on 2 and 1 on 3) reflected so much of the incident wave energy that if the generator were operated continuously, the reflected waves would return to the wave generator and be re-reflected by the generator blade. These re-reflected waves would then be superimposed on the incident waves producing a complex, undefined wave system. This complex wave system was avoided by operating the generator intermittently. During intermittent operation, waves were generated until the first reflected wave returned to the generator. Generation was then stopped, and the water was allowed time to calm before another burst of waves was generated.

During intermittent generation, transient conditions induced by the starting and stopping of the wave generator are prevalent, and each burst of waves contains a distribution of wave heights. However, each distribution is almost exactly reproducible and similar in all wave tanks for similar values of d/L_0 .

(2) Wave Height Distribution - Figure 10 illustrates the similarity of wave height distributions in the three wave tanks resulting from intermittent generator operation at wave periods used in most tests, and with d/L_0 about 0.20. Measurements of 15 bursts of about 10 waves each in each tank were used to plot these curves. Typical bursts of waves for these conditions are shown on Figure 11. H_m is the modal wave height of each burst (average height of the waves of fairly consistent height in the center of the burst) and H_s is the significant wave height (average of the highest 1/3 of the waves). The curve provided by the Denison - Fort Peck data (Saville, McClendon, and Cochran, May 1962) shows the distribution of wave heights in a typical reservoir with respect to the significant wave height. Although the position of the Denison - Fort Peck distribution is offset with respect to the tank distributions because each is plotted with respect to a different wave height of the distribution, the relative shapes of the curves illustrate that the tank wave heights were fairly uniform in comparison to the typical reservoir wave heights.

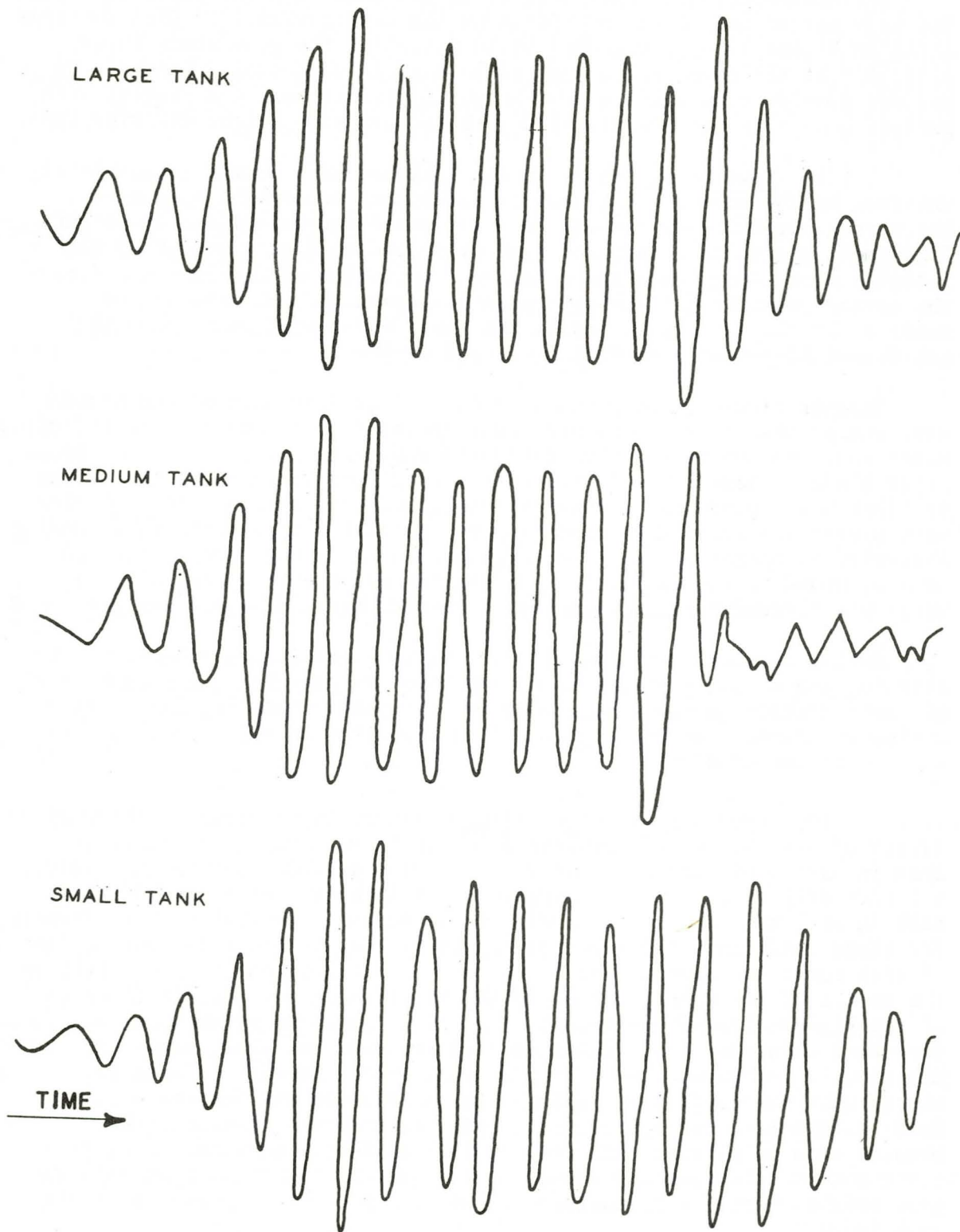


Figure 11. Sample Wave Gage Records

The average of the highest waves from the 15 individual bursts corresponds to about the 95 percent frequency level of the curves in Figure 10. These curves show that for most tests in this study, the highest wave in each burst is about 20 percent higher than the modal wave height, and about 15 percent higher than the significant wave height. The highest wave, the significant wave height and the modal wave height of each burst are nearly equal when the wave period is long.

(3) Effective Wave Height - Each 10 percent increment increase in wave height during testing provided a noticeable increase in the damage rate. Because the highest wave in each burst was more than 10 percent higher than the significant wave height or modal wave height in most tests, these high waves alone have a potential for causing appreciable damage if they exist in significant numbers. Most slopes were tested with at least 100 bursts of waves of each wave generator setting providing at least 100 of these highest waves at the common wave periods, and more at longer wave periods.

Other investigators have used the modal wave height or the significant wave height as the effective wave height of a burst of waves. In this study, the highest wave in each burst was considered the effective wave because:

- 1) The highest wave was significantly larger than the modal or significant wave height of each burst of waves during most model tests.
- 2) Highest waves existed in significant numbers.
- 3) During testing, increases in wave height as little as 10 percent produced significant increases in damage. The highest waves in a burst were usually more than 10 percent higher than the modal waves.
- 4) Wave height distributions were similar in all wave tanks.
- 5) The highest wave is easiest to define and measure.

To analyze the data, the highest wave in each burst of waves generated intermittently and the average wave height during continuous generation were used. All wave heights were converted to deepwater equivalent wave heights for data analysis.

b. Wave Damage on Models. Movement of the armor was monitored with photography, visually (counting armor units that are washed downslope by wave action), and by surveys which provided average armor surface profiles. The average cross-section area of damage was determined by comparing the average surface profile of the armor after damage with the original average surface profile. Profiles were compared by superimposing one profile on the other such that the cross-section area of the erosion, A , is equal to the cross-section area of accretion, A' , as shown in Figure 12. Damage in square feet is the area, A .

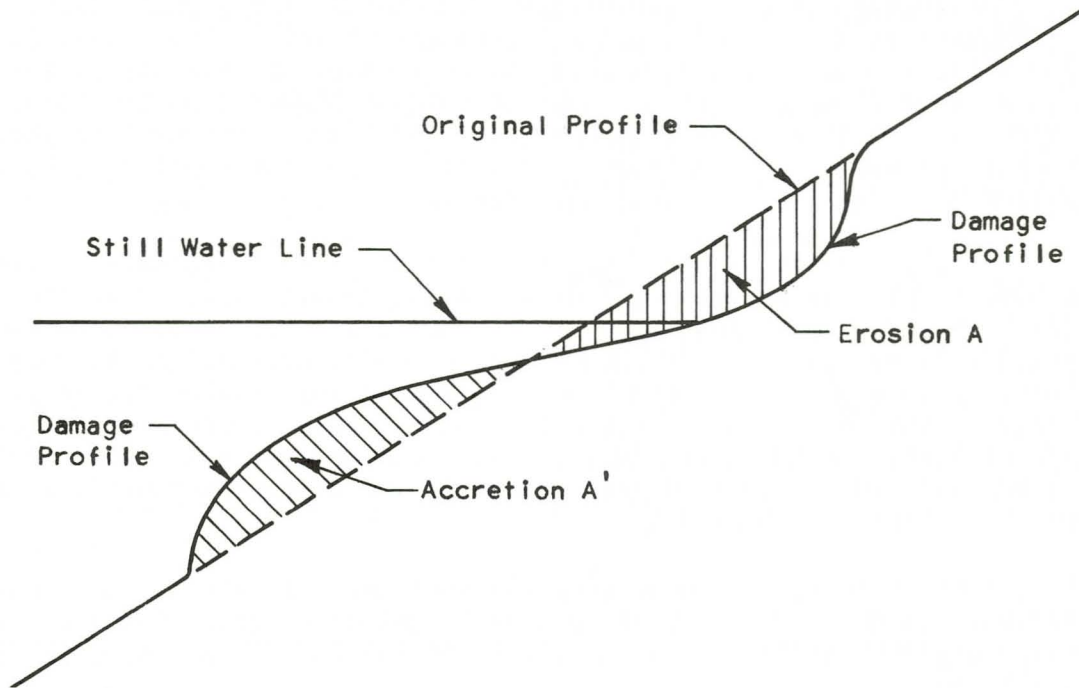


Figure 12. Damage Profile

To allow comparisons of damage and damage rates of all models regardless of model size, damage is expressed in dimensionless terms. Dimensionless damage, B , is the average number of armor units removed from a strip 1-armor-unit wide extending up and downslope parallel to the tank walls. Therefore,

$$B = \frac{JD}{b}$$

where

B is dimensionless damage,
 D is a representative linear dimension of an armor unit, and
 J is the total number of armor units removed from a test section of width b .

$$V = JW/(1-n) \gamma$$

is the volume occupied by J armor units if

W is the weight of a single armor unit,
 γ is the unit weight of the armor material, and
 n is the porosity of the armor layer.

The projected area of a section cut through J displaced armor units is

$$\frac{V}{b} = A = \frac{JW}{(1-n)\gamma b}$$

therefore,

$$\frac{J}{b} = \frac{(1-n)\gamma A}{W}$$

and

$$B = \frac{JD}{b} = \frac{(1-n)\gamma AD}{W} \quad (4.1)$$

Equation (4.1) provides for the computation of dimensionless damage, B, if either the total number of armor units removed (J) or the average cross-section area of damage (A) is known, as long as D and W are defined. In the data analysis in Section V, the median size (W_{50}) is shown to be the best representative size of the gradation. Therefore, the following values are assigned:

$$W = W_{50}$$

$$D = D_{50}$$

where

W_{50} is the median weight of the armor gradation

and D_{50} is a characteristic linear dimension of an armor unit of weight W_{50} ; approximately equivalent to the "sieve diameter", i.e., the square opening through which a stone will barely pass.

A number of measurements indicated that D_{50} could be computed by the equation

$$D_{50} = (W_{50}/0.65\gamma)^{1/3}$$

for stones. The height of a tribar leg was used as the characteristic linear dimension in tribar models.

Dimensionless damage can be computed from Equation (4.2) if the number of armor units removed (J) is known, and from Equation (4.3) if the cross-section area of damage (A) is known.

$$B_J = \frac{JD_{50}}{b} = 1.15 \frac{J(W_{50}/\gamma)^{1/3}}{b} \quad (4.2)$$

$$B_A = \frac{(1-n)\gamma AD_{50}}{W_{50}} \quad (4.3)$$

c. Determination of Zero-damage and Limited-damage Wave Heights.

The ability of each model to resist wave action is represented by two conditions of stability - zero-damage stability and limited-damage stability - determined by the zero-damage wave height and the limited-damage wave height. Zero-damage wave height is the highest wave during a test that did not remove armor units from the slope; limited-damage wave height is the highest wave during a test that did not remove underlayer material.

For the determination of these wave heights, dimensionless damage was plotted as a function of wave height for each model (Figures 45 through 58, Appendix C). Each data point on these figures is assumed to represent the maximum amount of damage or the equilibrium condition for the respective wave height. In other words, if more waves of each wave height had attacked the model, additional damage would have been slight. Figure 13 illustrates the validity of this assumption. Damage is plotted as a function of total number of high waves for tests L-1.1 and L-2.1. Vertical lines represent changes in wave height. Wave heights are indicated along the top of each graph between vertical lines. The attack of each of the wave heights shown was accompanied by attack from about 10 times as many modal waves that were about 20 percent lower than the indicated high waves. Both graphs in Figure 13 indicate that the damage rate became nearly zero, i.e., the model was in equilibrium with respect to damage during the attack of each wave height before the wave height was increased.

Zero-damage wave heights were determined by the extension of straight lines through the points on the damage curves to the zero-damage ordinate. In some tests, the removal of a few individually unstable armor units indicated an initial insignificant damage rate. In such cases, the intersection of two straight lines, one drawn through the data points representing "real" damage and one through the points representing insignificant damage determined the zero-damage wave height as in test L-7.1 (Figure 49, Appendix C).

A dimensionless damage number (B_J for tribars and placed stone models, B_A for dumped stone models) that represented the model condition just prior to underlayer erosion (limited-damage condition) was determined for each test by reviewing the test records and photographs. These limited-damage values were averaged for each type test, and are listed on page 52. The limited-damage wave height for each test was then determined by the intersection of this average limited-damage value and the damage curve for the test.

d. Photography. In addition to still photography, time-lapse photography was used to allow reviewing the events that occurred during each model test. Time-lapse movies were made by exposing about 16 frames of 16-millimeter film between bursts of waves during intermittent generation and at intervals of about 100 waves during continuous wave generation.

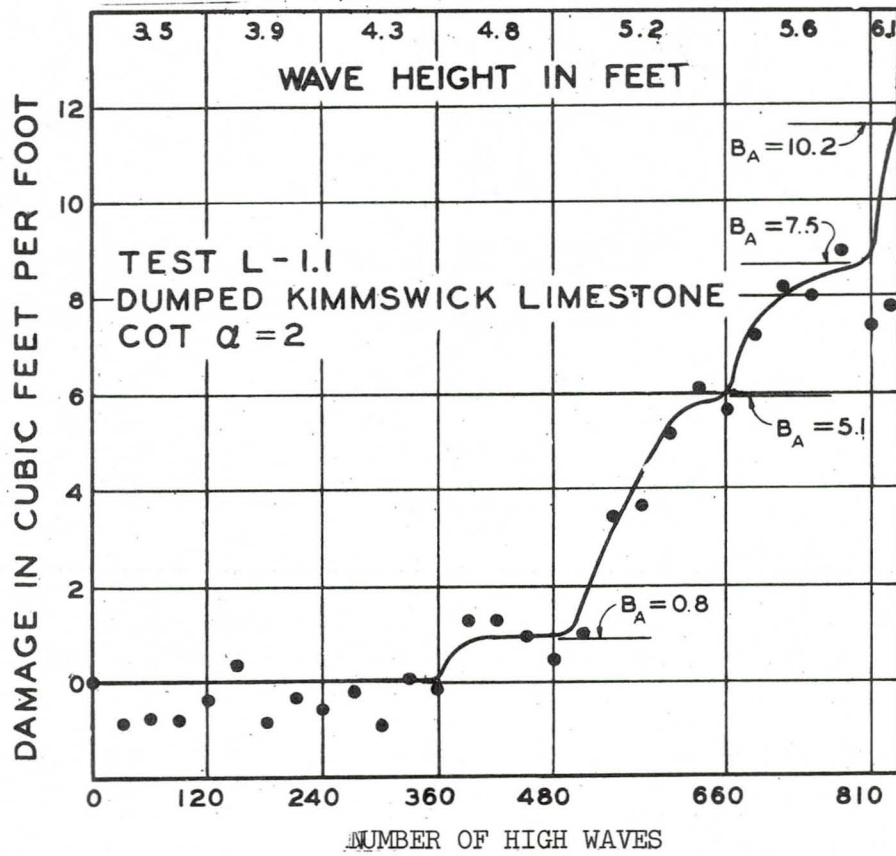
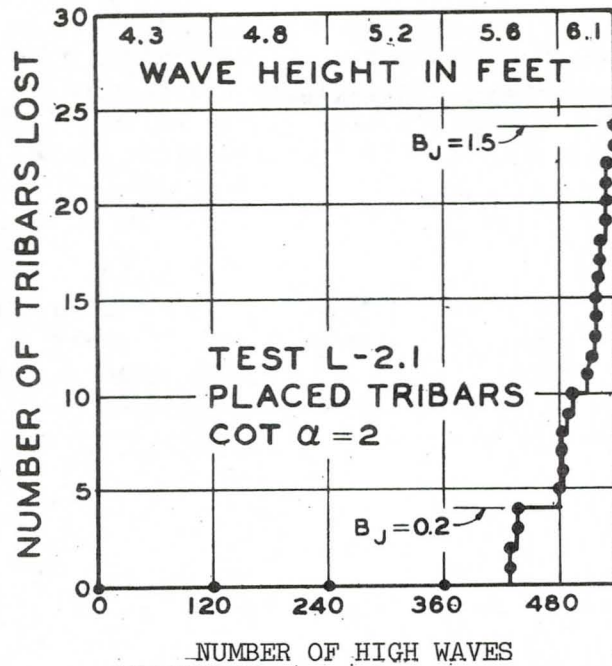


Figure 13. Typical Damage Development

e. Other Measurements. Water temperature used to determine viscosity was not measured during testing, but was estimated later from ambient temperatures. Indoor tank water temperatures were estimated at 65 degrees Fahrenheit; outdoor tank (large tank) temperatures were estimated equal to the average mean daily temperature recorded at the Dalecarlia Reservoir (adjacent to CERC) and compiled by the U. S. Department of Commerce.

Section V. TEST RESULTS

1. General

The analysis of the test data proceeds from the dimensionless analysis developed in Section II, Analytical Considerations. The stability number N will be evaluated for zero damage wave heights. Consequently, the damage parameter $J(W/\gamma)^{1/3}/b$ can be eliminated as a dependent variable and Equation (2.1) becomes:

$$\begin{aligned}
 N_{ZD} &= \frac{H_{ZD}}{(W/\gamma)^{1/3}(S-1)} \\
 &= f [\text{underlayers, } d/(W/\gamma)^{1/3}, (W_{85}/W_{15})^{1/3} \\
 &\quad R_N, gT^2/(W/\gamma)^{1/3}, \text{ Armor shape and placement,} \\
 &\quad \text{Cot } \alpha, C/(W/\gamma)^{1/3}\gamma] \tag{5.1}
 \end{aligned}$$

Each dimensionless parameter in Equation (5.1) relates to a variable as shown in Table 3.

TABLE 3
Variables Represented by Dimensionless Parameters

<u>Model Variable</u>	<u>DEPENDENT</u>	<u>Dimensionless Parameter</u>
Stability (Zero-damage wave height)	DEPENDENT	$N_{ZD} = \frac{H_{ZD}}{(W/\gamma)^{1/3}(S-1)}$
	INDEPENDENT	
Underlayer thickness		----
Water depth		$d/(W/\gamma)^{1/3}$
Armor gradation uniformity		$(W_{85}/W_{15})^{1/3}$
Model size		$R_N = \frac{\gamma_f}{\mu} \left(\frac{W}{\gamma}\right)^{1/3} \left(\frac{H_{ZD}}{g}\right)^{1/2}$
Wave period		$gT^2/(W/\gamma)^{1/3}$
Armor unit shape and placement		----
Embankment slope		$\text{cot } \alpha$
Armor thickness		$c/(W/\gamma)^{1/3}\gamma$

In effect, the wave height is the dependent variable for these tests as conducted.

Only a few of the possible combinations of variables were tested because of the large number involved. The Kimmswick limestone was most intensively tested, both as to the number of tests and the variables, and hence more conclusions are based on Kimmswick limestone than on other armor. Boulders, Sioux quartzite and tribars were tested only on a 1 on 2 slope. Tribars, with the exception of three small-tank tests, were tested as overlay on boulders. Since each armor type was tested in at least two tanks, data on armor size and scale effect is available for each type. Data on wave period for several slopes are available on Kimmswick limestone and tribars. Data from Occoquan granite tested by CERC are used to extend the wave period data.

The damage curve, photographs, notes, and time-lapse movies of each model test were examined to determine:

zero-damage wave height, H_{ZD} , (highest wave that did not remove a significant number of armor units) and

limited damage wave height, H_{LD} , (highest wave that did not remove a significant amount of underlayer material).

Limited damage wave heights were not used to correlate the data because the determination of these wave heights is quite subjective; however, the significance of limited damage stability is discussed in Paragraph 12.

Table 9, Appendix D, gives the model test conditions and results. The table lists the depth of water, the wave period and the zero-damage wave height, and describes the armor layer in terms of armor thickness, gradation, porosity and median weight. Table 10, Appendix E, gives the test results in the dimensionless terms of Equation (5.1) and is the source of data plotted in the figures in this section. Both tables are arranged by slopes and type of armor.

2. Effect of Underlayers on Zero-damage Stability

Underlayer design was not systematically investigated. Underlayer gradation was always in accordance with standard filter criteria for relative stone size in armor and underlayer (EM-1110-345-282, U.S. Army Corps of Engineers, 1955). The underlayer material was never drawn through the armor material by wave action, but was eroded only after substantial armor erosion had occurred and the underlayer was exposed to direct wave action.

Underlayer thickness was varied in one group of tests as shown in Table 4. The variation in stability is less than 8 percent which is less than the usual data scatter of about 15 percent. It is concluded that the variation in underlayer thickness occurring in the tests in this investigation did not affect stability.

TABLE 4

Effect of Underlayer Thickness

Test	Layer Thickness (inches)		Median Stone Size (inches)		Stability N_{ZD}
	Armor	Spalls	Armor	Spalls	
<u>Dumped Kimmswick Limestone, cot $\alpha = 2$</u>					
M-1.6A	4.0	1.5	2.0	0.4	2.16
M-1.6B	4.0	3.0	2.0	0.4	2.16
M-1.6C	4.0	4.5	2.0	0.4	2.29

In some flat slope tests (1 on 7 and 1 on 10) in the small tank, waves higher than the zero-damage wave tended to move the armor stone upslope and downslope in phase with the wave with no net displacement. This movement, although not destructive to the armor layer, tended to mix the armor and underlayer materials, and ultimately the underlayer material that mixed into the armor layer was washed away.

The underlayer characteristics should have an influence on stability since some wave energy is dissipated in the underlayers. However, within the variations in underlayer thickness and stone size in this investigation, the effects can be neglected and Equation (5.1) becomes

$$N_{ZD} = f [d/(w/\gamma)^{1/3}, (W_{85}/W_{15})^{1/3}, R_N, gT^2/(W/\gamma)^{1/3}, \text{armor unit shape and placement, cot } \alpha, c/(W/\gamma)^{1/3}\gamma] \quad (5.2)$$

3. Effect of Water Depth on Zero-damage Stability

There was very little variation in the depth parameter, $d/(W/\gamma)^{1/3}$, in this study; therefore, the effects of water depth on zero-damage stability were not determined. Because water depths in the wave tanks were sufficient to prevent the waves from breaking due to depth limitations, and all wave heights were converted to deepwater wave heights of equivalent energy, water depth is not considered an important variable in the results of these model tests. Equation (5.2) then becomes

$$N_{ZD} = f [(W_{85}/W_{15})^{1/3}, R_N, gT^2/(W/\gamma)^{1/3}, \text{armor unit shape and placement, cot } \alpha, c/(W/\gamma)^{1/3}\gamma] \quad (5.3)$$

4. Effect of Armor Gradation Uniformity on Zero-damage Stability

Armor gradation uniformity is represented quantitatively by the cube root of the ratio of the 85 percent weight and 15 percent weight of the gradation, $(W_{85}/W_{15})^{1/3}$. This computation converts the ratio of "diameter" to make gradation uniformity dimensionally similar to the conventional "uniformity coefficients".

Three gradations of Kimmswick limestone were tested:

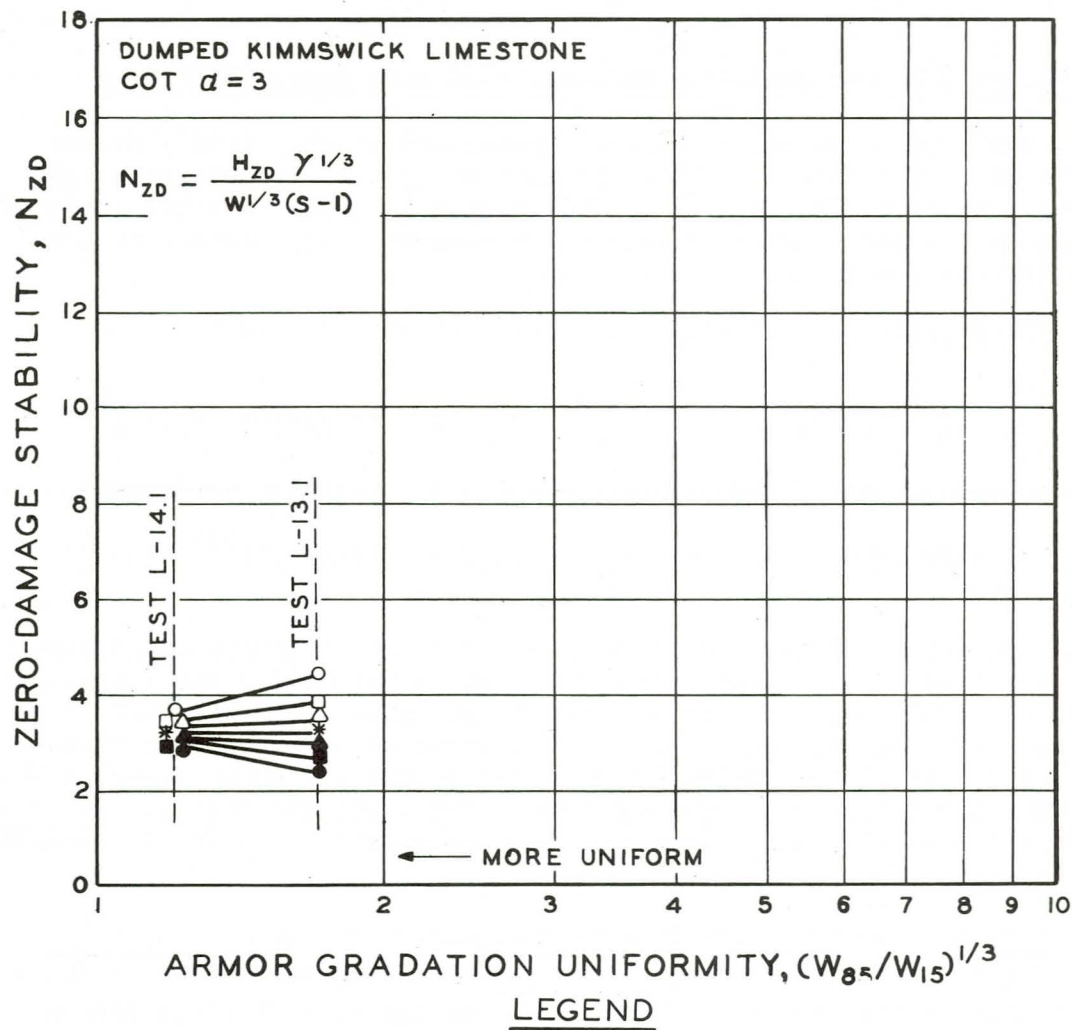
Narrow gradation	$1.0 < (W_{85}/W_{15})^{1/3} < 1.3$
EM gradation (EM-1110-2-2300)	$1.3 < (W_{85}/W_{15})^{1/3} < 2.5$
Wide gradation ("quarry run")	$2.5 < (W_{85}/W_{15})^{1/3} < 9.0$

Armor gradations of tests M-19, M-15 and M-17 are examples of narrow, EM, and wide gradations, respectively. Gradation curves for these tests are shown on Figure 41, Appendix B. Narrow gradations have been used to upgrade existing riprap or where a thin layer of armor is most economical because of excessive hauling costs. Wide gradations have been used when abundant quantities of unprocessed stone are available nearby. EM gradations are used most often in design and are specified in EM 1110-2-2300 (U. S. Army Corps of Engineers, 1959).

Although the armor consists of a gradation of stone sizes $(W_{85}/W_{15})^{1/3} > 1$, it is convenient in making computations to assign a single representative size. Usually the median size (W_{50}) is chosen by investigators as the representative size.

If a representative size can be assigned such that the stability of the graded armor is the same as that of a single-sized armor of the representative size, that size is regarded as the best representation of the gradation for stability studies. To determine the best representative size, the zero-damage stability number, N_{ZD} , was computed for each of a series of tests of various gradation uniformities using W_{10} , W_{25} , W_{40} , W_{50} , W_{60} , W_{75} , and W_{90} as trial representative sizes. W is the armor size in pounds; the subscript indicates the percent of the gradation by weight that is smaller than W . The best representative size is the size level (W_{10} , W_{25} , etc.) that provides zero-damage stability numbers that are most nearly independent of gradation uniformity.

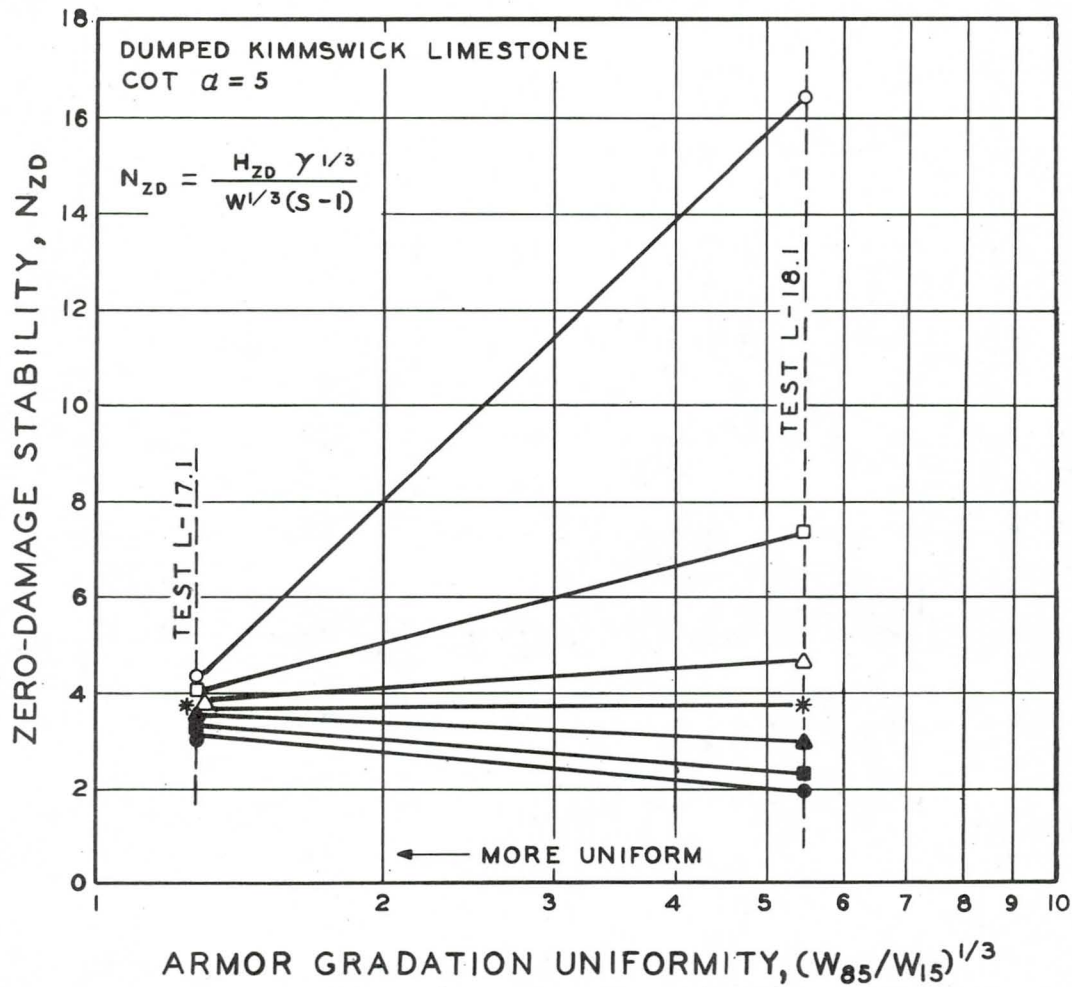
Zero-damage stability, computed using the various size levels, is plotted as a function of gradation uniformity for both small and large scale tests at embankment slopes of 1 on 3 and 1 on 5 on Figures 14 through 17. Gradation curves for these tests are shown in Figures 41 and 44 in Appendix B. Figures 14 through 17 indicate that the zero-damage stability number is independent of gradation uniformity when the median weight (W_{50}) of the gradation is used in the computation of the



LEGEND

<u>SYMBOL</u>	<u>REPRESENTATIVE SIZE USED TO COMPUTE N_{ZD}</u>
○	W_{10}
□	W_{25}
△	W_{40}
*	W_{50}
▲	W_{60}
■	W_{75}
●	W_{90}

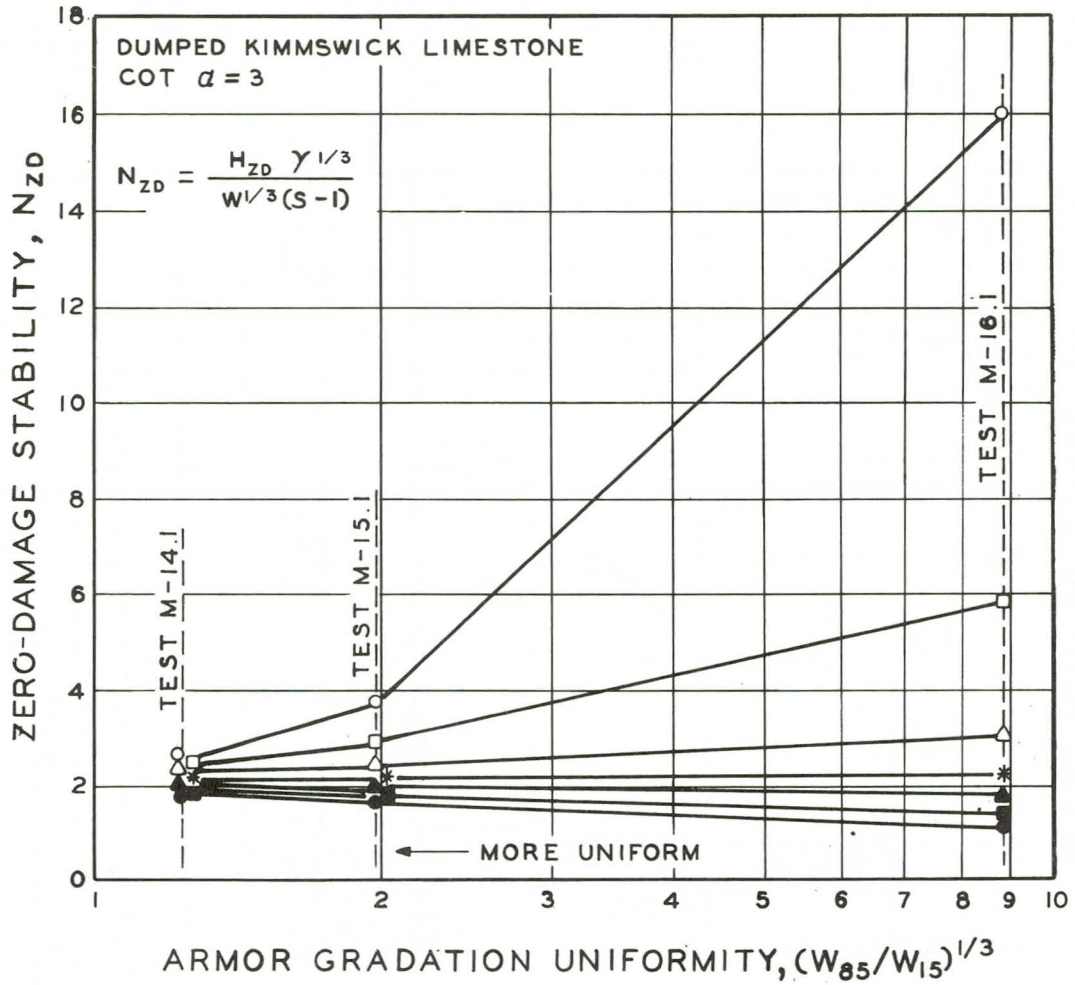
Figure 14. Determination of Best Representative Size of Graded Armor on a 1 on 3 Embankment Slope with Large-Scale Models



LEGEND

<u>SYMBOL</u>	<u>REPRESENTATIVE SIZE USED TO COMPUTE N_{ZD}</u>
○	W_{10}
□	W_{25}
△	W_{40}
*	W_{50}
▲	W_{60}
■	W_{75}
●	W_{90}

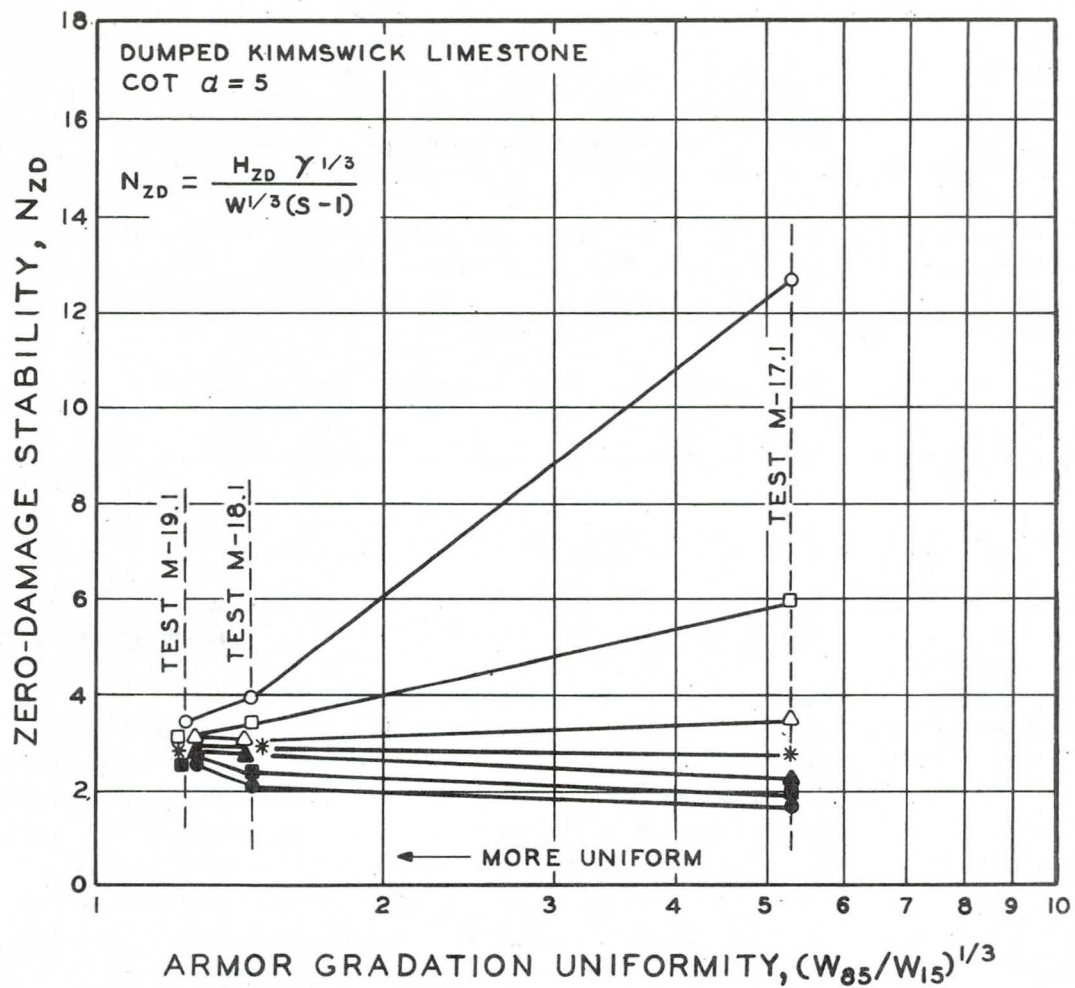
Figure 16. Determination of Best Representative Size of Graded Armor on a 1 on 5 Embankment Slope with Large-Scale Models



LEGEND

<u>SYMBOL</u>	<u>REPRESENTATIVE SIZE USED TO COMPUTE N_{ZD}</u>
○	W_{10}
□	W_{25}
△	W_{40}
*	W_{50}
▲	W_{60}
■	W_{75}
●	W_{90}

Figure 15. Determination of Best Representative Size of Graded Armor on a 1 on 3 Embankment Slope with Small-Scale Models



LEGEND

<u>SYMBOL</u>	<u>REPRESENTATIVE SIZE USED TO COMPUTE N_{ZD}</u>
○	W_{10}
□	W_{25}
△	W_{40}
*	W_{50}
▲	W_{60}
■	W_{75}
●	W_{90}

Figure 17. Determination of Best Representative Size of Graded Armor on a 1 on 5 Embankment Slope with Small-Scale Models

stability number. It is concluded, therefore, that the median size (W_{50}) satisfactorily represents riprap gradation. Beaudevin (1955) states a similar finding, "A mixture of stones of various sizes possesses a characteristic weight equal to or in excess of the average weight of the stones".

The median weight was used as the representative size of the gradations. Because the zero-damage stability number (N_{ZD}) is independent of gradation uniformity when the median weight is used to represent the size of graded armor, Equation (5.3), becomes

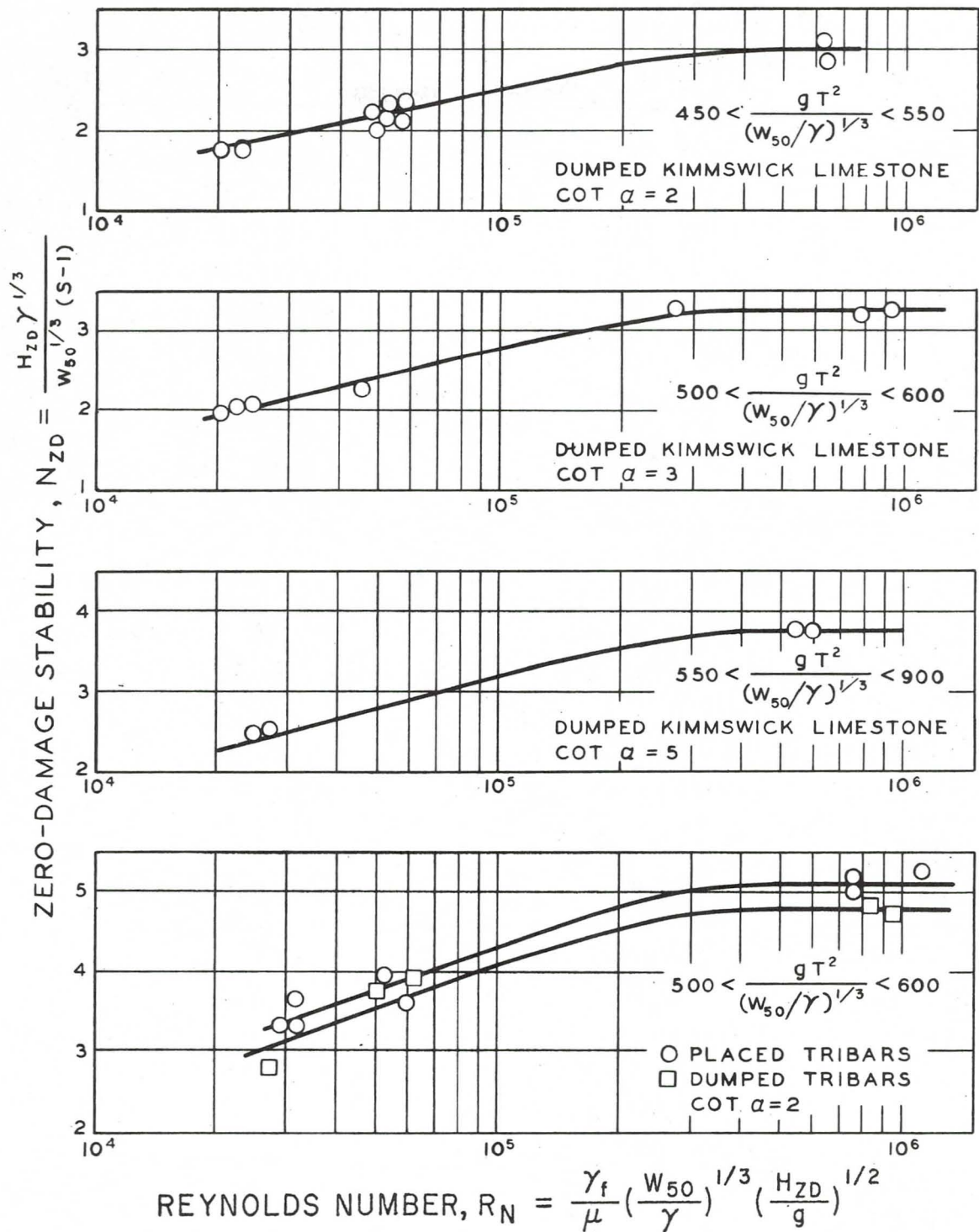
$$N_{ZD} = f [R_n, gT^2/(W_{50}/\gamma)^{1/3}, \text{armor shape and placement,} \\ \cot \alpha, c/(W_{50}/\gamma)^{1/3}\gamma] \quad (5.4)$$

5. Effect of Viscosity on Zero-damage Stability (Scale Effect)

The effect of viscosity was investigated by analyzing data from both small and large scale tests on similar models. Reynolds number is plotted against zero-damage stability number in Figure 18 for a variety of armor types and slopes. In order to avoid scatter because of possible wave period effects, the plots on Figure 18 are grouped within limited ranges of the wave period parameter $gT^2/(W_{50}/\gamma)^{1/3}$. All the plots show similar results. Armor stability, expressed by N_{ZD} , is lower for the small scale tests with low Reynolds numbers than for the large scale tests with high Reynolds numbers. For R_n less than 10^5 , N_{ZD} clearly increases with R_n . For R_n greater than 3×10^5 , N_{ZD} approaches a constant value that is independent of R_n . The constant value for the large scale tests is designated N_{ZD}^1 . Since the test waves in the large tank ranged up to 6.5 feet in height, N_{ZD}^1 is assumed to be the stability number for prototype scale conditions.

Each N_{ZD} value on Figure 18 was divided into its corresponding N_{ZD}^1 value to obtain $F_R = N_{ZD}^1/N_{ZD}$. F_R is plotted against R_n in Figure 19. Although the plotted points represent three types of armor on three different slopes, they seem to define a single function for F_R and R_n . Figure 19 indicates that the zero damage stability numbers obtained for the small scale models in this investigation must be increased 20 to 70 percent, depending on the model Reynolds number, in order to approach the zero damage stability numbers obtained from the large scale tests in which $R_n > 2 \times 10^5$.

Since the fluid properties, μ and γ_f , are the same for all models and prototypes where water is the fluid, variation in values of R_n depend solely on geometric scale (discounting temperature variations). F_R , therefore can be looked upon as a correction factor for scale effect. The zero damage stability number N_{ZD} for each model test was adjusted to the equivalent large scale value N_{ZD}^1 by multiplying by F_R obtained from Figure 19.



Since the effect of viscosity is accounted for by F_R , Equation (5.4) may be expressed,

$$\begin{aligned}
 N'_{ZD} &= F_R N_{ZD} = \frac{F_R H_{ZD}}{(W_{50}/\gamma)^{1/3}} (S-1) \\
 &= f, [gT^2/(W_{50}/\gamma)^{1/3}, \text{Armor slope and placement,} \\
 &\quad \cot \alpha, C/(W_{50}/\gamma)^{1/3}\gamma]
 \end{aligned}
 \tag{5.5}$$

$$F_R = f_2(R_n) \text{ from Figure 19}$$

6. Effect of Wave Period on Zero-damage Stability

The standard wave periods of the models were:

- 3.7 seconds in the large tank,
- 1.5 seconds in the medium tank, and
- 1.2 seconds in the small tank.

Deepwater wave steepness, H/L , developed in the tanks by waves of these periods are similar to the wave steepness observed in reservoirs during storms. Some tribar models and some dumped Kimmswick limestone models were tested over a wide range of wave periods to provide data for the determination of the effect of wave period on zero-damage stability.

The results of the tests shown in Figures 20 and 21 indicate that zero-damage stability is a function of wave period as represented by the wave parameter. The wave parameter $gT^2/(W_{50}/\gamma)^{1/3}$ as developed in Section II is the ratio of wave length to armor size since T^2 in the numerator is directly proportional to wave length and the denominator may be considered a linear measure of armor size. This parameter permits comparison of data from all tanks. The zero-damage stability number has been corrected for scale effect so that the values plotted represent large-scale zero-damage stability ($N'_{ZD} = F_R N_{ZD}$).

The test results plotted in figures 20 and 21 indicate that zero-damage stability is a function of wave period. Stability numbers $N'_{ZD} = F_R N_{ZD}$ are plotted against the dimensionless wave period parameter $gT^2/(W_{50}/\gamma)^{1/3}$. It is significant that in the dimensionless representation the points for both large scale and corrected small scale tests seem to follow the same function. Data for the graph where $\cot \alpha = 2 \frac{1}{2}$ in Figure 20 were provided by the CERC tests of large-scale models of constant stone weight.

The effect of wave period on embankment slopes of 1 on 7 and 1 on 10 for small model tests is shown in Figure 23. Since there were no large scale tests on these slopes to provide scale correction data, the zero-damage stabilities have not been corrected for scale effect; however,

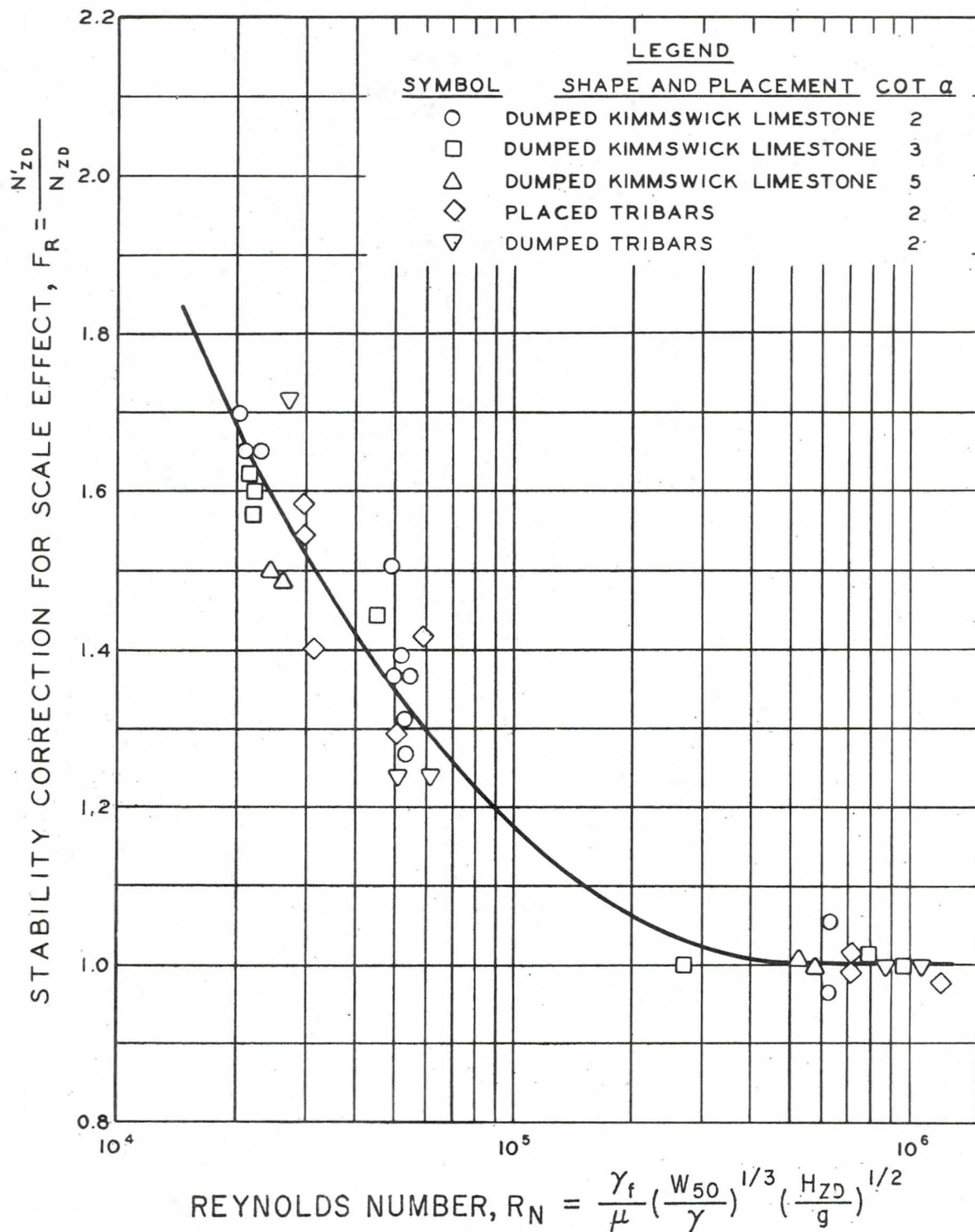
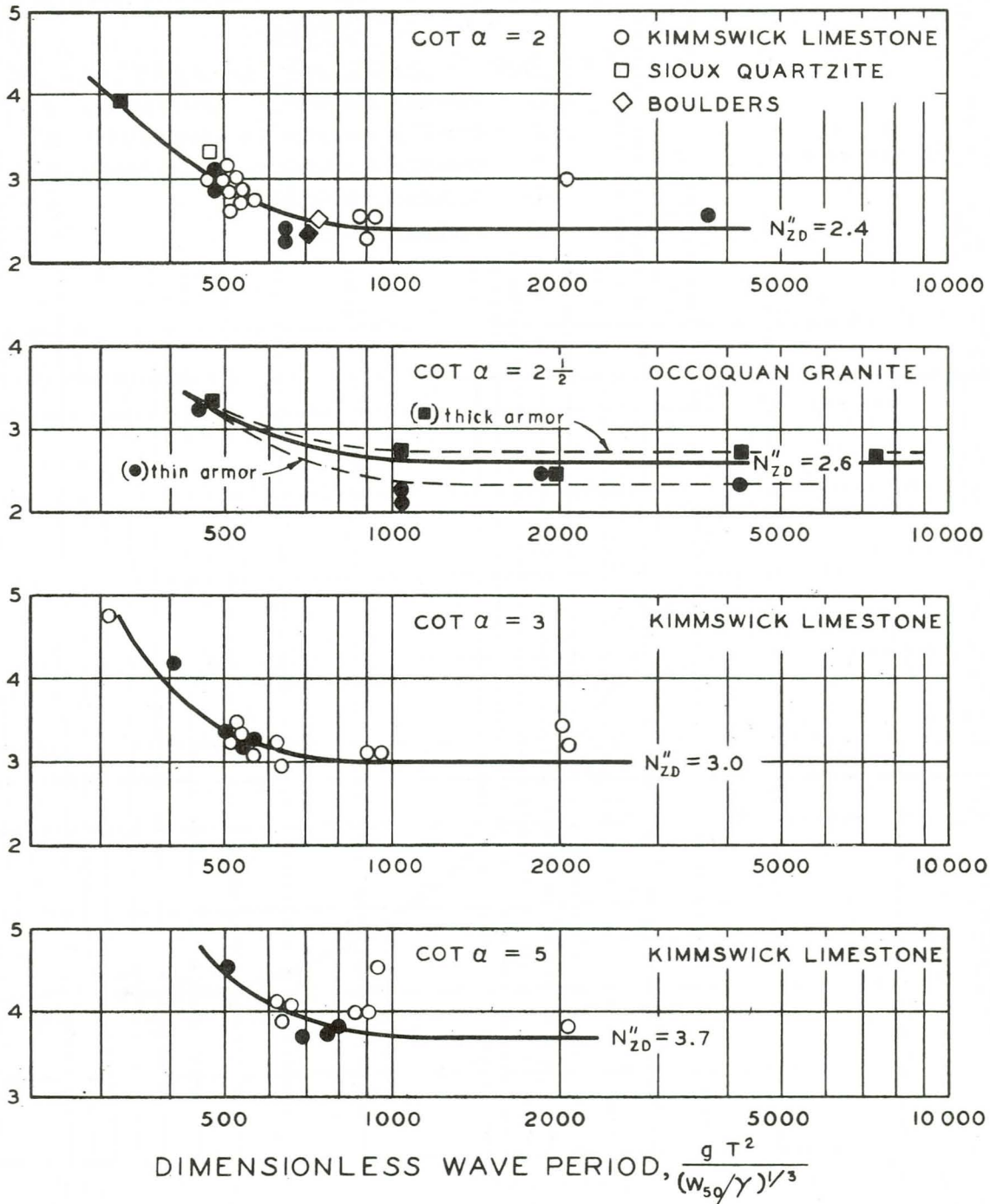


Figure 19. Stability Correction for Scale Effect as a Function of Reynolds Number

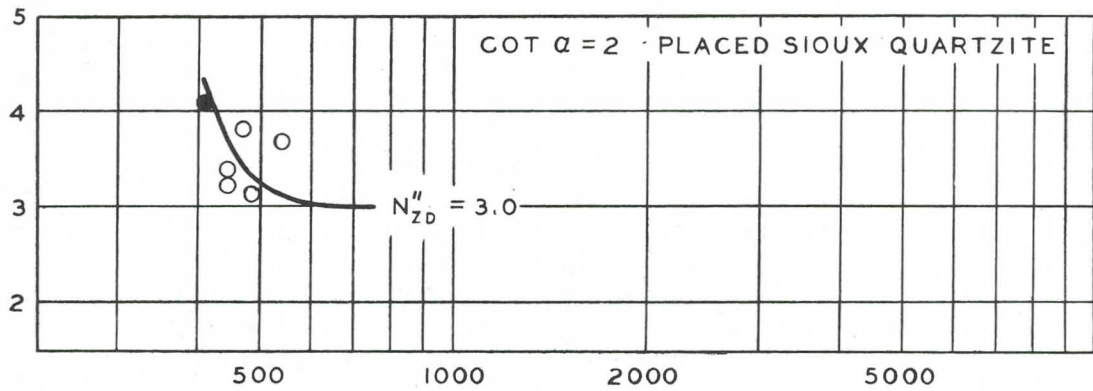
ZERO-DAMAGE STABILITY CORRECTED FOR SCALE EFFECT, $N'_{ZD} = F_R N_{ZD}$



Note: Solid symbols represent large-scale tests ($R_N > 2 \times 10^5$).
 Open symbols represent small-scale tests corrected for scale effect.

Figure 20. Effect of Wave Period on Zero-Damage Stability of Dumped Stone

ZERO-DAMAGE STABILITY CORRECTED FOR SCALE EFFECT, $N'_{ZD} = F_R N_{ZD}$



Note: Solid symbols represent large-scale tests ($R_N > 2 \times 10^5$)
 Open symbols represent small-scale tests corrected for scale effect.

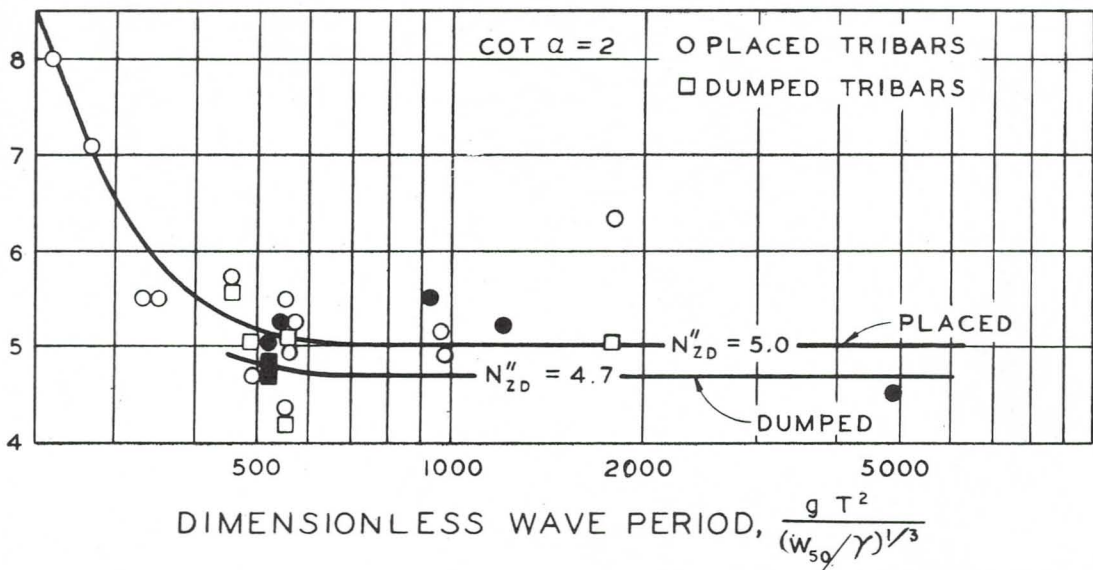


Figure 21. Effect of Wave Period on Zero-Damage Stability of Tribars and Placed Stone

these data indicate that wave period has a significant effect on the zero-damage stability of dumped stone on these flat embankment slopes.

Figure 22 is a consolidation of the curves in Figure 20 illustrating the consistency of the wave-period effect on the zero-damage stability of dumped stone on embankment slopes of 1 on 2, 1 on 2 1/2, 1 on 3, and 1 on 5. Dashed lines in Figure 22 are lines of constant deepwater wave steepness when $\gamma = 165$ lbs/cu ft. Stability is a function of wave period. For long period waves of steepness less than 0.03, armor stability approached a constant minimum value. For wave steepness greater than 0.03, however, stability increased as wave period decreased.

The function for the effects of wave period is implicit in the curves in Figures 20, 21 and 22. No attempt will be made to define the functions in mathematical terms. Each curve defines a minimum stability number N_{ZD}^u for long wave periods ($gT^2/(W_{50}/\gamma)^{1/3} > 800$ or $H_{ZD}/L < 0.03$). The values of N_{ZD}^u for various armor types and slopes are given in Table 5.

TABLE 5
Minimum Stability at Long Wave Periods
($H_{ZD}/L < 0.03$)

Armor	Placement	Embankment Slope	N_{ZD}^u
Tribars	Placed	1 on 2	5.0
Tribars	Dumped	1 on 2	4.7
Sioux quartzite	Placed	1 on 2	3.0
Sioux quartzite	Dumped	1 on 2	2.4
Boulders	Dumped	1 on 2	2.4
Kimmswick limestone	Dumped	1 on 2	2.4
Occoquan granite	Dumped	1 on 2 1/2	2.6
Kimmswick limestone	Dumped	1 on 3	3.0
Kimmswick limestone	Dumped	1 on 5	3.7

ZERO-DAMAGE STABILITY CORRECTED FOR SCALE EFFECT, $N'_{ZD} = F_R N_{ZD}$

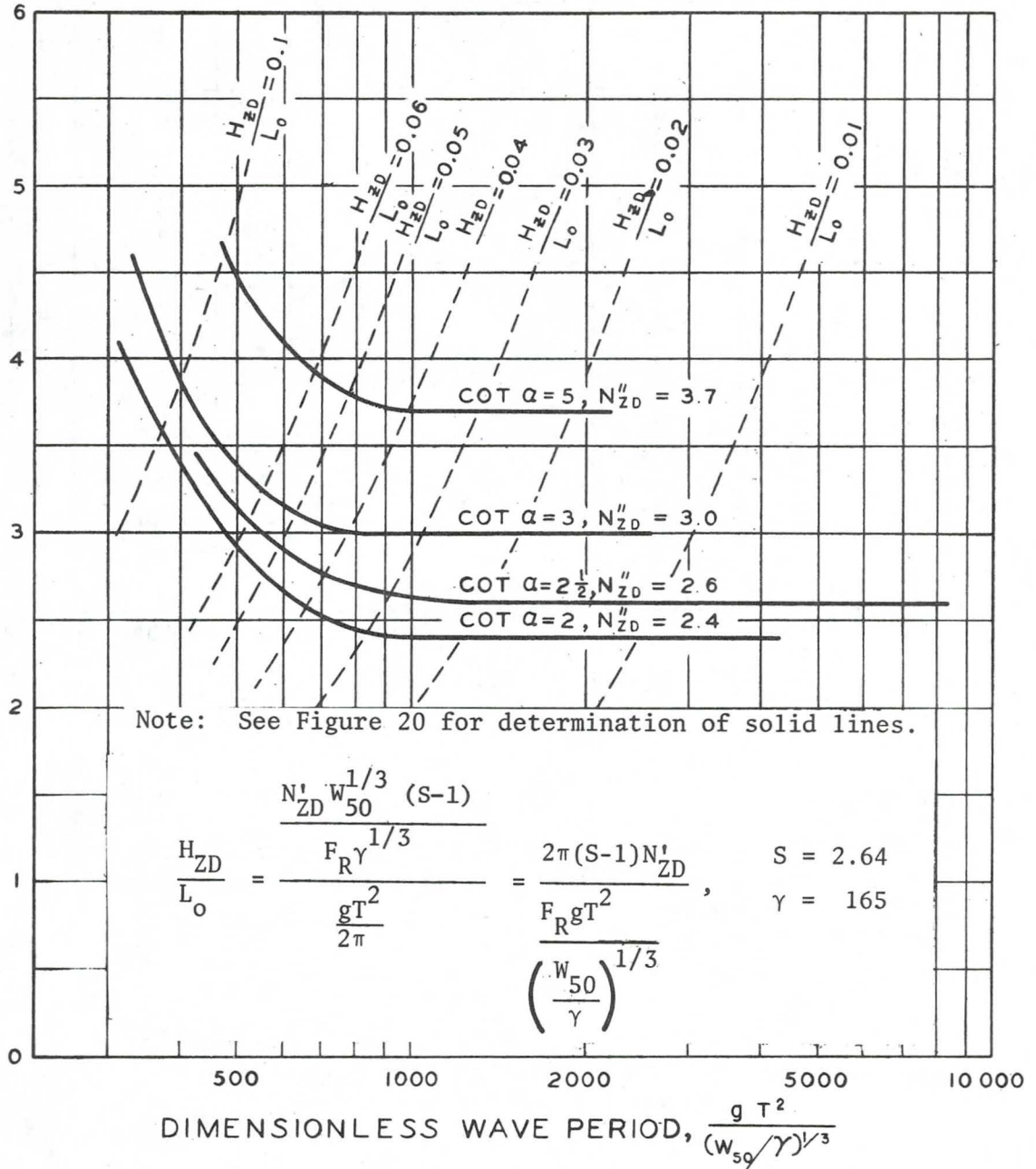
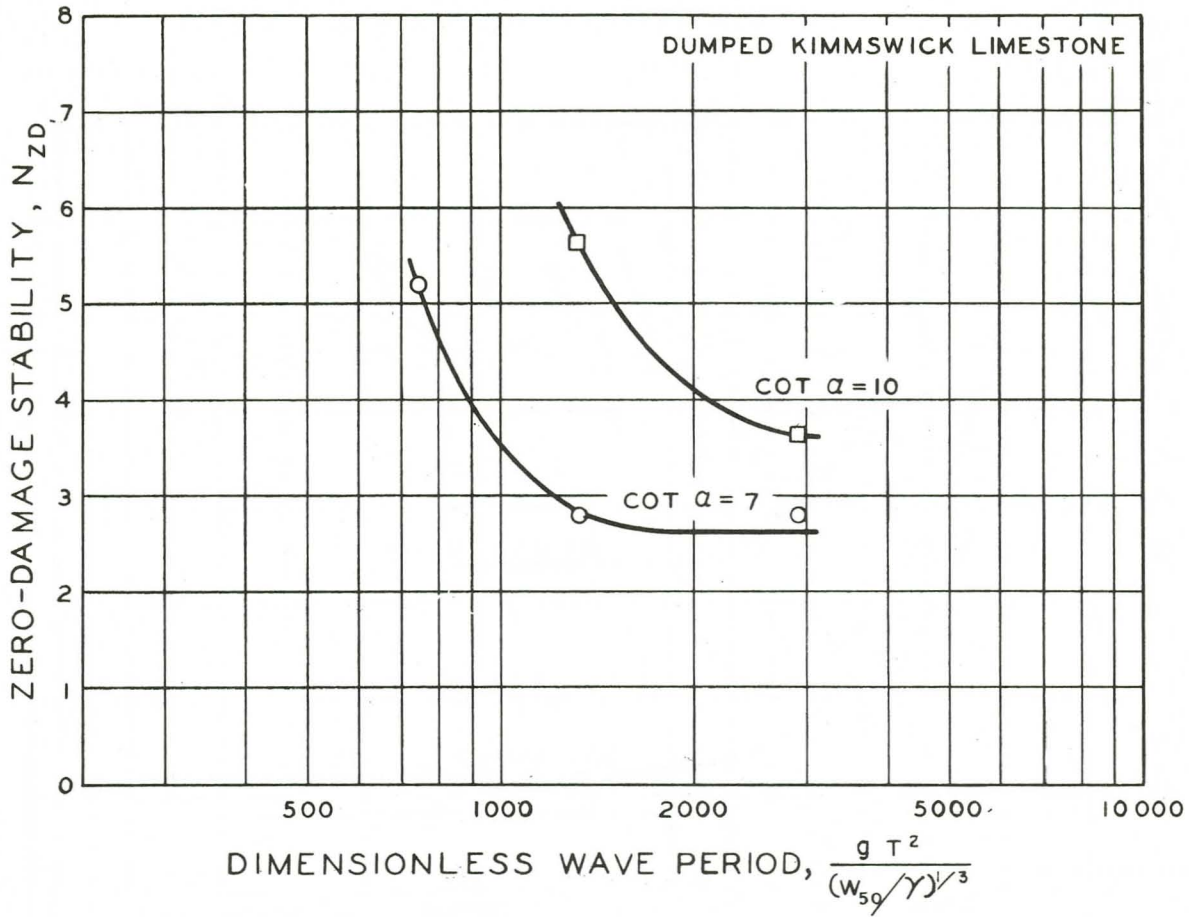


Figure 22. Effect of Wave Period on Zero-Damage Stability of Dumped Stone with Respect to Deepwater Wave Steepness



Note: These data are the results of small-scale model tests ($R_N = 1.5$ to 2.0×10^5) and are not corrected for scale effect

Figure 23. Effect of Wave Period on Zero-Damage Stability of Dumped Stone on Flat Embankment Slopes

7. Effect of Armor Shape and Placement on Zero-damage Stability

Zero-damage stability numbers in Table 5 indicate that placed armor is more stable than dumped armor. Placement procedures other than those used in these tests could result in greater stability if the individual stones are carefully wedged and chinked to provide a paved revetment.

A variation of stone shape was tested only for dumped placement on a 1 on 2 slope. There were two tests each on boulders and Sioux quartzite which are compared with a greater number of tests on Kimmswick limestone. On the basis of these tests, all three stone shapes (Kimmswick limestone, Sioux quartzite and boulders) tested on an embankment slope of 1 on 2 have equal stability (top graph of Figure 20); therefore, the results of stone model tests will no longer be referred to separately by material but by the broader categories of either dumped stone or placed stone. There is a significant difference in the shape of the tribars and the stone, and the tribars are definitely more stable than the stone on an embankment slope of 1 on 2.

Since meaningful quantitative expressions for armor shape and placement have not been developed, the effects of these variables cannot be contained in Equation 5.6 in explicit terms; instead, the zero-damage stability number remains a function of armor shape and placement that is implicit in the curves in Figures 20, 21 and 22 and in Table 5.

8. Effect of Embankment Slope on Zero-Damage Stability

Dumped stone tests on slopes of 1 on 2, 1 on 2 1/2, 1 on 3, and 1 on 5 provide the data for the determination of the effect of embankment slope on zero-damage stability. Values of N_{ZD} from Table 5 for dumped stone at long wave periods are plotted against $\cot \alpha$ in Figure 24 which shows how stability increases as the embankment slope is flattened.

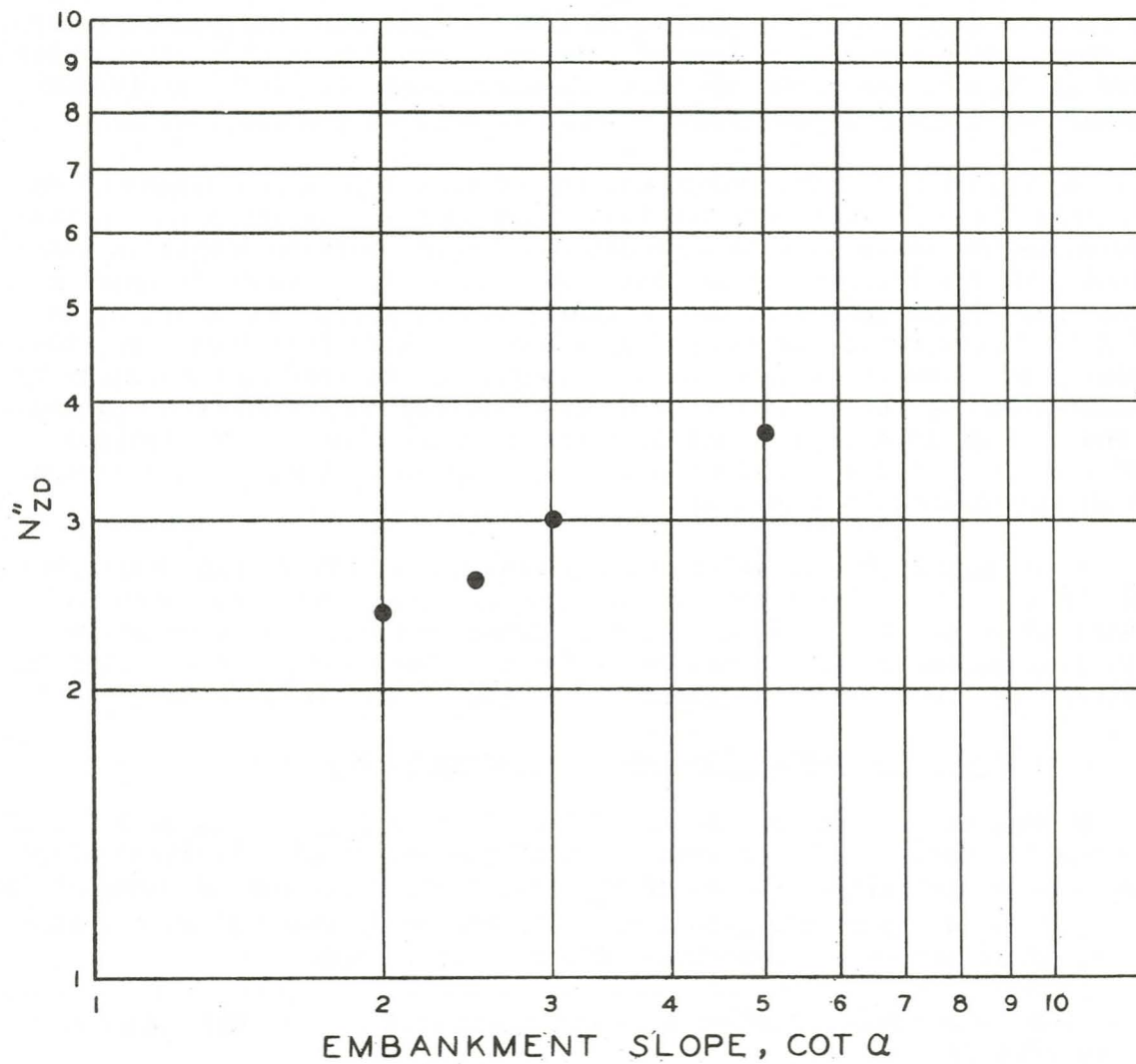
Some investigators offer explicit relationships for the embankment slope effect:

$$N_{ZD} = \frac{2.38 \cos \alpha - \sin \alpha}{(\text{constant})} \quad (\text{Irribarren, 1965})$$

$$N_{ZD} = \cot^{1/3} \alpha (\text{constant}) \quad (\text{Hudson, 1958})$$

$$N_{ZD} = (\text{constant}) \cos \alpha \text{ for } \cot \alpha \leq 2.6 \quad (\text{Svee, 1962})$$

$$N_{ZD} = \frac{1.11 \cos \alpha - \sin \alpha}{(\text{constant})} \text{ for } \cot \alpha \leq 2.6 \quad (\text{Hedar, 1960})$$



Note: N'' is the minimum zero-damage stability with respect to wave period of large model tests and small model tests corrected for scale effect. See Figure 19.

Figure 24. Effect of Embankment Slope on Zero-Damage Stability of Dumped Stone

The "constant" indicated in each of the above formulas does not have the same numerical value for all formulas, and in addition varies for such effects as type of armor. Svec and Hedar propose that the slope function is discontinuous near $\cot \alpha = 2.6$ where the stability ceases to be a function of the downrush of the wave and becomes a function of the uprush of the wave for flatter slopes. These two investigators provide more complex relationships between stability and slope for embankment slopes flatter than 1 on 2.6. Because the data collected by each of the investigators fit his own equation but not necessarily all of the other equations, it is apparent that differences in test and analysis procedures including unavoidable subjectivity in analysis have influenced the forms of these equations. In this investigation, no attempt is made to establish another explicit relationship from the data on Figure 24 nor to extrapolate to steeper or flatter slopes. Instead, the zero-damage stability number remains a function of embankment slope that is also implicit in the curves in Figure 22 or in Figure 24.

9. Effect of Armor Thickness on Zero-Damage Stability

Armor thickness is represented by dimensionless coverage, $c/(W_{50}/\gamma)^{1/3}\gamma$, in which

c = pounds of armor per square foot of embankment surface.

W_{50} = median weight of armor gradation in pounds.

γ = unit weight of armor material in pounds per cubic foot.

Dimensionless coverage is directly proportional to thickness for a given size stone if porosity does not vary ($c = \gamma Th(1-n)$). The thickness of the armor for dumped stone varied from about 1.4 to 2.9 times the D_{50} size. For this variation no effect was apparent, hence coverage is eliminated from Equations (5.5).

$$\begin{aligned} N'_{ZD} &= F_R N_{ZD} = \frac{F_R H_{ZD}}{(W_{50}/\gamma)^{1/3}(S-1)} \\ &= f_1 [gT^2/(W_{50}/\gamma)^{1/3}, \text{ armor slope and placement,} \\ &\quad \cot \alpha] \text{ from Figures 20, 21, and 22} \end{aligned} \tag{5.6}$$

$$F_R = f_2 [R_n] \text{ from Figure 19}$$

$$1.4 < Th/D_{50} < 2.9$$

10. Stability Equations

Solving Equation (5.6) for W_{50} gives the stable armor unit size for zero damage stability against wave action on an embankment slope:

$$W_{50} = \frac{H_{ZD}^3 \gamma}{(N'_{ZD}/F_R)^3 (S-1)^3} \quad (5.7)$$

N'_{ZD} and F_R are evaluated as in Equations (5.6). Equation (5.7) is a general relationship for any combination of wave period and geometric scale.

For values of $gT^2/(W_{50}/\gamma)^{1/3}$ greater than about 800, or for waves steeper than about 0.03, N'_{ZD} approaches a limiting minimum value that is independent of wave period. N''_{ZD} is a function only of armor shape and placement and embankment slope. Values of N''_{ZD} evaluated in this investigation are listed in Table 6. For prototype scale, the Reynolds number is high and $F_R = 1.0$. Substituting N''_{ZD} for N'_{ZD} and $F_R = 1.0$ in Equation (5.7) gives:

$$W_{50} = \frac{H_{ZD}^3 \gamma}{(N''_{ZD})^3 (S-1)^3} \quad (5.8)$$

Equation (5.8) with N''_{ZD} values from Table 6 could be adapted for prototype design. It yields values of W_{50} that are conservatively high because N''_{ZD} is a minimum limiting value with respect to wave period. Graphs of Equation (5.8) for each combination of armor and embankment slope in Table 6 are shown in Figure 25.

11. Data Scatter

In order to test the consistency of the relationships developed in this investigation, Equation (5.6) and Figures 19, 20, 21 and 22 were used to hind cast the zero damage wave height for each model test. The hind cast wave heights are plotted against the observed zero damage wave heights in Figure 26. 90 percent of the points scatter less than 15 percent from the line of perfect agreement between observed and hind cast values.

12. Reserve Stability

Each model had some stability beyond zero-damage, i.e., waves slightly larger than zero-damage height did not destroy the model. Therefore, a reserve of stability is available beyond zero-stability which varies with armor layer thickness, armor shape, armor placement and slope. A measure of reserve stability is the ratio of the limited-damage wave height and the zero-damage wave height. Limited-damage wave height, H_{LD} , is the highest wave tested that did not remove under-layer material, and limited

damage is the armor damage the model sustained from the attack of the limited-damage wave. Average limited-damage values are:

<u>Shape</u>	<u>Placement</u>	<u>Thickness</u>	<u>Cot α</u>	<u>Average Limited Damage</u>
Tribars	Placed	One layer	2	0.5
Tribars	Dumped	1 1/2 layers	2	1.5
Stone	Placed	One layer	2	1.2
Stone	Dumped	1.5 D ₅₀ to 2 D ₅₀	2	4.6
Stone	Dumped	1.5 D ₅₀ to 2 D ₅₀	3	5.0
Stone	Dumped	1.5 D ₅₀ to 2 D ₅₀	5	10.4

TABLE 6

Summary of Zero-damage Stability Numbers

<u>Shape</u>	<u>Placement</u>	<u>Embankment Slope</u>	<u>N''_{ZD}</u>	<u>(N''_{ZD})³</u>
Tribars	Placed	1 on 2	5.0	125
Tribars	Dumped	1 on 2	4.7	104
Stone	Placed	1 on 2	3.0	27
Stone	Dumped	1 on 2	2.4	14
Stone	Dumped	1 on 2 1/2	2.6	18
Stone	Dumped	1 on 3	3.0	27
Stone	Dumped	1 on 5	3.7	51

Figure 25 shows graphical solutions using these values in equation,

$$W_{50} = \frac{H_{ZD}^3 \gamma}{(N''_{ZD})^3 (S-1)^3}$$

Stability numbers were determined under the following test conditions:

The wave height is the equivalent deepwater wave height of the highest wave in each burst of test waves.

Water depth was sufficient to prevent breaking of waves due to depth limitations.

Placed tribar armor layers consisted of one layer of tribars.

Dumped tribar armor layers contained 1.5 times as many tribars per unit area as the placed tribar layers.

Text resumes on page 56

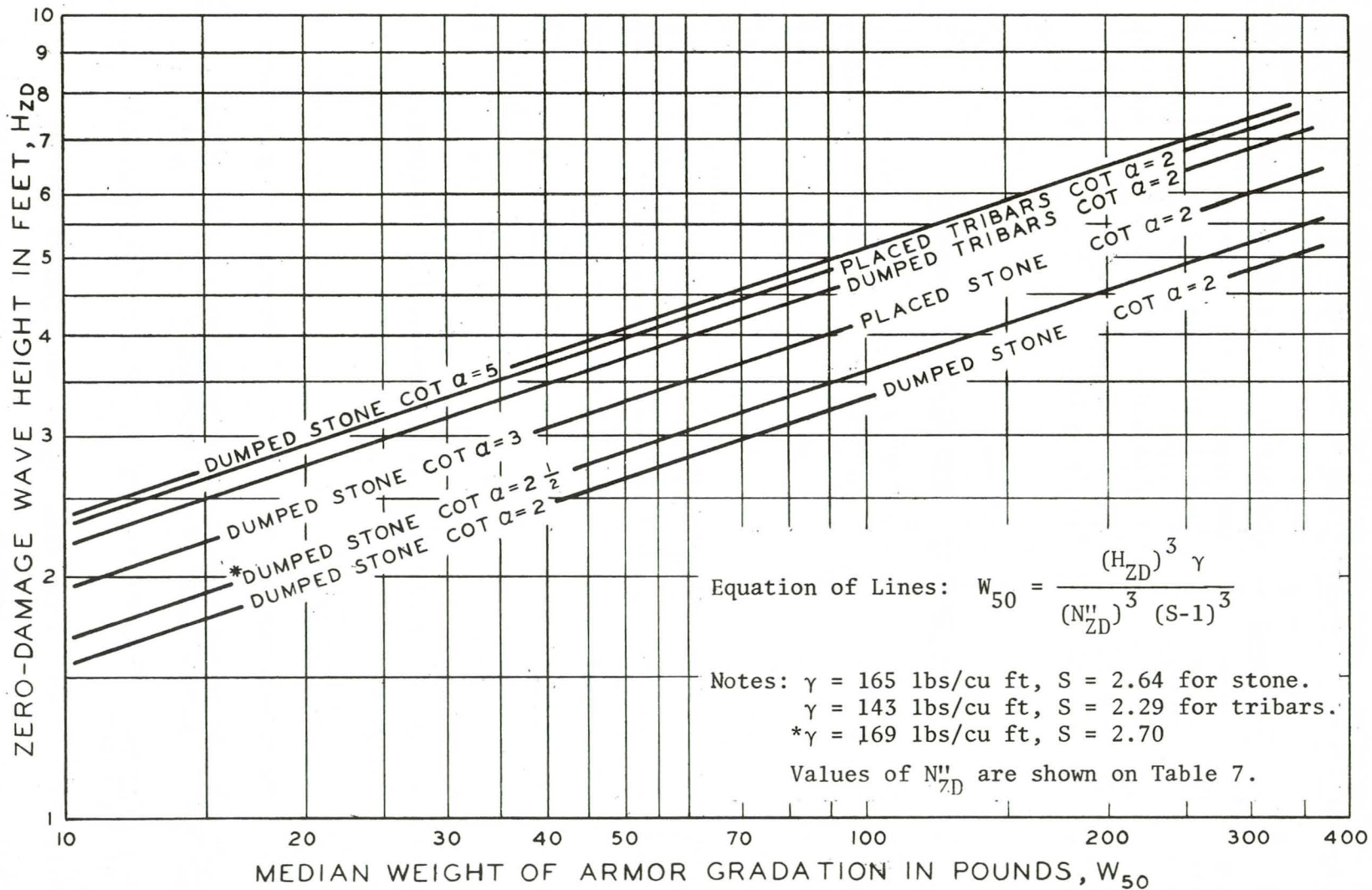
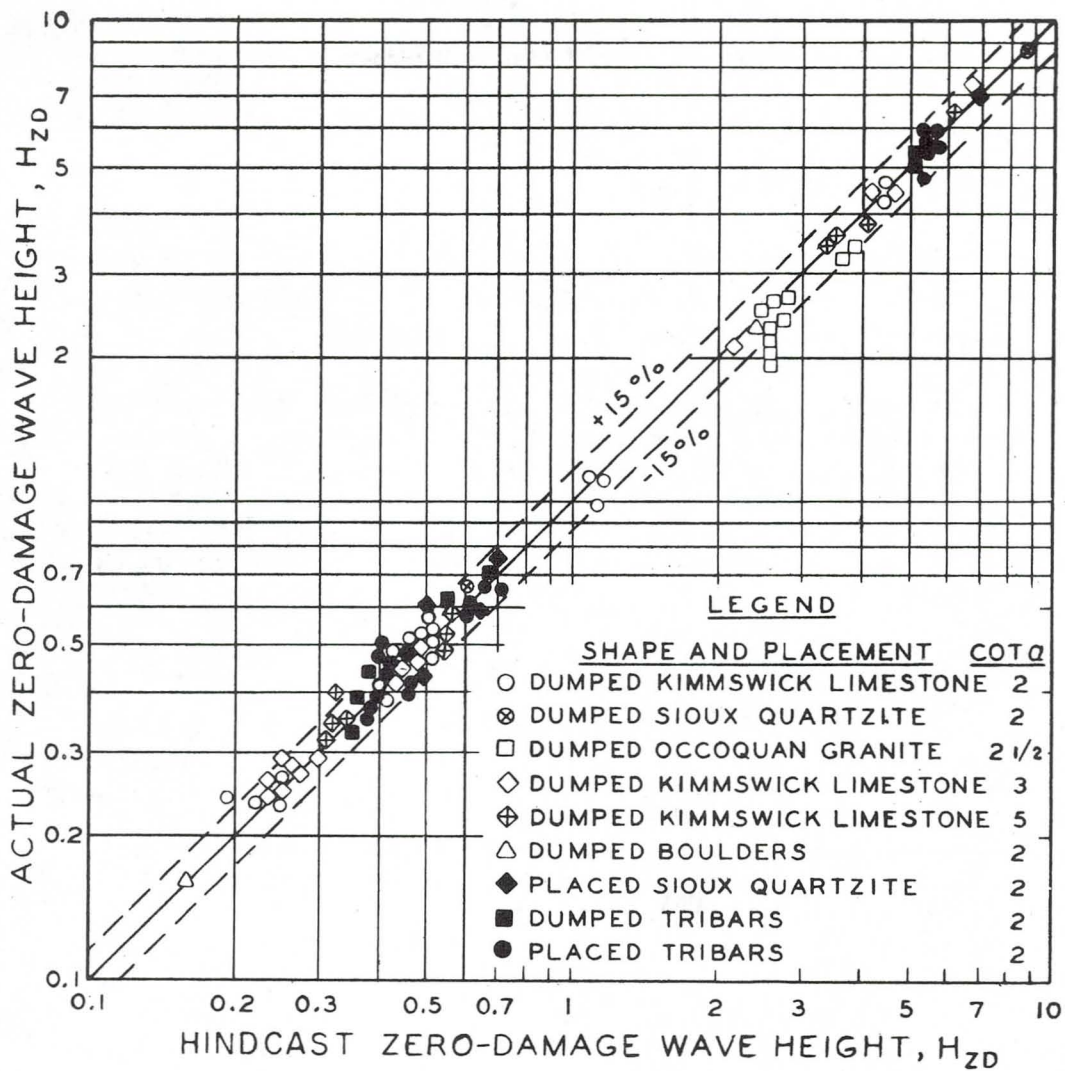


Figure 25. Zero-Damage Stability Curves for Stone and Tribars



NOTE: Figures 20, 21 and 19 were used to hindcast N_{ZD} for each model test. Hindcast zero-damage wave heights, H_{ZD} , were then determined by the equation

$$H_{ZD} = \frac{N_{ZD} W_{50}^{1/3} (S-1)}{\gamma^{1/3}}$$

Figure 26. A Comparison of the Hindcast Zero-Damage Wave Height and the Actual Zero-Damage Wave Height for each Model Test

Placed stone armor layers consisted of one layer of stone and the gradation uniformity, $(W_{85}/W_{15})^{1/3}$, was less than 2.

Dumped stone armor layer thickness varied from 1.4 to 2.9 times the size of the median weight stone and the gradation uniformity, $(W_{85}/W_{15})^{1/3}$, was less than 9.

Larger stability numbers were obtained from models tested at wave periods such that $gT^2/(W_{50}/\gamma)^{1/3} < 1,000$. Smaller stability numbers were obtained from small models ($R_N < 2 \times 10^5$).

The limited-damage wave height of each model test was determined by the intersection of the limited-damage value and the damage curve of the test (paragraph 3c, Section IV, and Figures 45 through 58 in Appendix C). Limited-damage wave height is plotted as a function of zero-damage wave height on Figures 27, 28, and 29. The reserve stability determined by the equation of the line drawn through the data points of each graph is shown in Table 7.

TABLE 7
Reserve Stability of Tribars and Stone

<u>Shape</u>	<u>Placement</u>	<u>Cot α</u>	<u>Reserve Stability*</u>
Tribars	Placed	2	5%
Tribars	Dumped	2	20%
Stone	Placed	2	5%
Stone	Dumped	2	20%
Stone	Dumped	3	30%
Stone	Dumped	5	40%

*Percent increase in wave height from zero to limited damage

Since reserve stability is probably dependent upon armor thickness, the values in this table are realistic only when the placed units are one layer thick and the dumped armor layers are from 1.5 D_{50} to 2.0 D_{50} thick. The models were in equilibrium at both zero-damage and limited-damage conditions. Figures 30 through 35 show photos of stages of damages near zero-damage and limited-damage conditions in six of the large-scale models. No alarming displacement of armor is evident, even at the limited damage stage.

13. Comparison of Results with Those of Other Investigators

Many other investigators have studied the stability of riprap with model tests. Dumped stone, zero-damage model test results of some of these investigators are shown on Figure 36 along with the results of this study. Some of the investigators noticed that stability was a function of wave period. In these cases, only the minimum stability with respect to wave period is shown. Numbers beside the symbols on the figure designate the Reynolds number times 10^{-4} of the models that determined the position of the symbol. Enlarged, solid symbols designate large-scale tests ($R_N > 2 \times 10^5$).

Text resumes on page 67

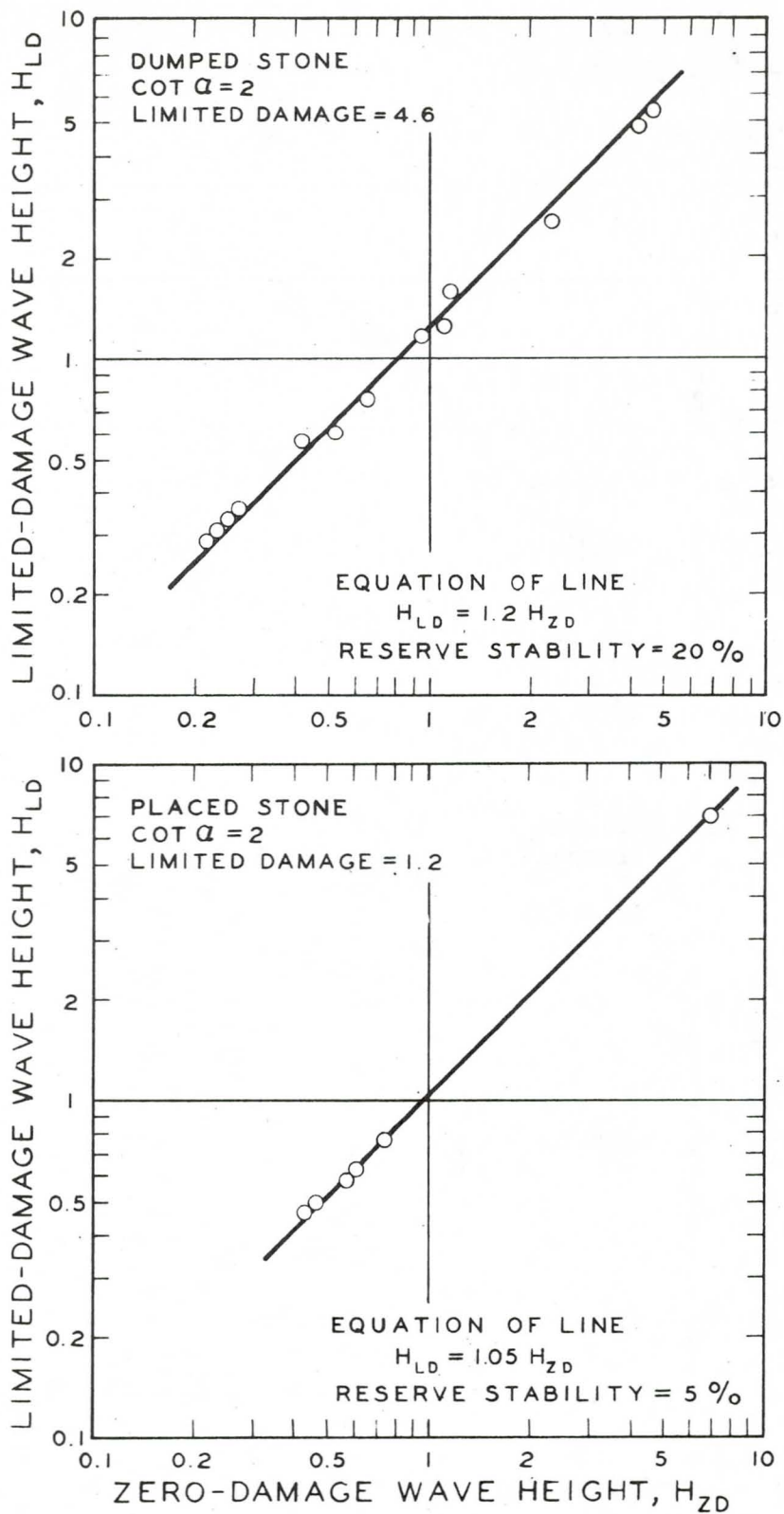


Figure 27. Determination of Reserve Stability of Stone on an Embankment Slope of 1 on 2

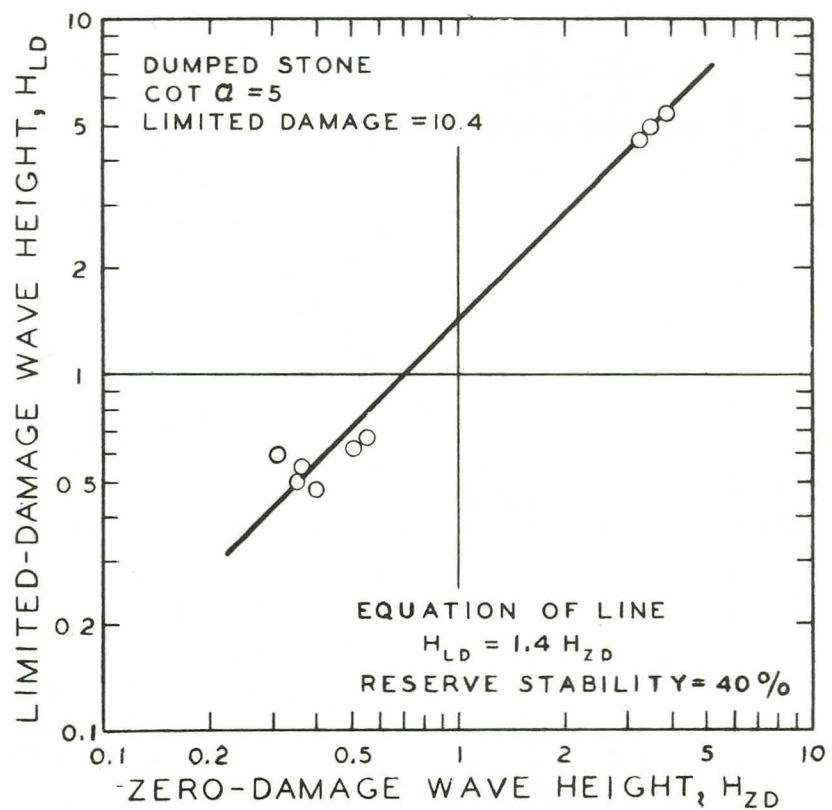
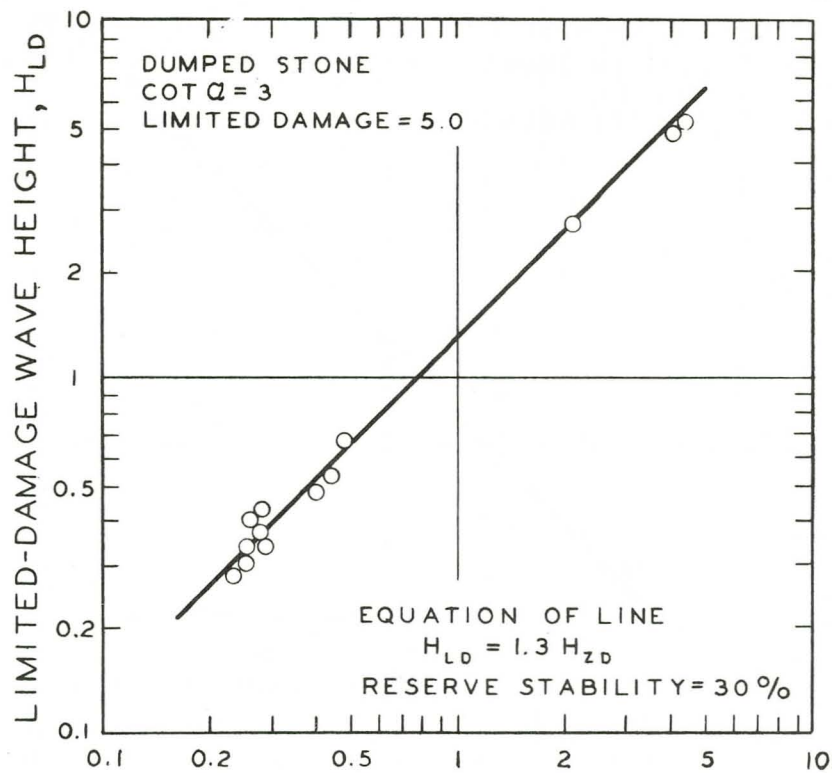


Figure 28. Determination of Reserve Stability of Dumped Stone on Embankment Slopes of 1 on 3 and 1 on 5

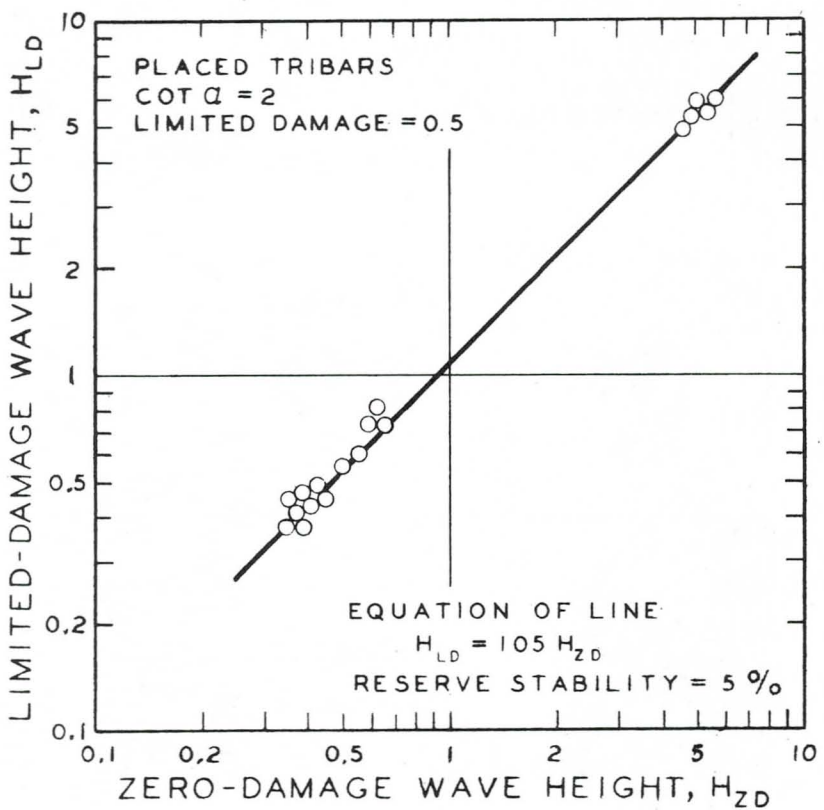
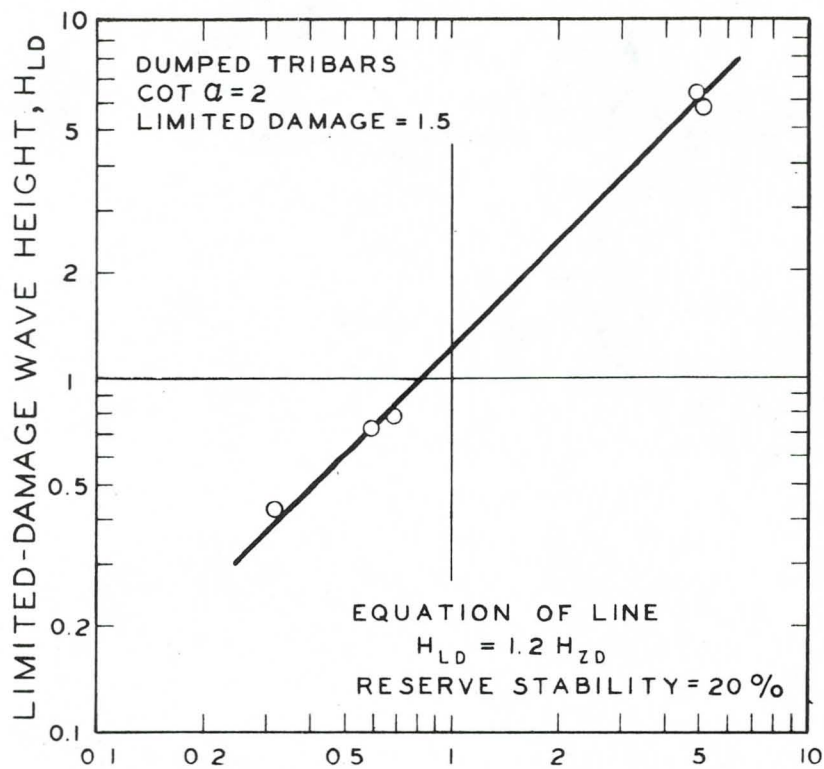


Figure 29. Determination of Reserve Stability of Tribars on an Embankment Slope of 1 on 2.



Damage = 4.0



Damage = 17.2



Damage = 17.2

Figure 30. Photographs Showing Equilibrium Stages of Damage of Test L-1.2 (Dumped Stone, $\cot \alpha = 2$, Limited Damage = 4.6)



Damage = 0.4



Damage = 0.6

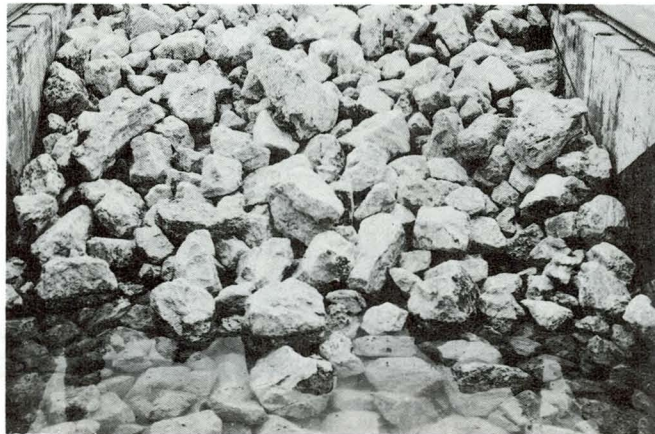


Damage = 3.0

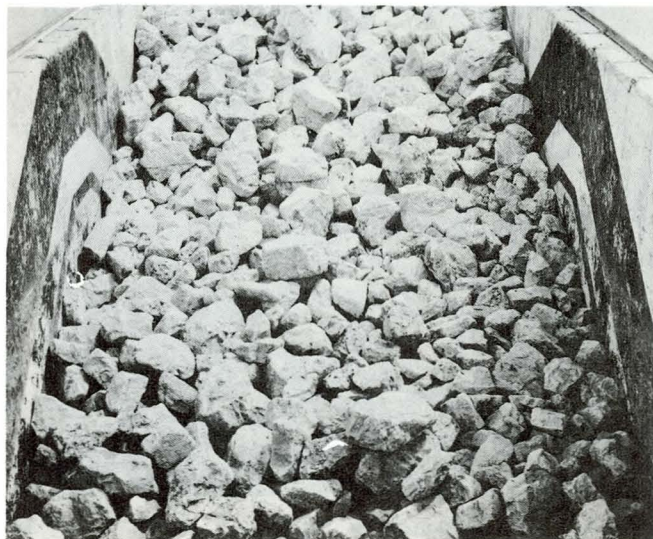
Figure 31. Photographs Showing Equilibrium Stages of Damage of Test L-7.1 (Placed Stone, $\cot \alpha = 2$, Limited Damage = 1.2)



Damage = 1.8

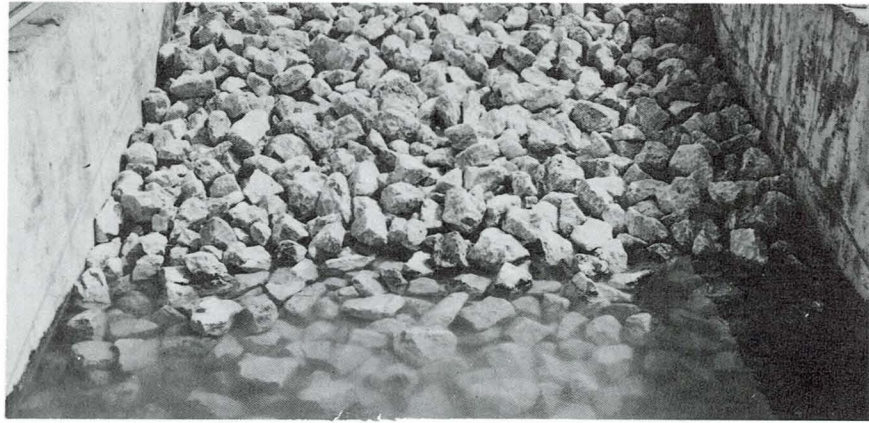


Damage = 5.7



Damage = 5.7

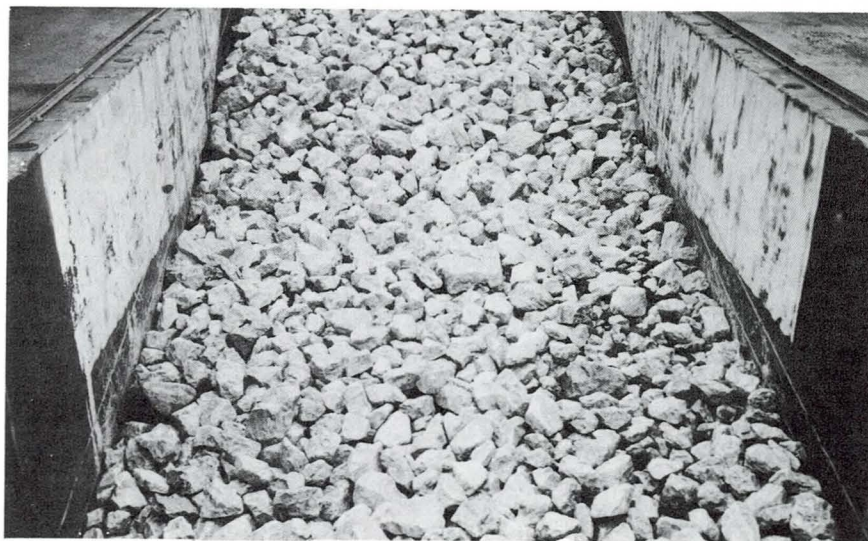
Figure 32. Photographs Showing Equilibrium Stages of Damage of Test L-13.1 (Dumped Stone, $\cot \alpha = 3$, Limited Damage = 5.0)



Damage = 1.1

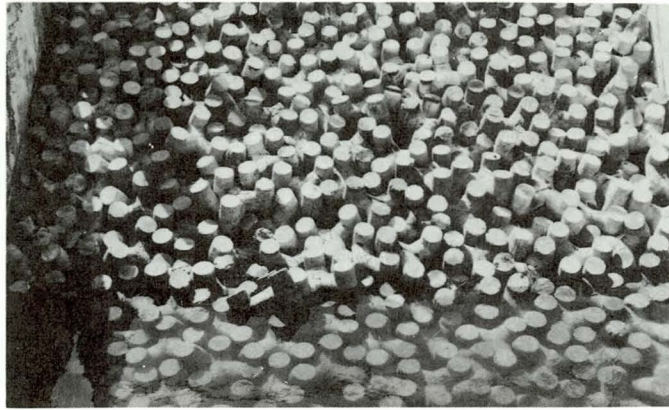


Damage = 6.8

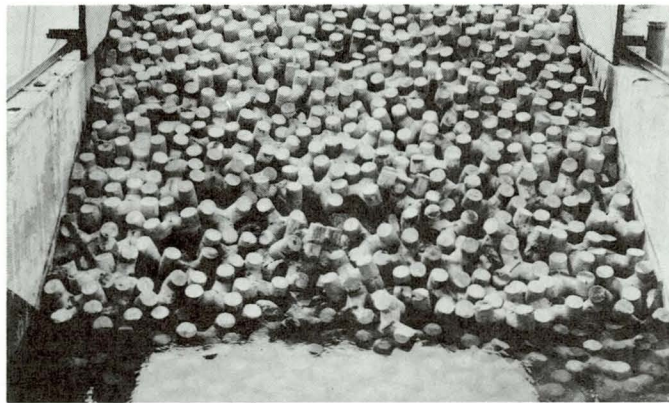


Damage = 12.5

Figure 33. Photographs Showing Equilibrium Stages of Damage of Test L-17.1 (Dumped Stone, $\cot \alpha = 5$, Limited Damage = 10.4)



Damage = 0

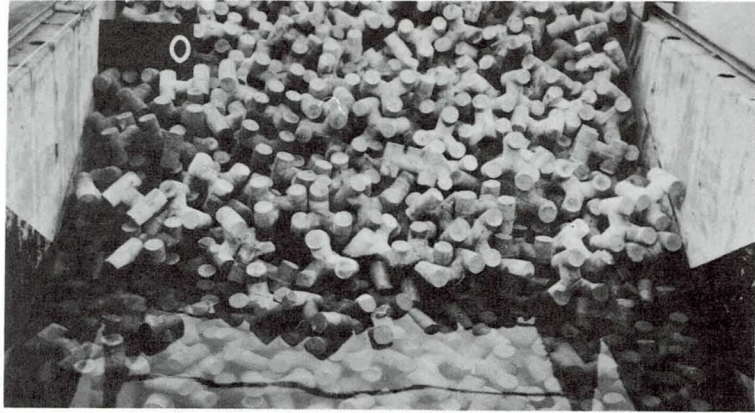


Damage = 0.6

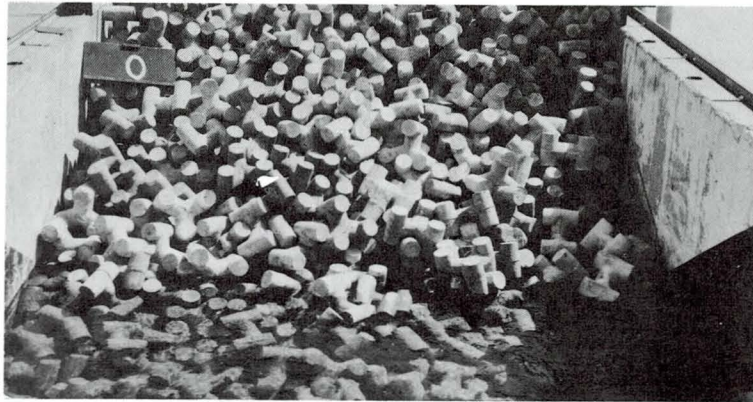


Damage = 1.5

Figure 34. Photographs Showing Equilibrium Stages of Damage of Test L-2.2 (Placed Tribars, $\cot \alpha = 2$, Limited Damage = 0.5)



Damage = 0



Damage = 0.5



Damage = 1.2

Figure 35. Photographs Showing Equilibrium Stages of Damage of Test L-5.1 (Dumped Tribars, $\cot \alpha = 2$, Limited Damage = 1.5)

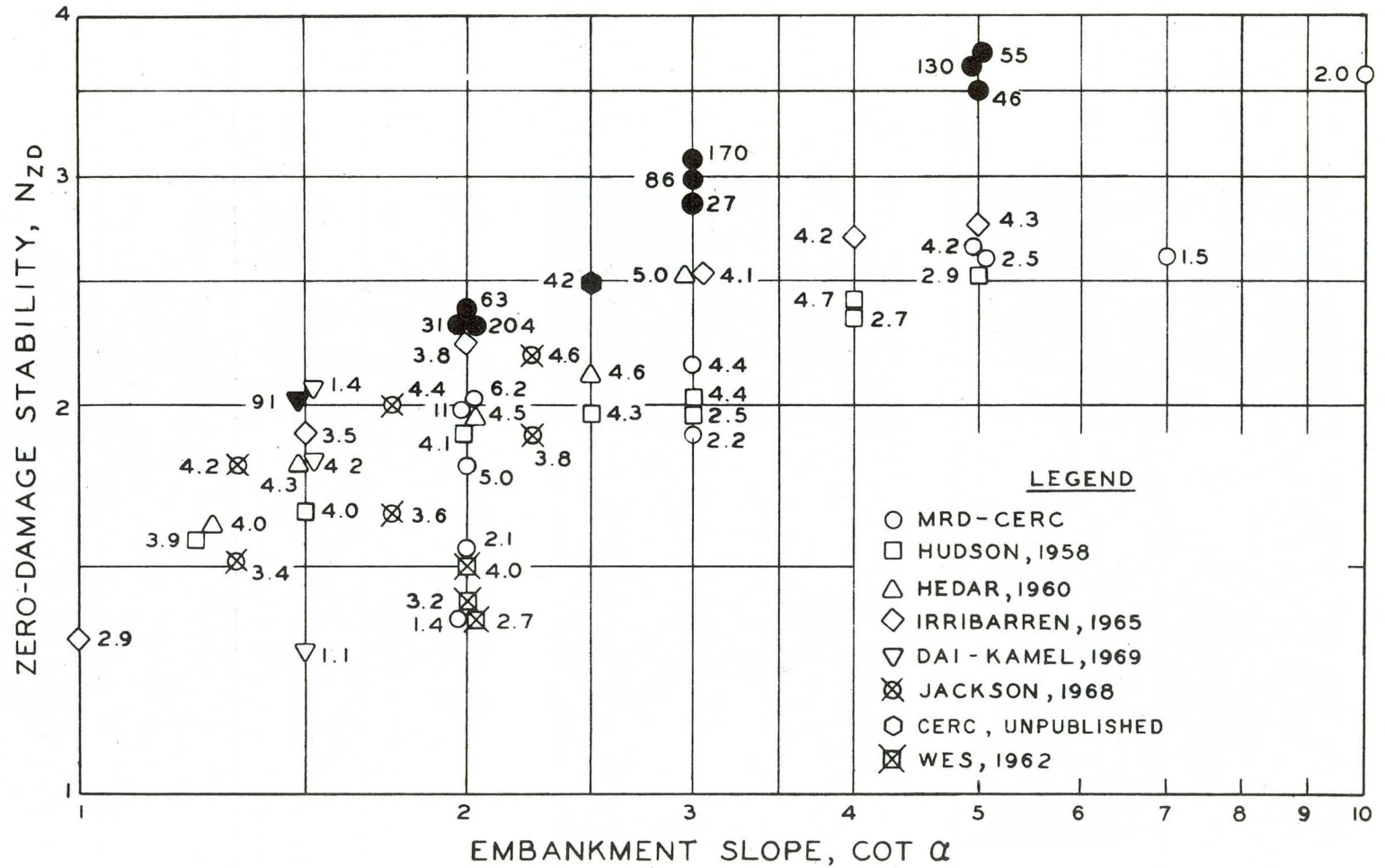


Figure 36. A Comparison of Zero-Damage Model Test Results of Dumped Stone Armor of Various Investigations. Some symbols represent the average of the results of a number of similar tests. Enlarged, solid symbols indicate large-scale tests ($R_N > 2 \times 10^5$). Numbers beside symbols indicate the approximate Reynolds number of the test or tests times 10^{-4} .

The numbers beside the symbol for each embankment slope indicate that the stability increases with model size or Reynolds number up to a certain point (about $R_N \times 10^{-4} < 10$). Considerable differences in the results of a number of independent investigations can be expected because the results of each investigation are to some degree a function of test equipment, model construction, test procedures, and the unavoidable subjectivity of the investigator in the data analysis. However, Figure 36 shows that the results of these independent investigations are similar when compared by the Reynolds numbers of the models tested, and are consistent with this investigation.

Section VI. SUMMARY AND CONCLUSIONS

Ninety models were tested in wave tanks to determine the effectiveness of several riprap designs in protecting embankment slopes from wave action in inland reservoirs. CERC's 635-foot, 85-foot, and 72-foot wave tanks were used.

Prototype riprap construction was simulated in the models as closely as possible. Each model consisted of an impervious core and layers of bedding, spalls and armor. Upgrading of undersized riprap by overlaying with armor of greater stability was represented in some models. Embankment slopes varied from 1 on 2 to 1 on 5 except for several at slopes of 1 on 7 and 1 on 10. Armor consisted of quarried stone, glacial boulders and tribars. The stone and boulders were typical of material used on prototype structures in the Missouri River Division. Several gradations of stone sizes were tested. Armor was dumped from a skip to form a layer 1.4 to 2.9 armor units thick or was placed by individual units in a single layer.

For model slopes of 1 on 3 or steeper waves were generated in bursts of 10 to 15 to avoid reflection effects in the wave tanks. The highest wave in the burst was chosen to represent the burst. Wave heights were increased progressively without rebuilding the model until extensive damage occurred. Riprap stability is based on the wave height at "zero-damage." All wave heights measured in the tanks were converted to equivalent deepwater values. Numerical and graphical methods of determining the zero-damage wave height from surveys of the slope were developed.

Relationships that define the effects of deepwater wave height, wave period, embankment slope and Reynolds number on size of stable armor units were experimentally determined. Model results are expressed by the stability equation,

$$W_{50} = \frac{H_{ZD}^3 \gamma}{\left(\frac{N'_{ZD}}{F_R}\right)^3 (S-1)^3} \quad (5.7)$$

$$N'_{ZD} = f_1 [gT^2/(W_{50}/\gamma)]^{1/3}, \text{ armor shape and placement} \\ \text{cot } \alpha] \text{ from Figures 20, 21, and 22}$$

$$F_R = f_2 [R_n] \text{ from Figure 19}$$

$$1.4 < \frac{Th}{D_{50}} < 2.9$$

For prototype embankment slopes R_n is high and $F_R = 1.0$. When $gT^2/(W_{50}/\gamma)^{1/3} > 800$, or $H_{ZD}/L < 0.03$, N'_{ZD} approaches a minimum limiting value, N''_{ZD} , which is independent of wave period and a function of armor slope and placement and embankment slope. Values of N''_{ZD} obtained from these tests are listed in Table 6. Substituting $F_R = 1.0$ and $N'_{ZD} = N''_{ZD}$ in Equation (5.7) gives,

$$W_{50} = \frac{H_{ZD}^3 \gamma}{(N''_{ZD})^3 (S-1)^3} \quad (5.8)$$

which gives conservative values for prototype design purposes since N''_{ZD} is a minimum limiting value with respect to wave period.

Each model was capable of resisting waves higher than the zero-damage wave height without serious damage. The difference between the zero-damage wave height and the highest wave that did not remove under-layer material is the reserve stability. Average values of reserve stability are listed in Table 7.

Additional conclusions are:

1. Underlayers graded according to the filter criteria in EM 1110-345-282, U.S. Army Corps of Engineers 1950, provided adequate protection against migration of underlayers or core material through the armor during wave action.

2. The median weight, W_{50} , of the armor layer gradation is a satisfactory "effective size" to represent the armor material.

3. Small-scale models with Reynolds number $< 2 \times 10^5$ are less stable than the larger-scale models. These differences are a function of Reynolds number and apparently are caused by viscous effects. Consequently, there is a "scale effect" that produces conservative results when stability determined in a small model is scaled up to prototype size on the basis of stability number alone. A correction factor for viscous effects was developed as a function of Reynolds number and is presented in Figure 19.

4. Stability is a function of wave period. Stability is greatest at short wave periods and decreases as the wave period increases. For wave periods corresponding to $gT^2/(W_{50}/\gamma)^{1/3} > 800$ or $H_{ZD}/L > 0.03$, the stability number approaches a minimum limiting value and is relatively independent of wave period.

5. No effect of armor unit shape was detected from tests on boulders and two types of quarried stone. Tribars are more stable than stone.

6. Individually placed armor units have more zero-damage stability than dumped armor units.

7. The zero-damage stability for dumped stone is not affected when the armor layer thickness is varied from 1.4 to 2.9 times the median stone size.

8. Stability increases with flatter embankment slopes. Simple mathematical expressions for the effect of slope on stability, suggested by other investigators were not verified.

9. Results of this study are similar to those of other investigators when differences in test conditions and methods of analysis are recognized. Differences in Reynolds number are a significant factor in comparing the results of various studies.

Section VII. RECOMMENDATIONS FOR ADDITIONAL TESTS
OF RIPRAP STABILITY

Conclusions of this study were determined from data provided by 34 large-scale and 56 small-scale model tests on steep embankment slopes (1 on 2, 1 on 2 1/2, 1 on 3 and 1 on 5) and five small-scale model tests on flatter embankment slopes (1 on 7 and 1 on 10). Significant statistical improvement of the steep embankment slope results with additional large-scale model tests is probably too costly to be justified. However, a few additional large-scale models with steep embankment slopes tested with long-period waves would check the results of this study.

A series of large-scale model tests of various armor thicknesses would provide desirable information concerning the most economical design armor thickness. Qualitative observations of these and other models by personnel of this study indicate a considerable savings may be possible in many designs if more information were available on the stability of "thin" armor layers.

All large-scale model tests should be paralleled with geometrically similar small-scale model tests to provide additional information regarding scale effects. Then, many of the "secondary" variables can be investigated systematically and economically with small-scale models.

The stability of dumped stone on slopes flatter than 1 on 5 should be investigated. The following items should be considered:

- underlayer design
- armor gradation uniformity
- model size (scale effect)
- wave period
- armor thickness
- embankment slope
- reserve stability
- equilibrium profile
- damage development

The suggested order of priority of the above recommendations follows:

1. Test a few large-scale models with long-period waves on slopes of 1 on 2 1/2 and 1 on 4.
2. Test various thicknesses of armor on large-scale models with long-period waves.
3. Parallel all large-scale model tests with geometrically similar small-scale tests.
4. Determine the effects of all pertinent variables on the stability of dumped stone on flat embankment slopes.
5. Test the effects of secondary variables with small-scale models.

LITERATURE CITED

- Barbe, R. and Beaudevin C. (1953), "Experimental Research on the Stability of a Rubble-Mound Breakwater Subjected to Wave Action" translated from *La Houille Blanche*, Vol. 8, pp. 346-359, by Jan C. Van Tienhoven, U.S. Army Engineer Waterways Experiment Station, Translation No. 54-11, November 1954.
- Beaudevin, C. (1955), "Stability of Rubble-Mound Breakwaters with a Protective Cover Layer of Loose Cap Rock", translated from *La Houille Blanche*, Vol. 10, No. A/1955, pp. 332-339, by Jan C. Van Tienhoven, U.S. Army Engineer Waterways Experiment Station.
- Dai, Y. B. and Kamel, A. M. (1969), "Scale Effect Tests for Rubble-Mound Breakwaters", U. S. Army Engineer Waterways Experiment Station, Research Report H-69-2.
- Hedar, P. A. (1960), "Stability of Rock Fill Breakwaters", Chalmers Tekniska Hogskola, Doktorsavhandlingar, Akademiforlaget-Gumperts, No. 26, Goteborg.
- Hudson, R. Y. (1958), "Design of Quarry-stone Cover Layers for Rubble-Mound Breakwaters", U. S. Army Engineer Waterways Experiment Station, Research Report 2-2.
- Irribarren, R. (1965), "Formule Pour le Calcul des Dignes en Enrochements Naturels on Elements Artificiels", XXIst International Navigation Congress, Stockholm.
- Jackson, R. A. (1968), "Design of Cover Layers for Rubble-Mound Breakwaters Subjected to Nonbreaking Waves", U. S. Army Engineer Waterways Experiment Station, Research Report No. 2-11.
- Karaki, S. S., Gray, E. E. and Collins, J. (1961), "Dual Channel Stream Monitor", *Proceedings, ASCE*, Paper 2976, November 1961.
- Saville, Thorndike, Jr., McClendon, E. W. and Cochran, A. L. (1962), "Freeboard Allowances for Waves in Inland Reservoirs", *Journal of the Waterways and Harbors Division, Proceedings, ASCE*, Paper 3138, pp. 93-124, May 1962.
- Svee, Roald (1962), "Formulas for Design of Rubble-Mound Breakwaters", *Journal of the Waterways and Harbors Division, Proceedings, ASCE*, Vol. 88, No. WW2, May 1962.
- U. S. Army Corps of Engineers (1959), "Earth Embankments", EM 1110-2-2300, April 1959.
- U. S. Army Corps of Engineers, Office of the Chief of Engineers (1955), "Drainage and Erosion Control, Subsurface Drainage Facilities for Airfields", including: Change 3, 15 June 1959, TM 5-820-2, formerly EM 1110-345-282, June 1955.

- U. S. Army Corps of Engineers, Office of the Chief of Engineers (1958), "Stone Protection (Slopes and Channels)", including Amendment 1, May 1959, CE 1308, July 1958.
- U. S. Army Engineer Waterways Experiment Station (1962), "Design of Riprap Cover Layers for Railroad Relocation Fills, Ice Harbor and John Day Lock and Dam Projects", Miscellaneous Paper No. 2-465, January 1962.
- U. S. Army Engineer Waterways Experiment Station (1960), "Standard Method Test for Specific Gravity, Absorption and Unit Weight of Coarse Aggregate and Riprap", Handbook for Concrete and Cement, CRD-C 107-60.
- U. S. Army Coastal Engineering Research Center (1966), "Shore Protection, Planning and Design", Technical Report No. 4, Third Edition, June 1966.

BIBLIOGRAPHY

- Carvalho, Jose Joaquim Reis de e Vera Cruz, Daniel (1961), "On the Stability of Rubble-Mound Breakwaters", *Proceedings of the Seventh Conference on Coastal Engineering*, The Hague, Netherlands, August 1960.
- Hedar, P. A. (1964), "Filter as Protection Against Erosion", Swedish Geotechnical Institute, Reprints and Preliminary Reports No. 6, Stockholm 1964.
- Holmes, P. D. L. and Park, A. G. (1966), "Hydraulic Model Studies for a Mound Type Breakwater", *The Dock and Harbor Authority*, June 1966.
- Kreeke, Jacobus van de (1969), "Damage Function of Rubble-Mound Breakwaters", *Journal of the Waterways and Harbors Division, ASCE*, Paper 6743, August 1969, and Discussion by P. M. Brun, Juan B. Font, A. M. Kamel, A. Brantzaeg, and L. G. Hulman, *Journal of the Waterways and Harbors Division*, Vol. 96, No. WW2, May 1970.
- Metelitsyna, G. G. (1967), "Determination of the Stone and Concrete Block Weight in Protective Linings of Structures Subject to Wave Action", translated from *Giodrotekhnicheskoe Stroitel'stvo*, No. 5, pp. 38-43, May 1967, for ASCE.
- U. S. Army Engineer Waterways Experiment Station (1961), "Wave Forces on Rubble-Mound Breakwaters and Jetties", Miscellaneous Paper No. 2-453, September 1961.

APPENDIX A

MODEL DESCRIPTIONS

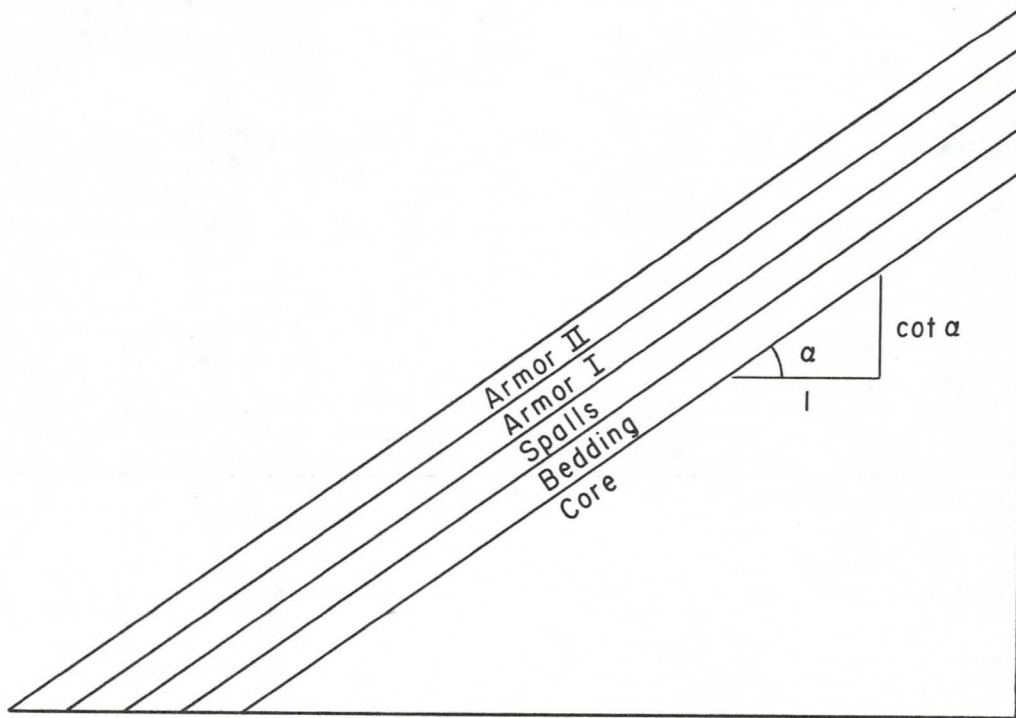


Figure 37. Model Layer Configuration and Nomenclature

Armor II is an overlay of existing armor and was not present in all models. Underlayers are Armor I, Spalls and Bedding if Armor II is present, and Spalls and Bedding if Armor II is not present.

TABLE 8

Model Descriptions

Figure 38 (Appendix B) shows size characteristics of the materials.

<u>Model No.</u>	<u>Layer</u>	<u>Layer Thickness (inches)</u>	<u>Figure Showing Gradation</u>	<u>Material</u>
S-1	Core		38	Sand
	Bedding	1.25		Crushed Stone
	Spalls	1.0		Crushed Stone
	Armor	2.5		Kimmswick Limestone
S-2	Core		38	Sand
	Bedding	.685		Sand
	Spalls	.46		Rounded Gravel
	Armor I	2.0		Rounded Boulders
	Armor II	1 layer		Sioux Quartzite
S-3	Core		38	Sand
	Bedding	.685		Sand
	Spalls	.46		Rounded Gravel
	Armor I	2.0		Rounded Boulders
	Armor II	1 layer		Sioux Quartzite
S-4, S-5 S-6, S-7 S-8, S-9 S-10, S-11	Core		38	Sand
	Bedding	.685		Sand
	Spalls	.46		Rounded Gravel
	Armor I	2.0		Rounded Boulders
	Armor II	1 layer		Tribars (placed)
S-12	Core		38	Tribars
	Bedding	.685		Sand
	Spalls	.46		Rounded Gravel
	Armor	2.0		Rounded Boulders
	Core			39
Bedding	.4	Sand		
Spalls	.5	Crushed Stone		
Armor	1.4	Kimmswick Limestone		
S-15 S-16	Core		39	
	Bedding	.75		Rounded Gravel
	Spalls	1.25		Sioux Quartzite
	Armor	3.0		Tribars

TABLE 8 (Continued)

<u>Model No.</u>	<u>Layer</u>	<u>Layer Thickness (inches)</u>	<u>Figure Showing Gradation</u>	<u>Material</u>
S-17	Core		39	Sand
	Bedding	1.0		Crushed Stone
	Spalls	2.0		Sioux Quartzite
	Armor	1 layer		Tribars (placed)
S-18	Core		40	Sand
	Bedding	.5		Sand
	Armor I	.75		Crushed Stone
	Armor II	1.0		Kimmswick Limestone
S-19	Core		40	Sand
S-20	Bedding	.5		Sand
S-21	Spalls	.75		Crushed Stone
S-22	Armor	1.0		Kimmswick Limestone
S-25	Core		40	Sand
S-26	Bedding	.5		Sand
	Spalls	.75		Crushed Stone
	Armor	1.37		Kimmswick Limestone
M-1A	Core		40	Sand
	Bedding	2.0		Crushed Stone
	Spalls	1.5		Crushed Stone
	Armor	4.0		Kimmswick Limestone
M-1B	Core		40	Sand
M-2A	Bedding	2.0		Crushed Stone
	Spalls	3.0		Crushed Stone
	Armor	4.0		Kimmswick Limestone
M-1C	Core		40	Sand
	Bedding	2.0		Crushed Stone
	Spalls	4.5		Crushed Stone
	Armor	4.0		Kimmswick Limestone
M-2B	Core		40	Sand
	Bedding	2.0		Crushed Stone
	Spalls	3.0		Crushed Stone
	Armor	2.5		Kimmswick Limestone

TABLE 8 (Continued)

<u>Model No.</u>	<u>Layer</u>	<u>Layer Thickness (inches)</u>	<u>Figure Showing Gradation</u>	<u>Material</u>
M-2C	Core		40	Sand
	Bedding	2.0		Crushed Stone
	Spalls	3.0		Crushed Stone
	Armor	5.5		Kimmswick Limestone
M-4	Core		41	Sand
M-5	Bedding	1.0		Sand
	Spalls	.75		Rounded Gravel
	Armor I	2.5		Rounded Boulders
	Armor II	1 layer		Tribars (placed)
M-6	Core		41	Sand
	Bedding	1.0		Sand
	Spalls	.75		Rounded Gravel
	Armor I	2.5		Rounded Boulders
	Armor II	1 layer		Sioux Quartzite
M-7	Core		41	Sand
M-8	Bedding	1.0		Sand
	Spalls	.75		Rounded Gravel
	Armor I	2.5		Rounded Boulders
	Armor II	3.9		Tribars (dumped)
M-9	Core		41	Sand
M-10	Bedding	1.0		Sand
	Spalls	.75		Rounded Gravel
	Armor	2.5		Rounded Boulders
	Overlay	1 layer		Sioux Quartzite (placed)
M-11	Core		41	Sand
	Bedding	1.0		Sand
	Spalls	.75		Rounded Gravel
	Armor	2.5		Rounded Boulders
	Overlay	3.8		Sioux Quartzite
M-13	Core		41	Sand
	Bedding	1.00		Sand
	Spalls	.75		Rounded Gravel
	Armor	2.5		Rounded Boulders
M-14	Core		41	Sand
M-15	Bedding	1.0		Crushed Stone
	Spalls	1.0		Crushed Stone
	Armor	2.5		Kimmswick Limestone

TABLE 8 (Continued)

<u>Model No.</u>	<u>Layer</u>	<u>Layer Thickness (inches)</u>	<u>Figure Showing Gradation</u>	<u>Material</u>
M-16	Core		41	Sand
	Bedding	1.0		Crushed Stone
	Armor	3.5		Kimmswick Limestone
M-18	Core		41	Sand
M-19	Bedding	1.0		Crushed Stone
	Spalls	1.0		Crushed Stone
	Armor	3.0		Kimmswick Limestone
M-20	Core		40	Sand
	Bedding	1.0		Sand
	Spalls	.75		Crushed Stone
	Armor I	1.0		Crushed Stone
	Armor II	1.5		Kimmswick Limestone
M-21	Core		40	Sand
	Bedding	1.00		Sand
	Armor	3.25		Kimmswick Limestone
M-17	Core		41	Sand
	Bedding	1.0		Crushed Stone
	Armor	4.0		Kimmswick Limestone
L-1	Core		42	Bank Run Gravel
	Bedding	6.00		Crushed Stone
	Spalls	9.00		Kimmswick Limestone
	Armor	25.00		Kimmswick Limestone
L-2	Core		43	Bank Run Gravel
L-3	Bedding	6.00		Crushed Stone
L-5	Spalls	4.00		Rounded Boulders
	Armor I	18.00		Rounded Boulders
	Armor II	1 layer (L-2)		Tribars (placed)
	Armor II	20.00 (L-3, L-5)		Tribars
L-6	Core		43	Bank Run Gravel
L-7	Bedding	6.00		Crushed Stone
	Spalls	4.00		Rounded Boulders
	Armor I	18.00		Rounded Boulders
	Armor II	1 layer (L-7)		Sioux Quartzite (placed)
	Armor II	32.50 (L-6)		Sioux Quartzite

TABLE 8 (Continued)

<u>Model No.</u>	<u>Layer</u>	<u>Layer Thickness (inches)</u>	<u>Figure Showing Gradation</u>	<u>Material</u>
L-9	Core Bedding Spalls Armor I Armor II	6.00 5.00 12.00 1 layer	43	Bank Run Gravel Crushed Stone Kimmswick Limestone Kimmswick Limestone Tribars
L-10	Core Bedding Spalls Armor	3.50 3.00 9.00	44	Bank Run Gravel Crushed Stone Kimmswick Limestone Kimmswick Limestone
L-11	Core Bedding Spalls Armor	6.00 4.00 18.00	44	Bank Run Gravel Crushed Stone Rounded Boulders Rounded Boulders
L-12	Core Bedding Spalls Armor	3.00 4.00 11.50	44	Bank Run Gravel Crushed Stone Kimmswick Limestone Kimmswick Limestone
L-13	Core Bedding Spalls Armor	3.00 4.00 22.00	44	Bank Run Gravel Crushed Stone Kimmswick Limestone Kimmswick Limestone
L-14	Core Bedding Spalls Armor I Armor II	3.00 4.00 5.00 14.00	44	Bank Run Gravel Crushed Stone Crushed Stone Kimmswick Limestone Kimmswick Limestone
L-15	Core Bedding Spalls Armor	3.00 4.00 30.00	44	Bank Run Gravel Crushed Stone Crushed Stone Kimmswick Limestone
L-16	Core Bedding Spalls Armor	3.00 4.00 22.00	44	Bank Run Gravel Crushed Stone Kimmswick Limestone Kimmswick Limestone

TABLE 8 (Continued)

<u>Model No.</u>	<u>Layer</u>	<u>Layer Thickness (inches)</u>	<u>Figure Showing Gradation</u>	<u>Material</u>
L-17	Core		44	Bank Run Gravel
	Bedding	3.00		Crushed Stone
	Spalls	4.00		Kimmswick Limestone
	Armor	10.50		Kimmswick Limestone
L-18	Core		44	Bank Run Gravel
	Bedding	3.00		Crushed Stone
	Armor	18.00		Kimmswick Limestone
L-19	Core		44	Bank Run Gravel
	Bedding	3.00		Crushed Stone
	Spalls	4.00		Crushed Stone
	Armor	17.00		Kimmswick Limestone

APPENDIX B

GRADATION CURVES

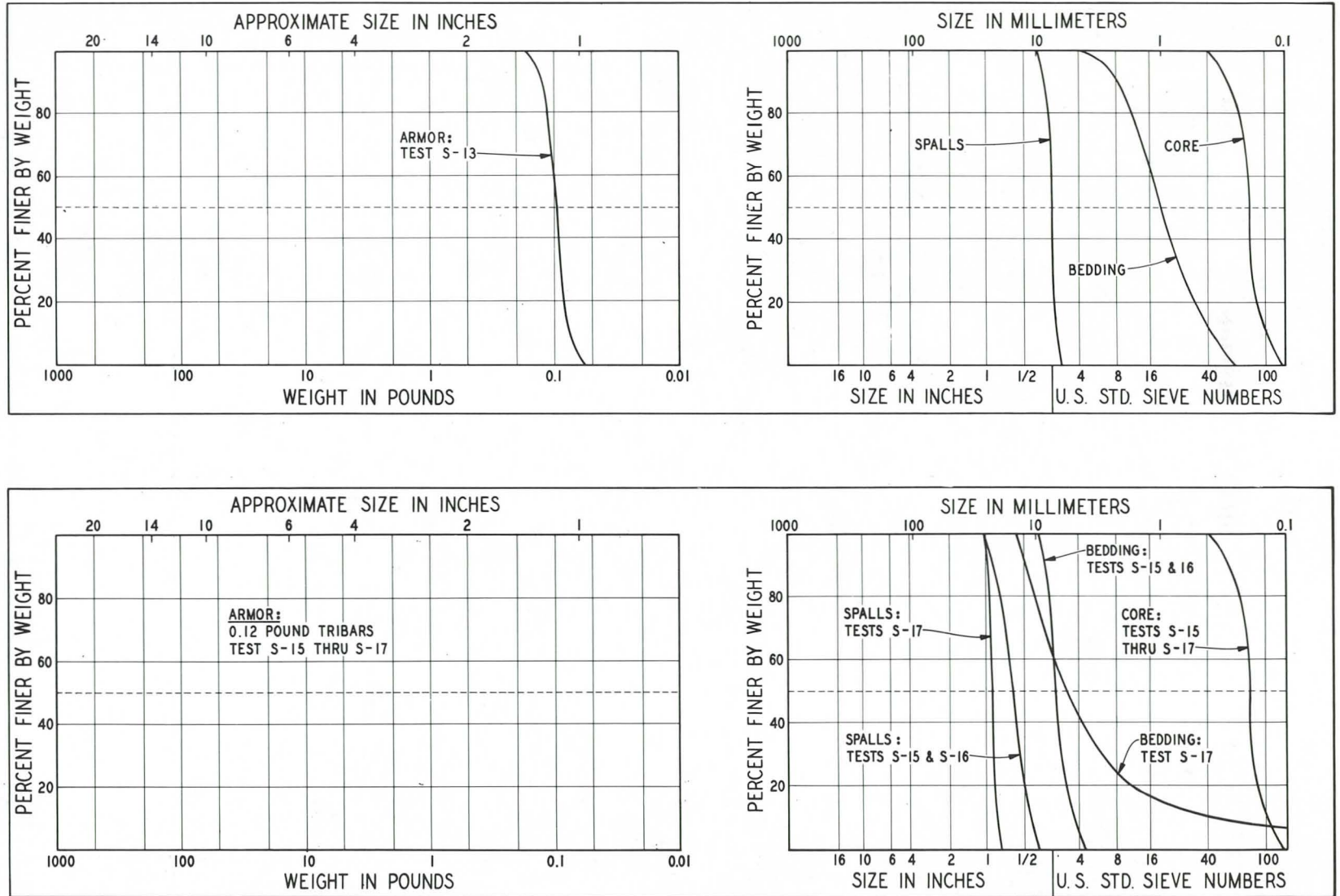


Figure 39. Gradation Curves

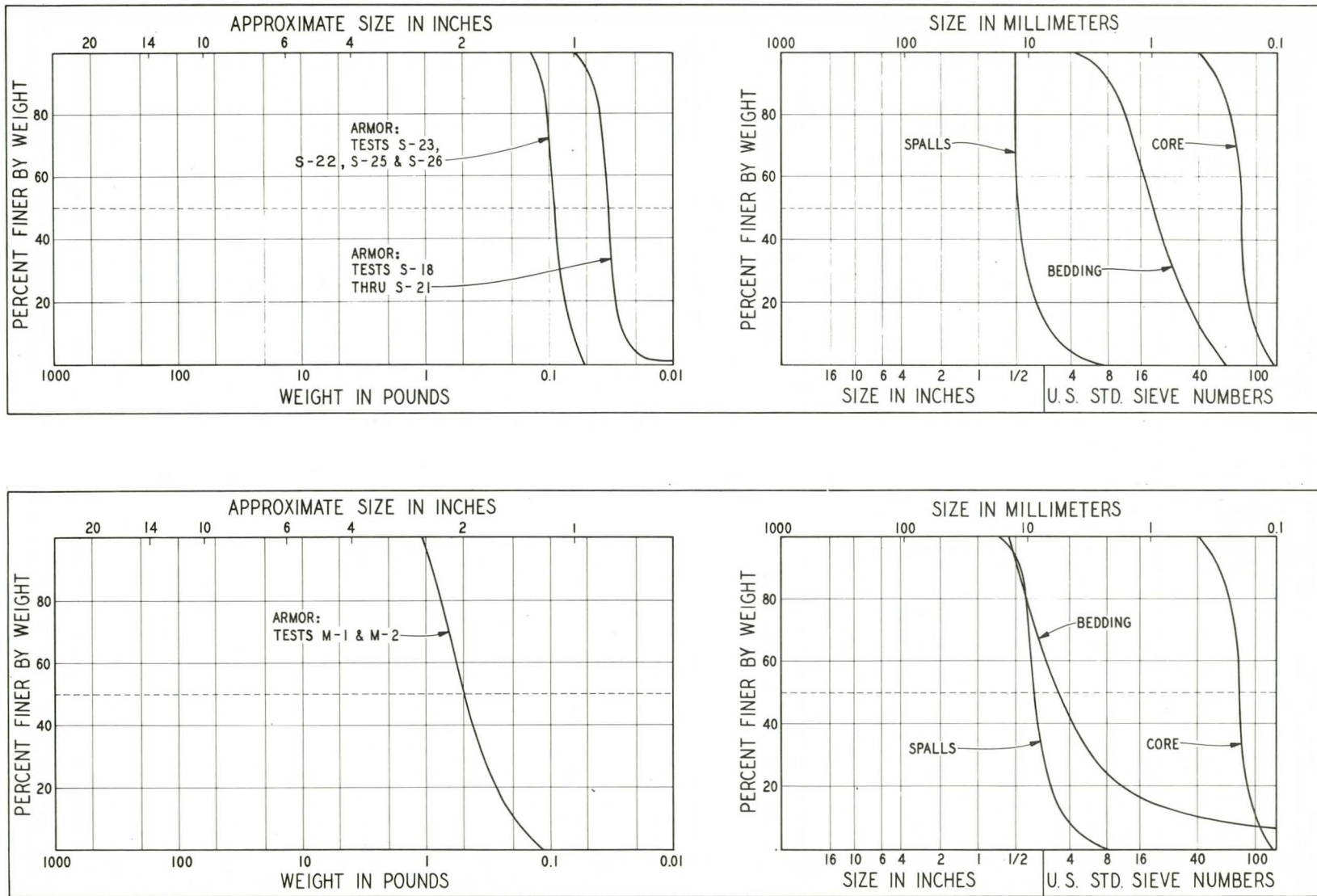


Figure 40. Gradation Curves

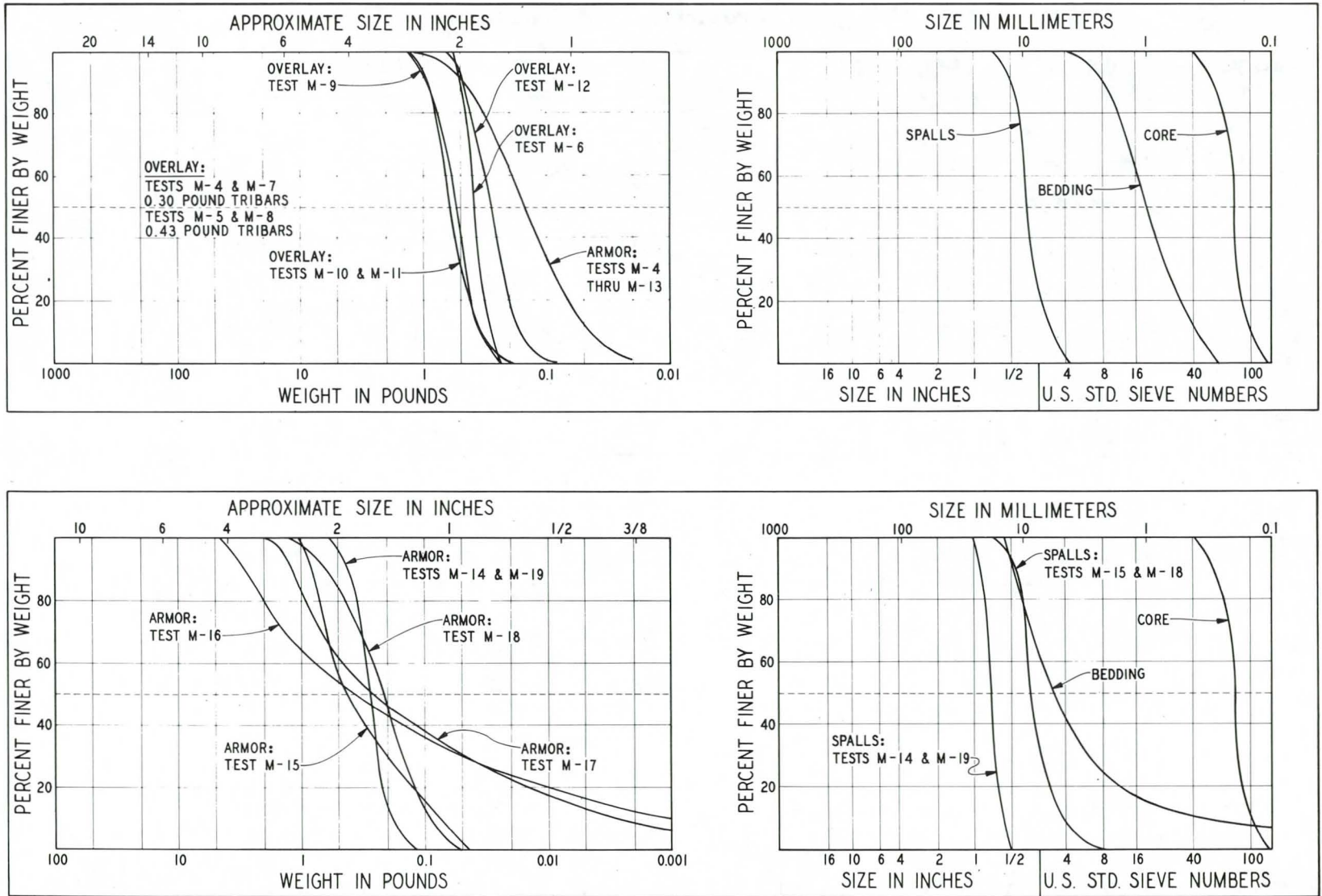


Figure 41. Gradation Curves

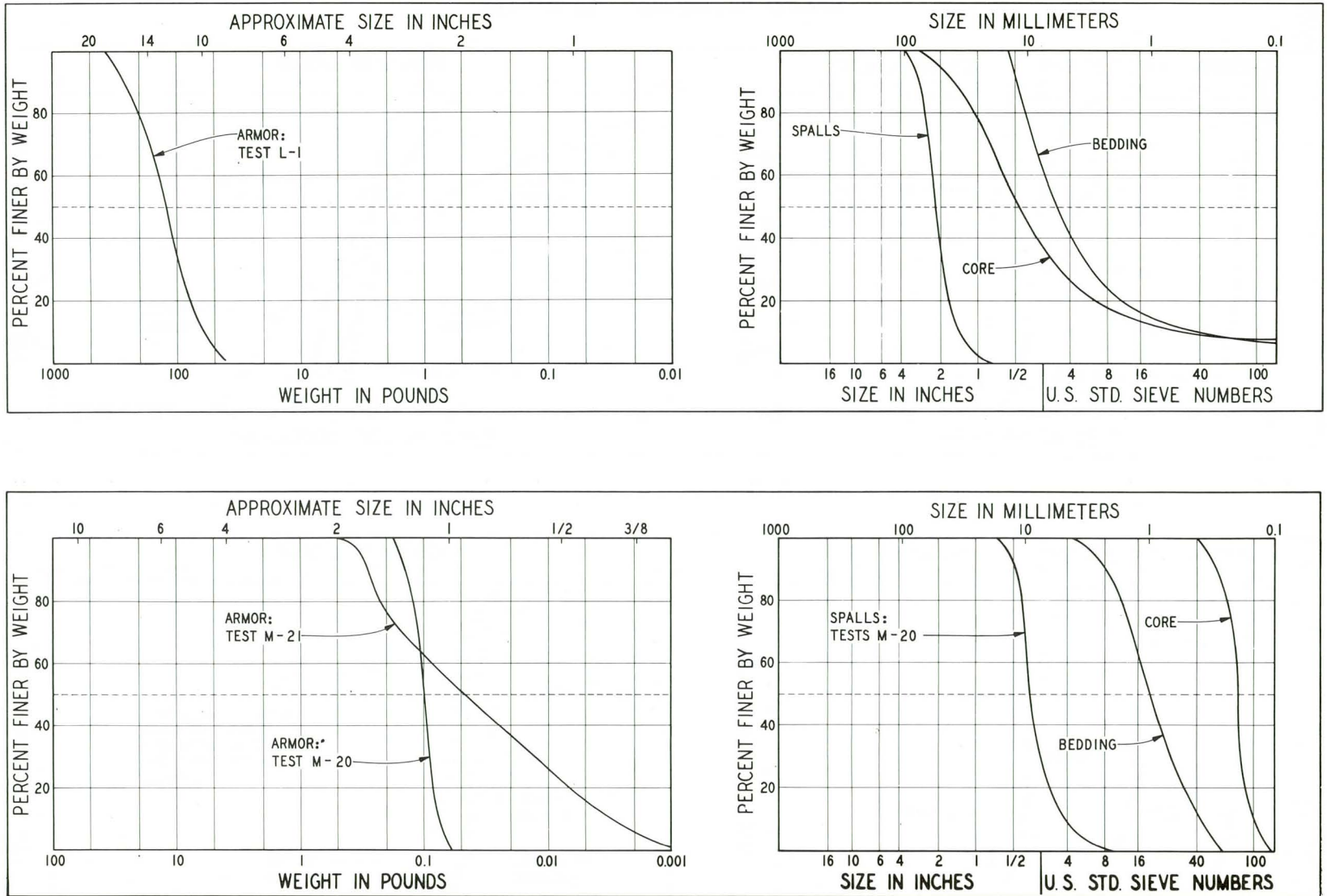
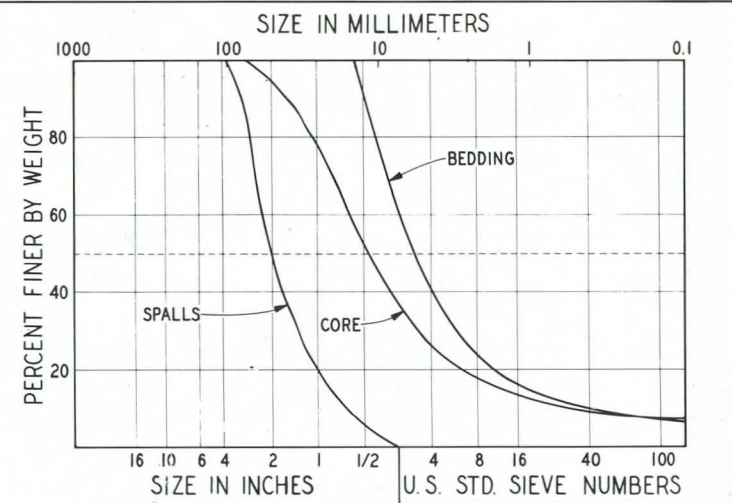
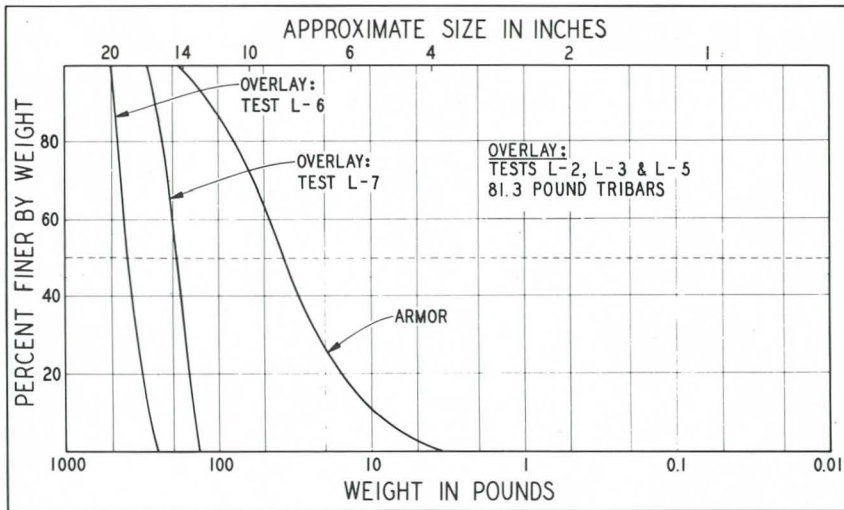


Figure 42. Gradation Curves



87

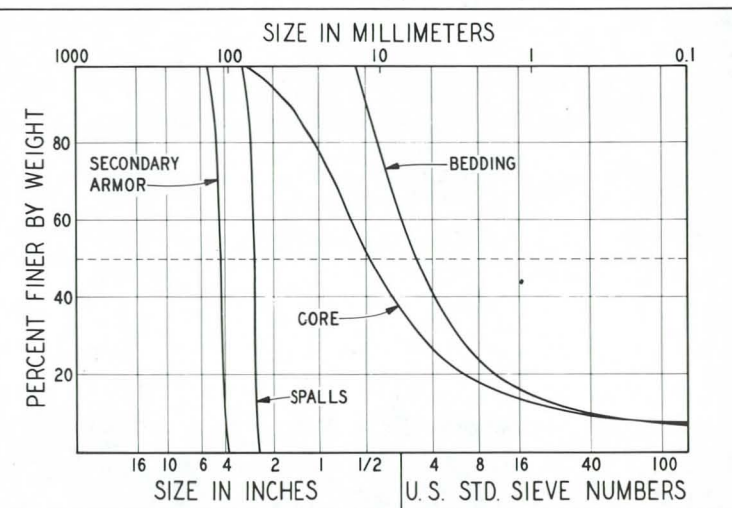
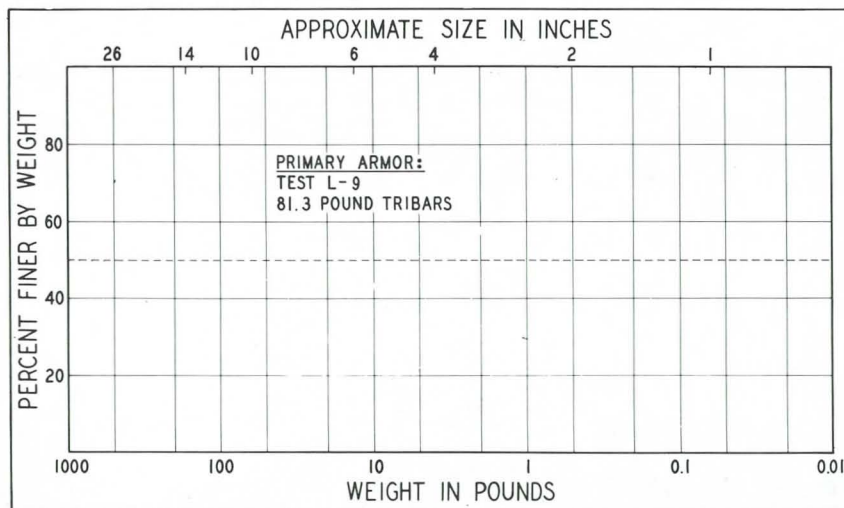


Figure 43. Gradation Curves

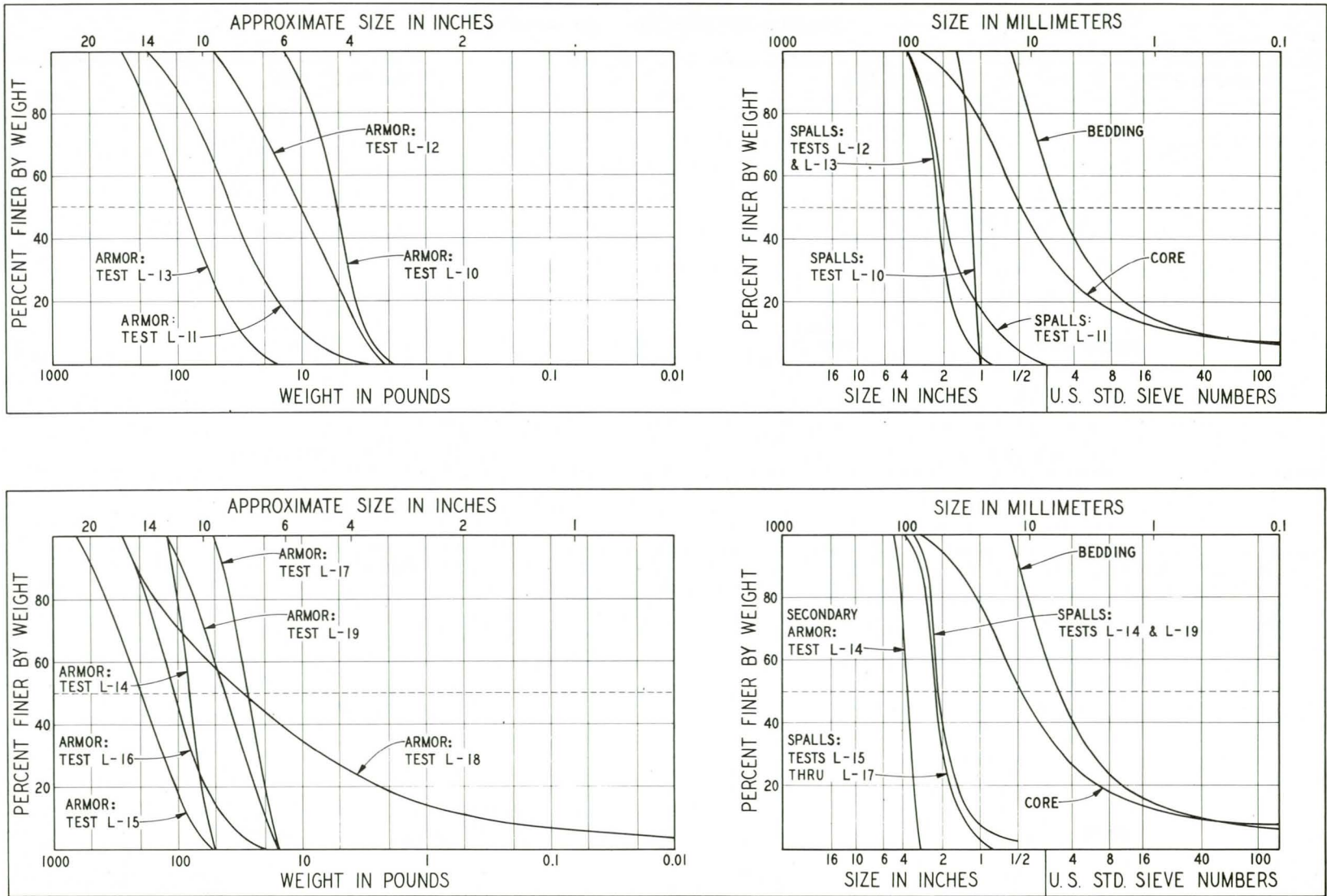


Figure 44. Gradation Curves

APPENDIX C

DAMAGE CURVES

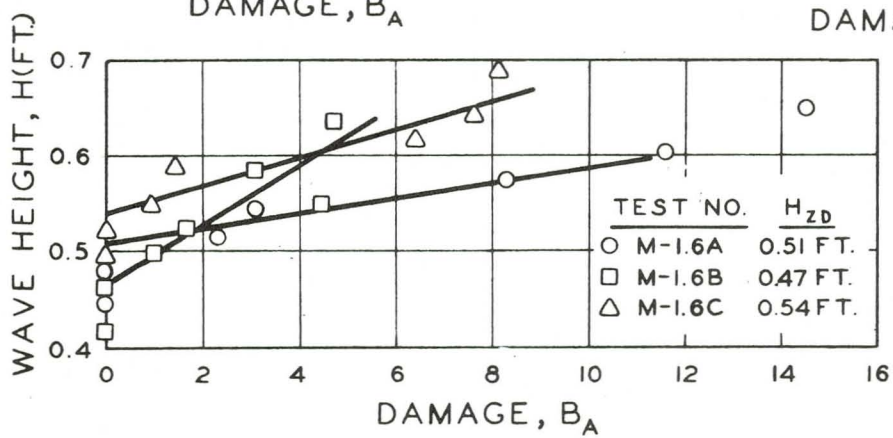
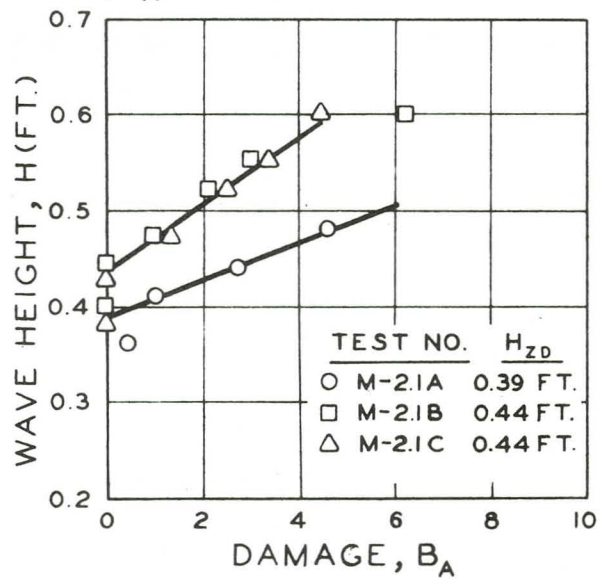
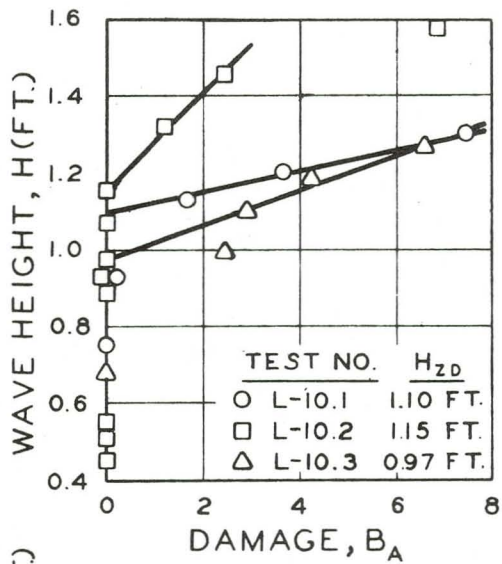
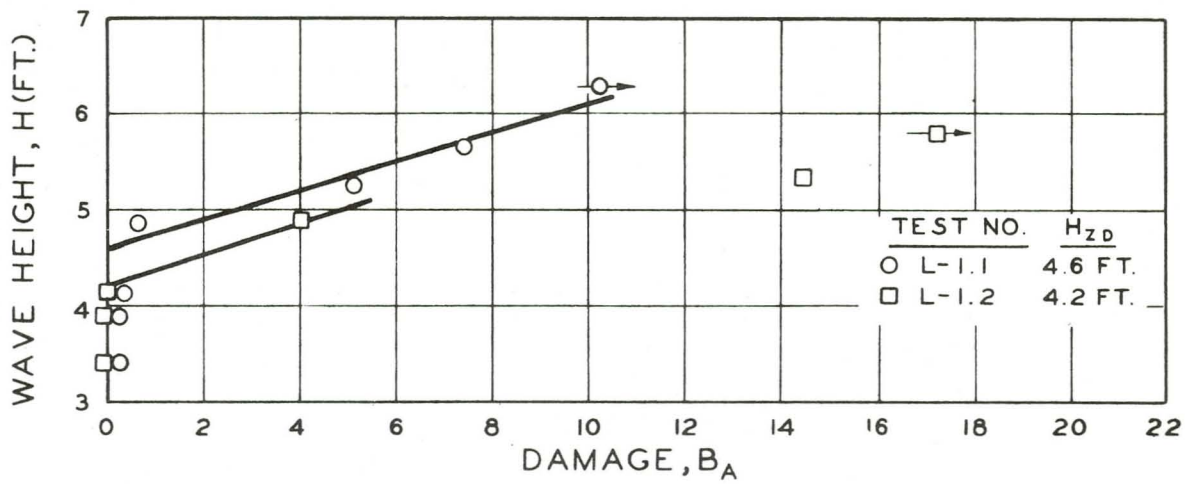


Figure 45. Damage Curves of Dumped Kimmswick Limestone Tests, $\cot \alpha = 2$

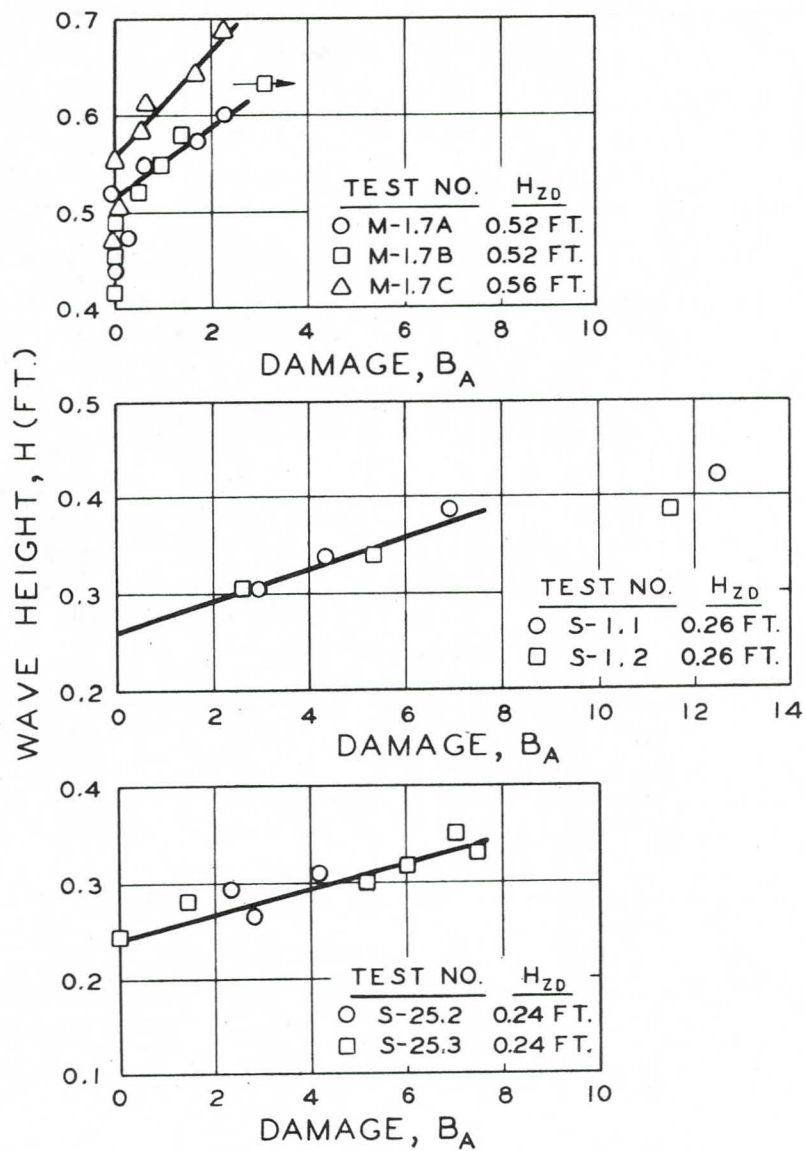


Figure 46. Damage Curves of Dumped Kimmswick Limestone Tests, $\cot \alpha = 2$

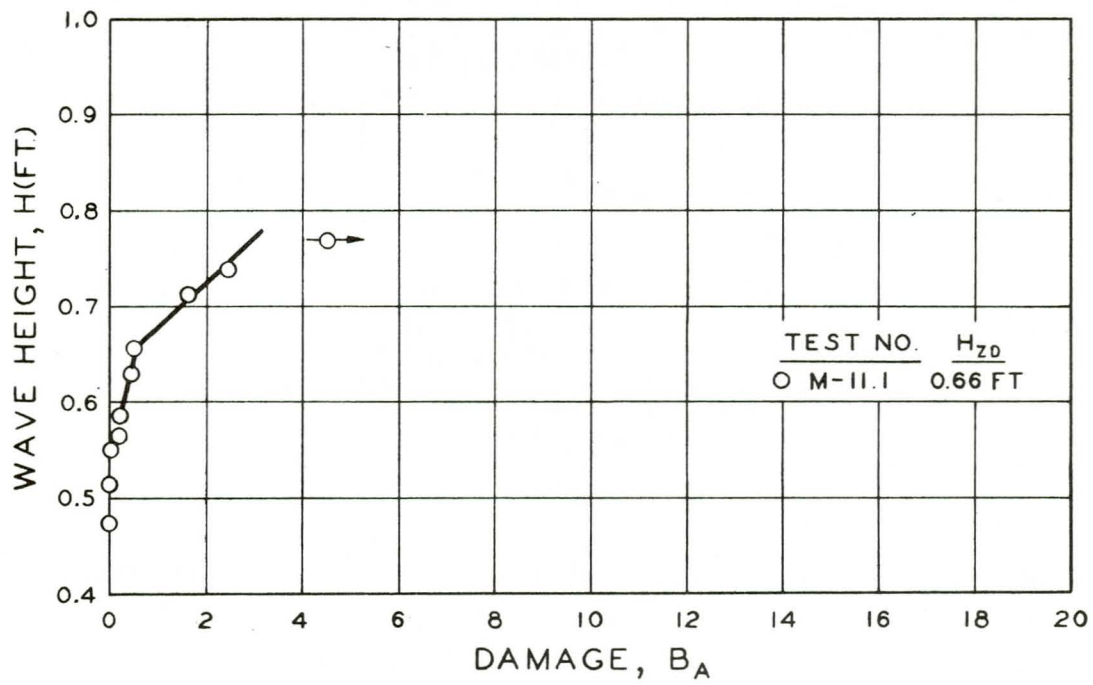
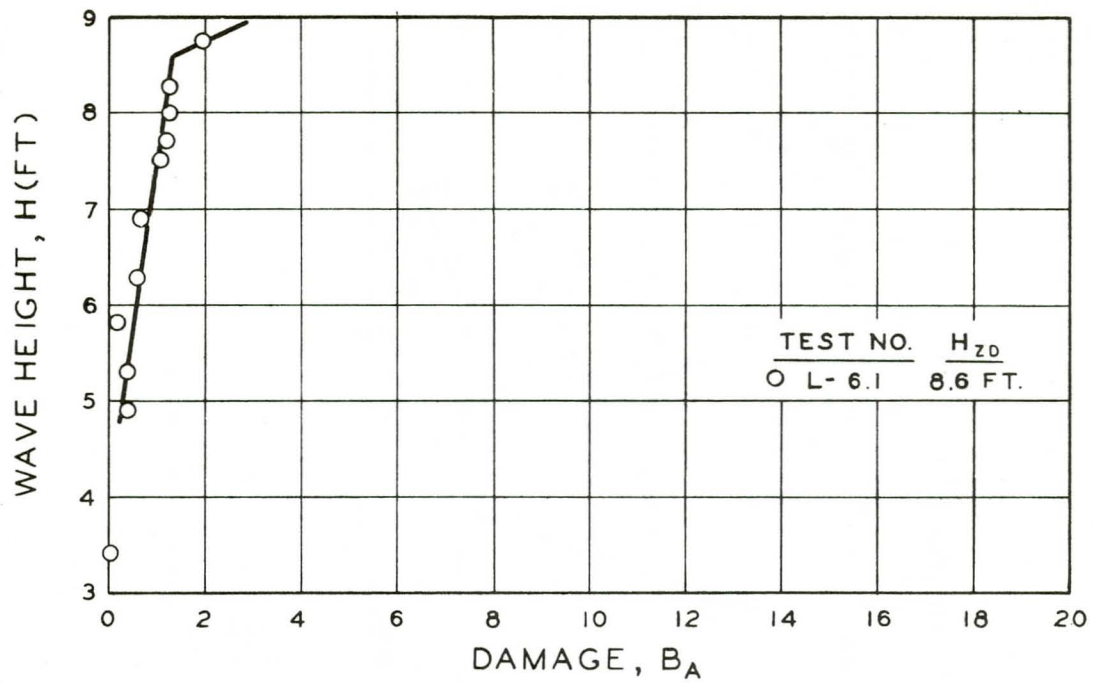


Figure 47. Damage Curves of Dumped Sioux Quartzite Tests, $\cot \alpha = 2$

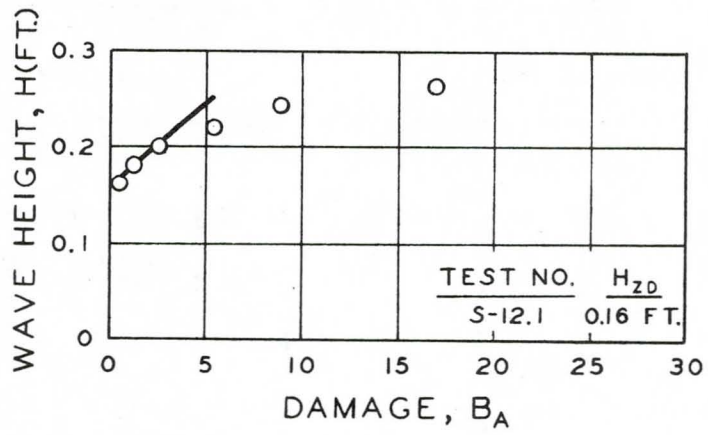
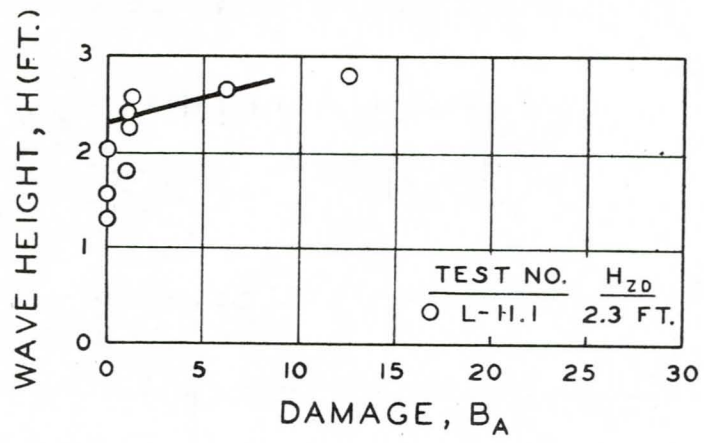


Figure 48. Damage Curves of Dumped Boulder Tests, $\cot \alpha = 2$

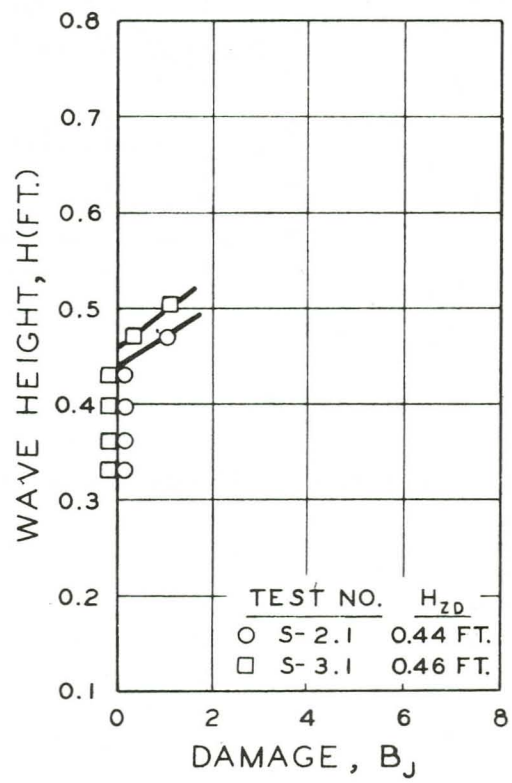
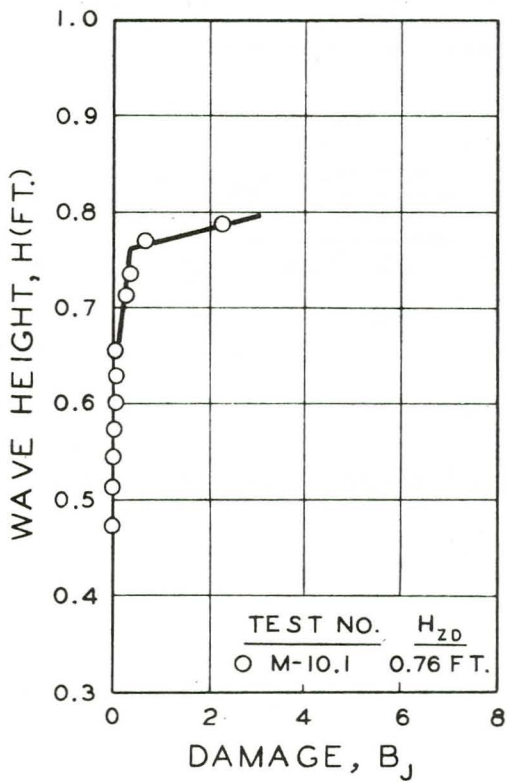
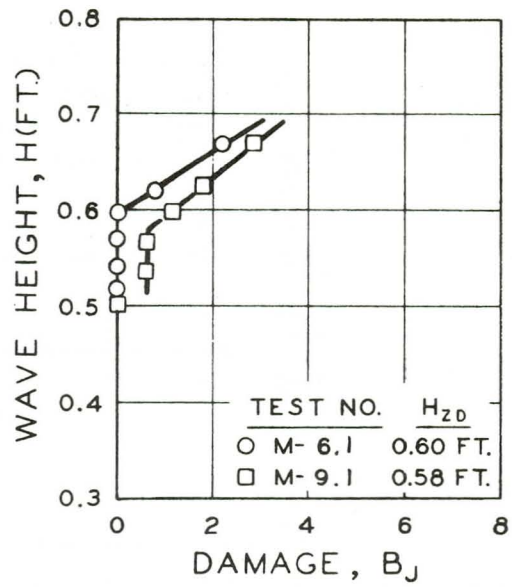
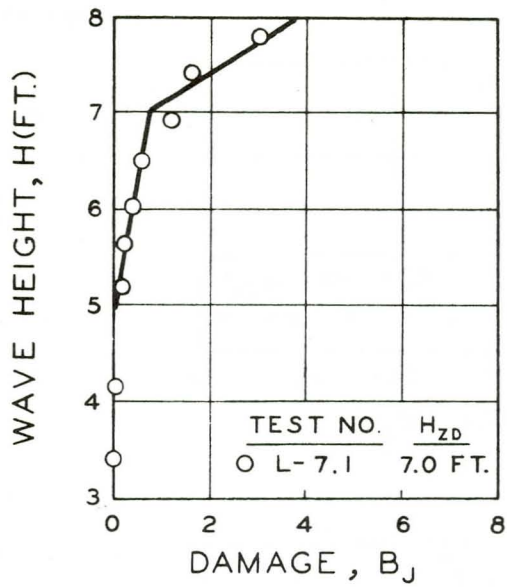


Figure 49. Damage Curves at Placed Sioux Quartzite Tests,
 $\cot \alpha = 2$

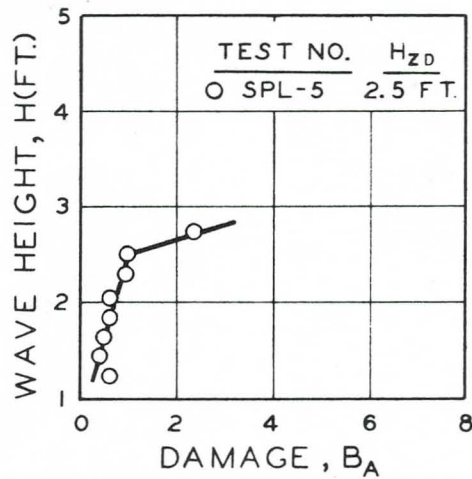
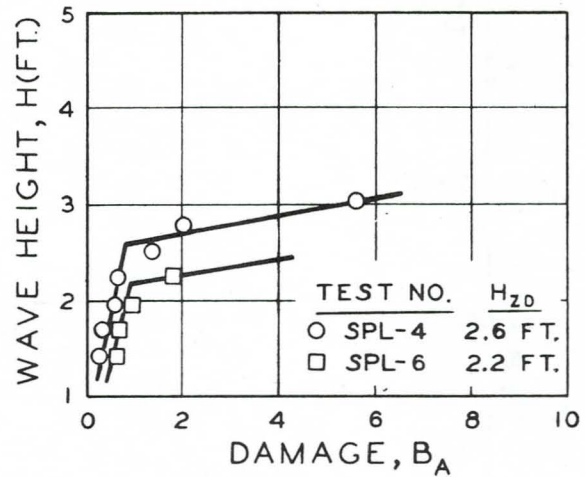
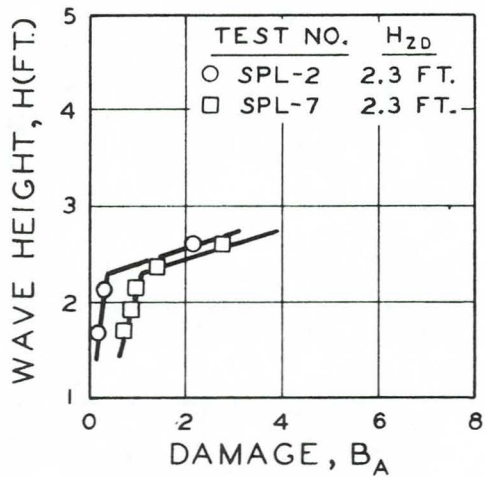
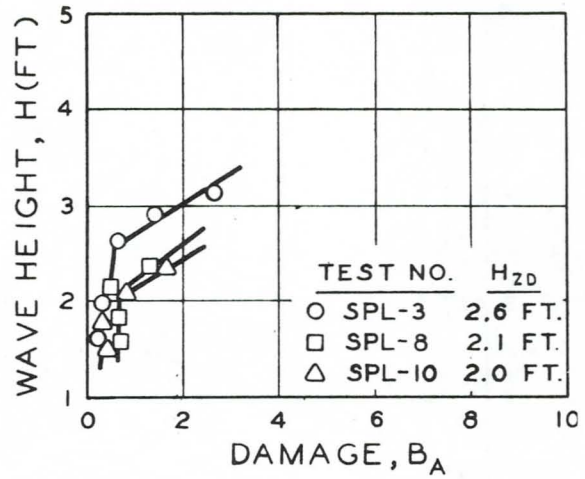
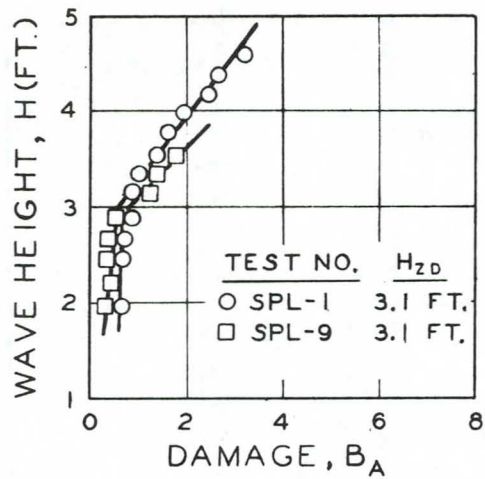


Figure 50. Damage Curves of Dumped Occoquan Granite Tests, $\cot \alpha = 2 \frac{1}{2}$

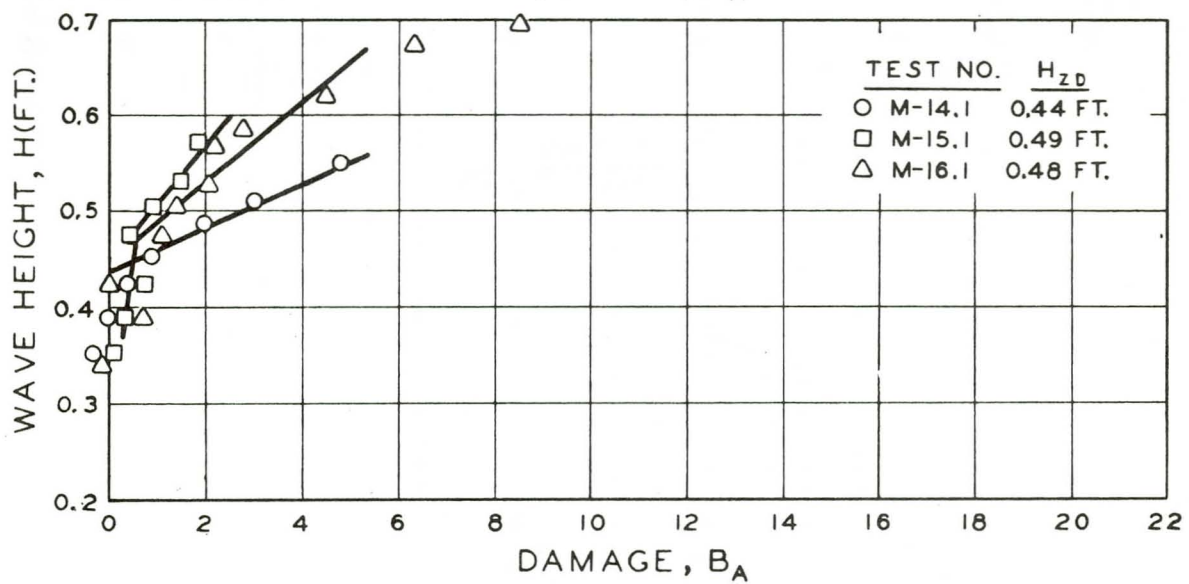
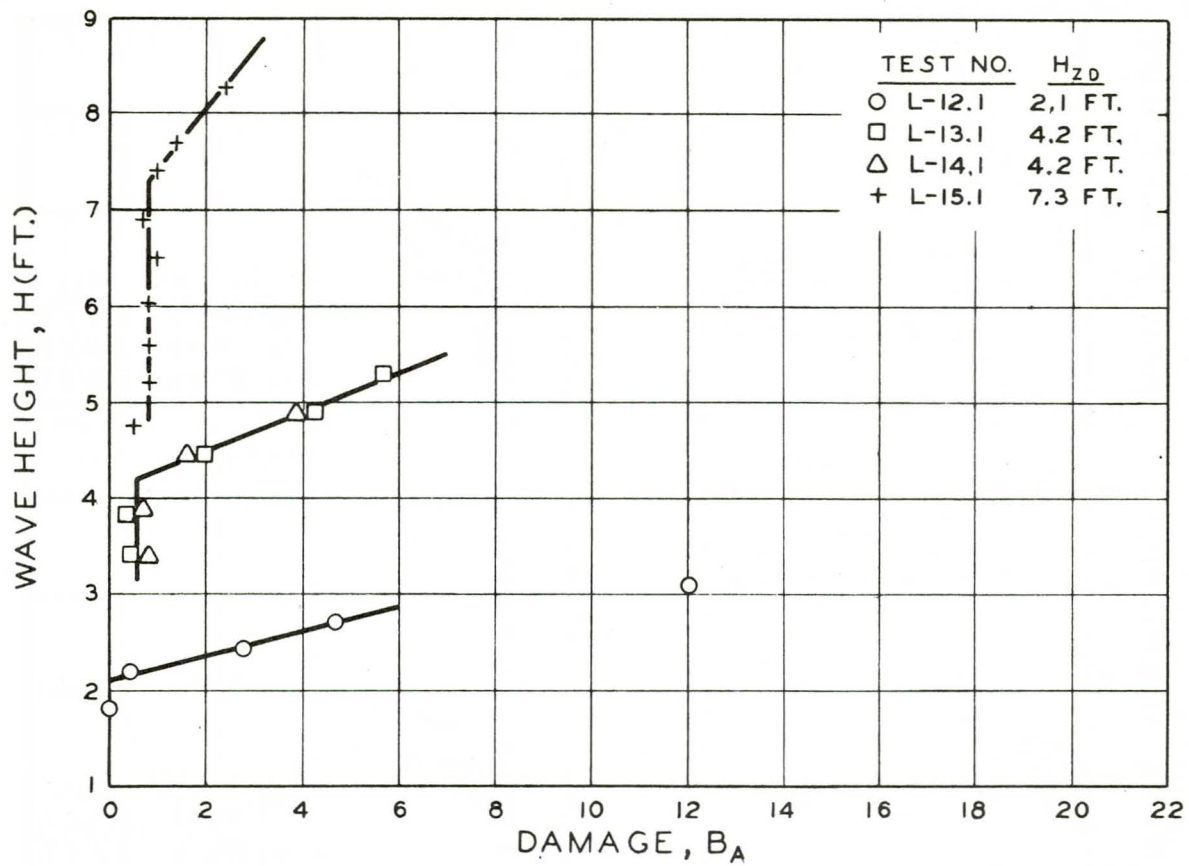


Figure 51. Damage Curves of Dumped Kimmswick Limestone Tests, $\cot \alpha = 3$

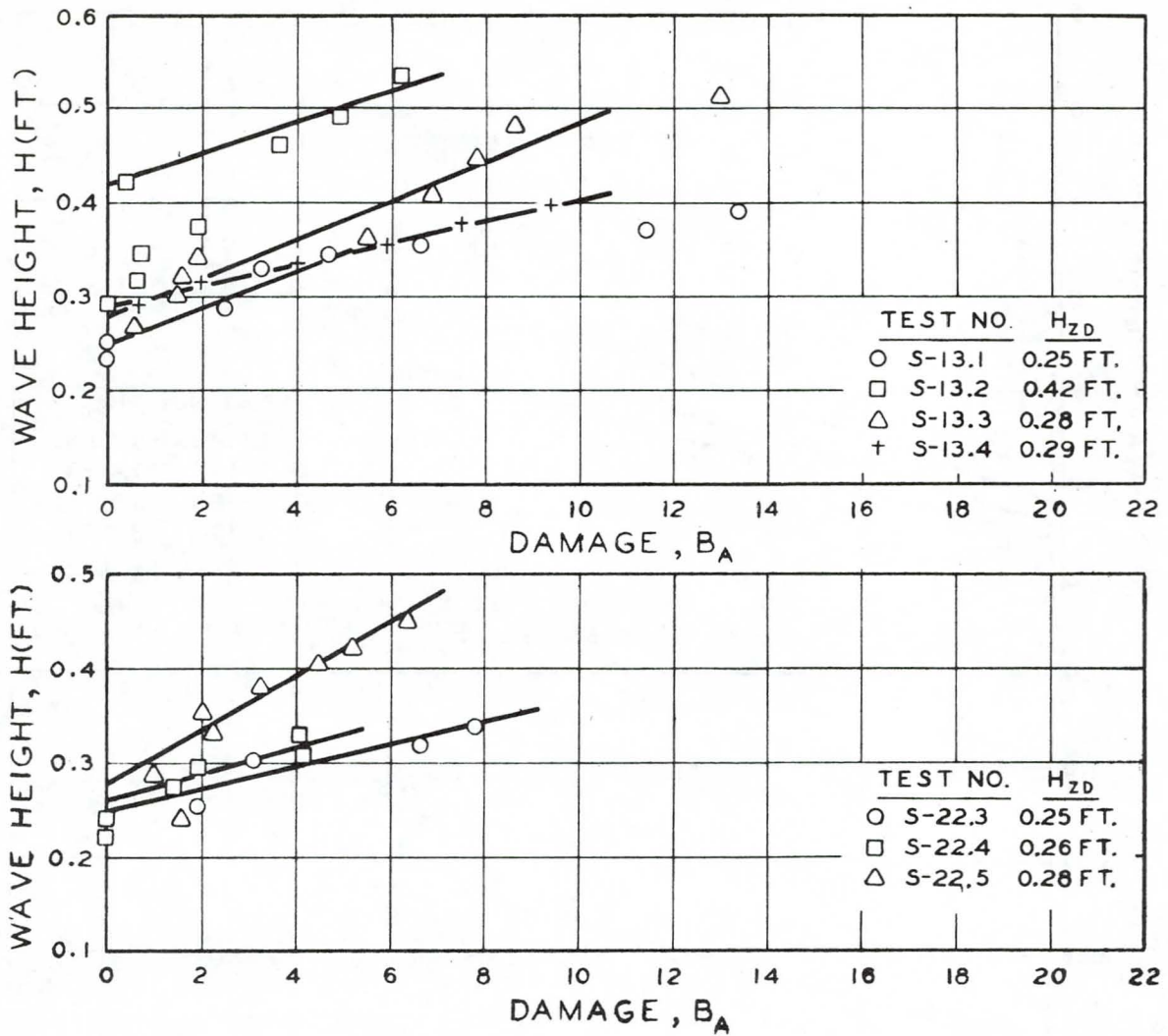


Figure 52. Damage Curves of Dumped Kimmswick Limestone Tests, $\cot \alpha = 3$

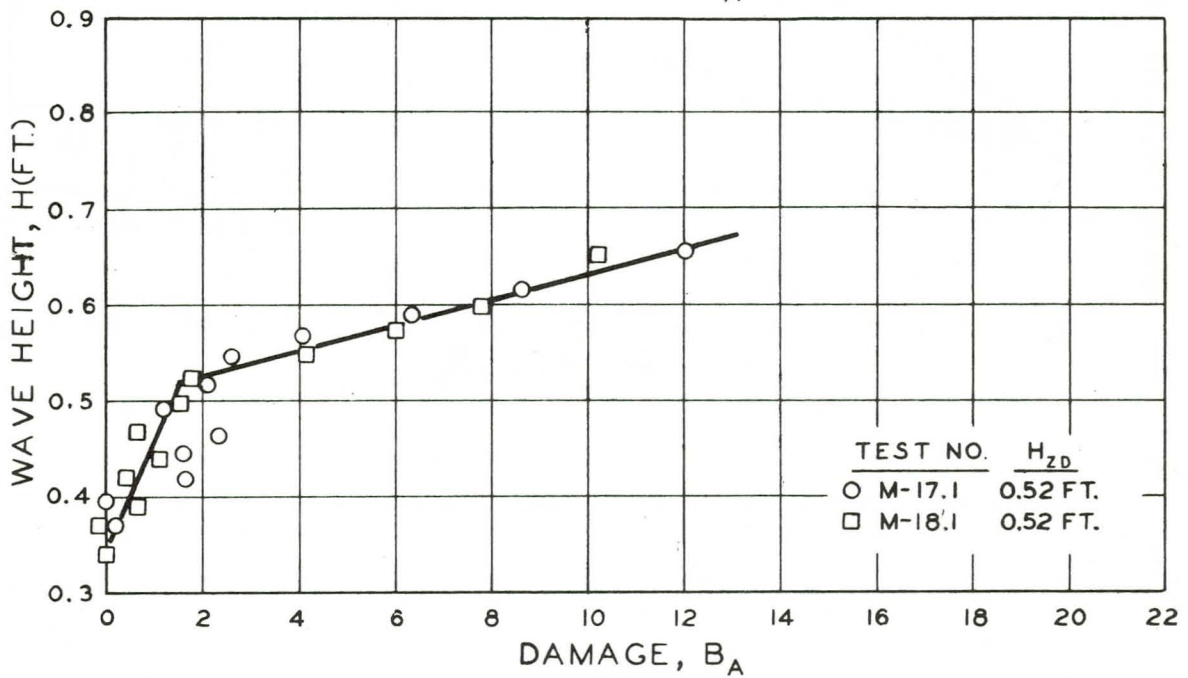
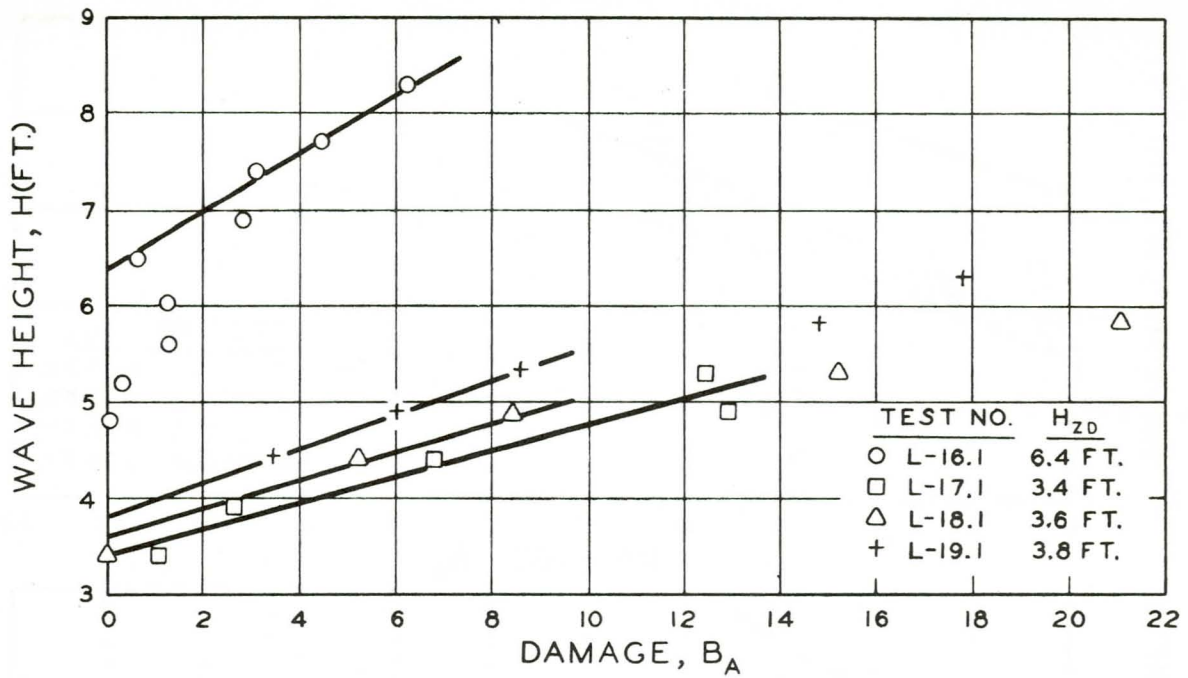


Figure 53. Damage Curves of Dumped Kimmswick Limestone Tests, $\cot \alpha = 5$

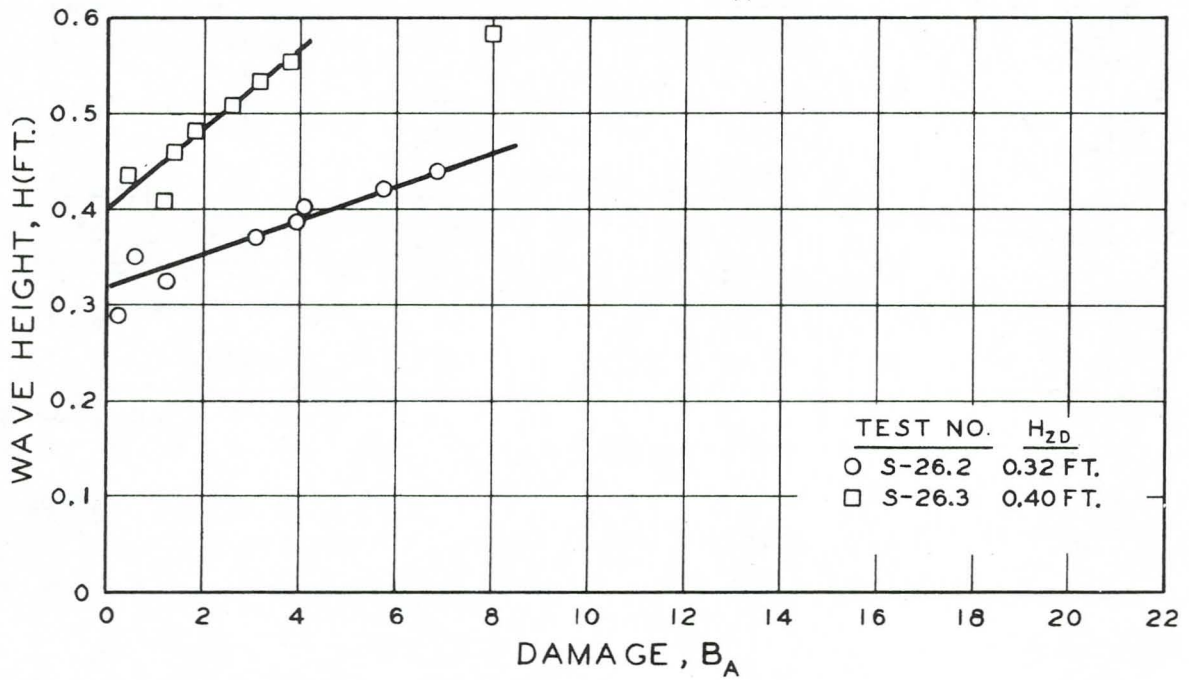
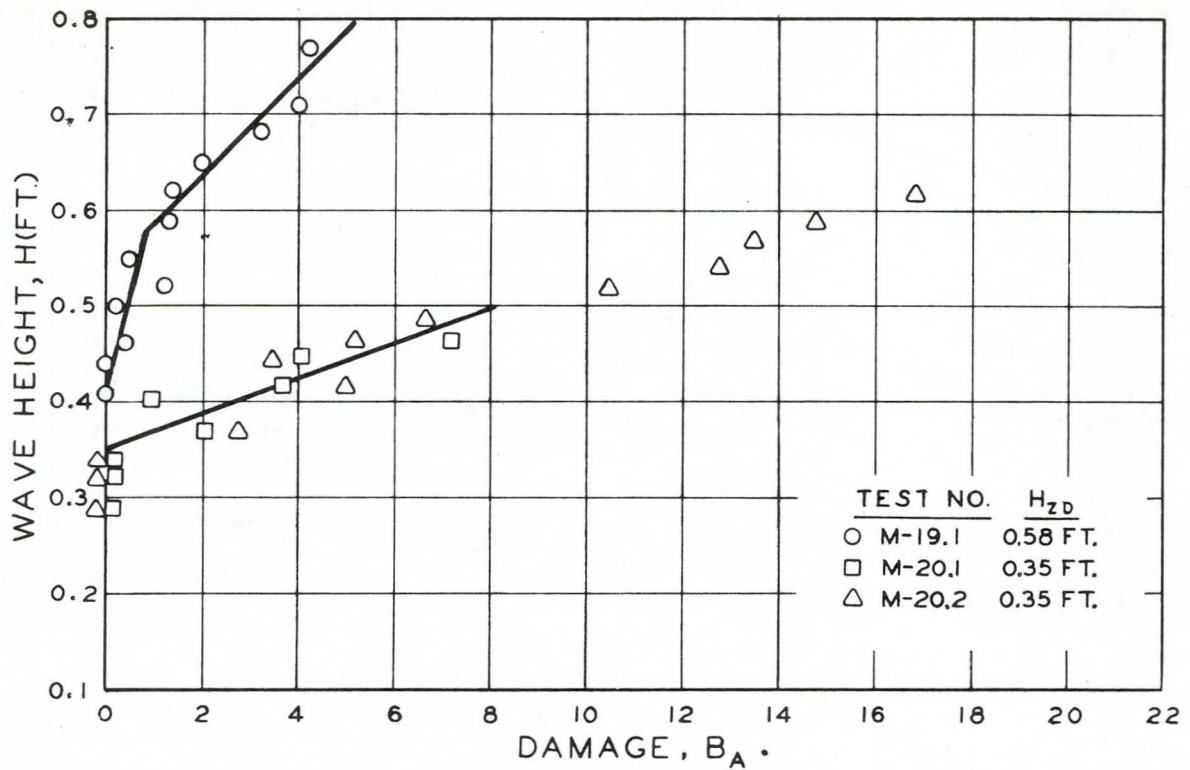


Figure 54. Damage Curves of Dumped Kimmswick Limestone Tests,
 $\cot \alpha = 5$

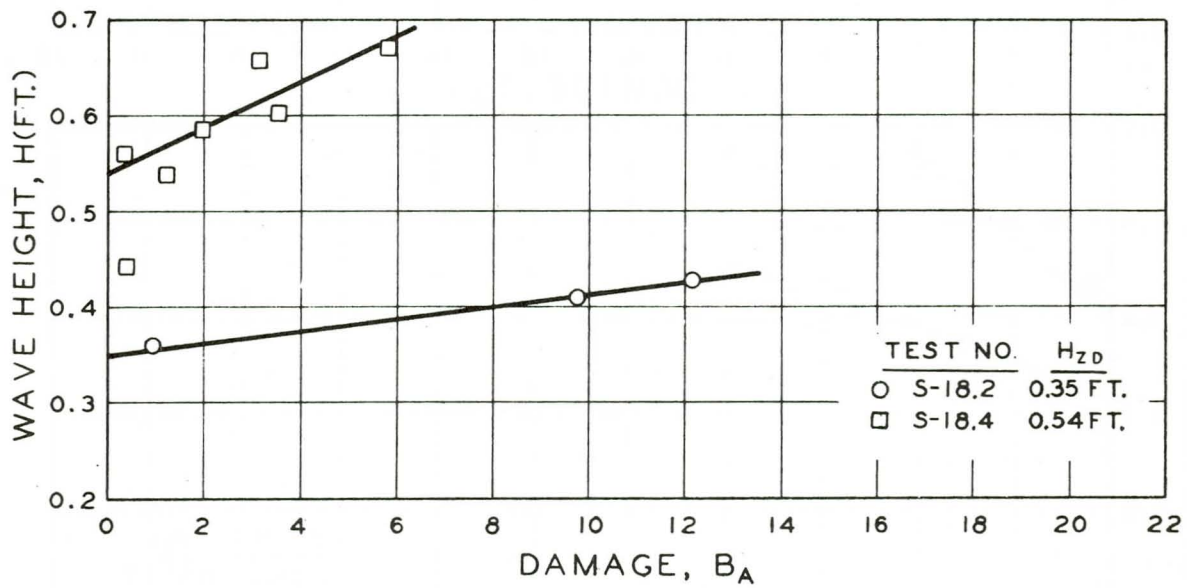
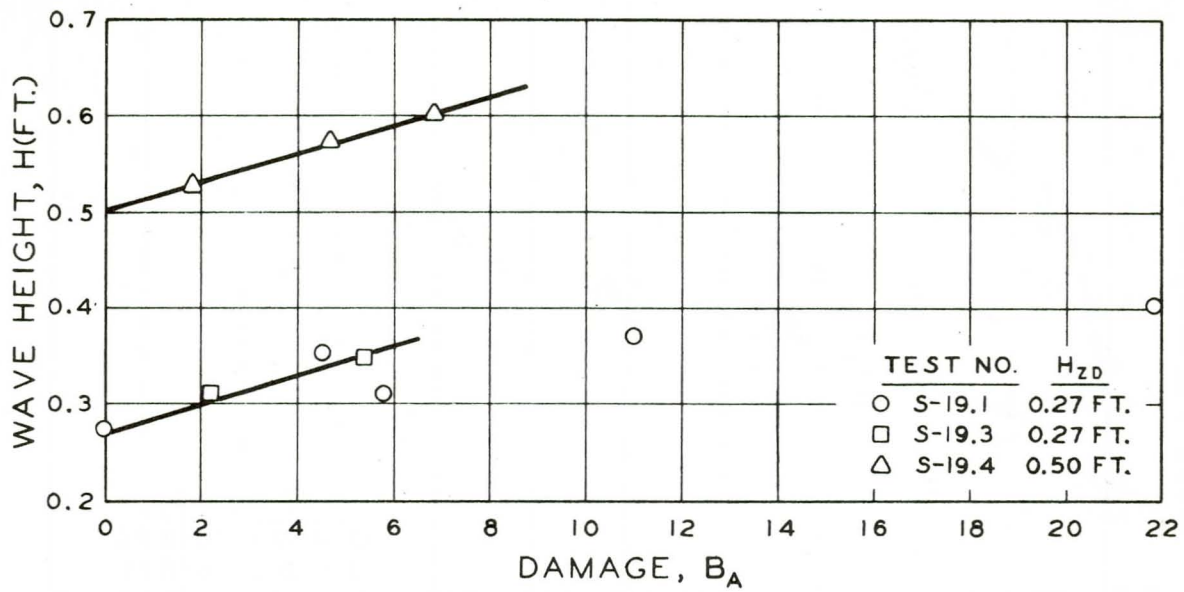


Figure 55. Damage Curves of Dumped Kimmswick Limestone Tests.
cot α = 7 and 10.

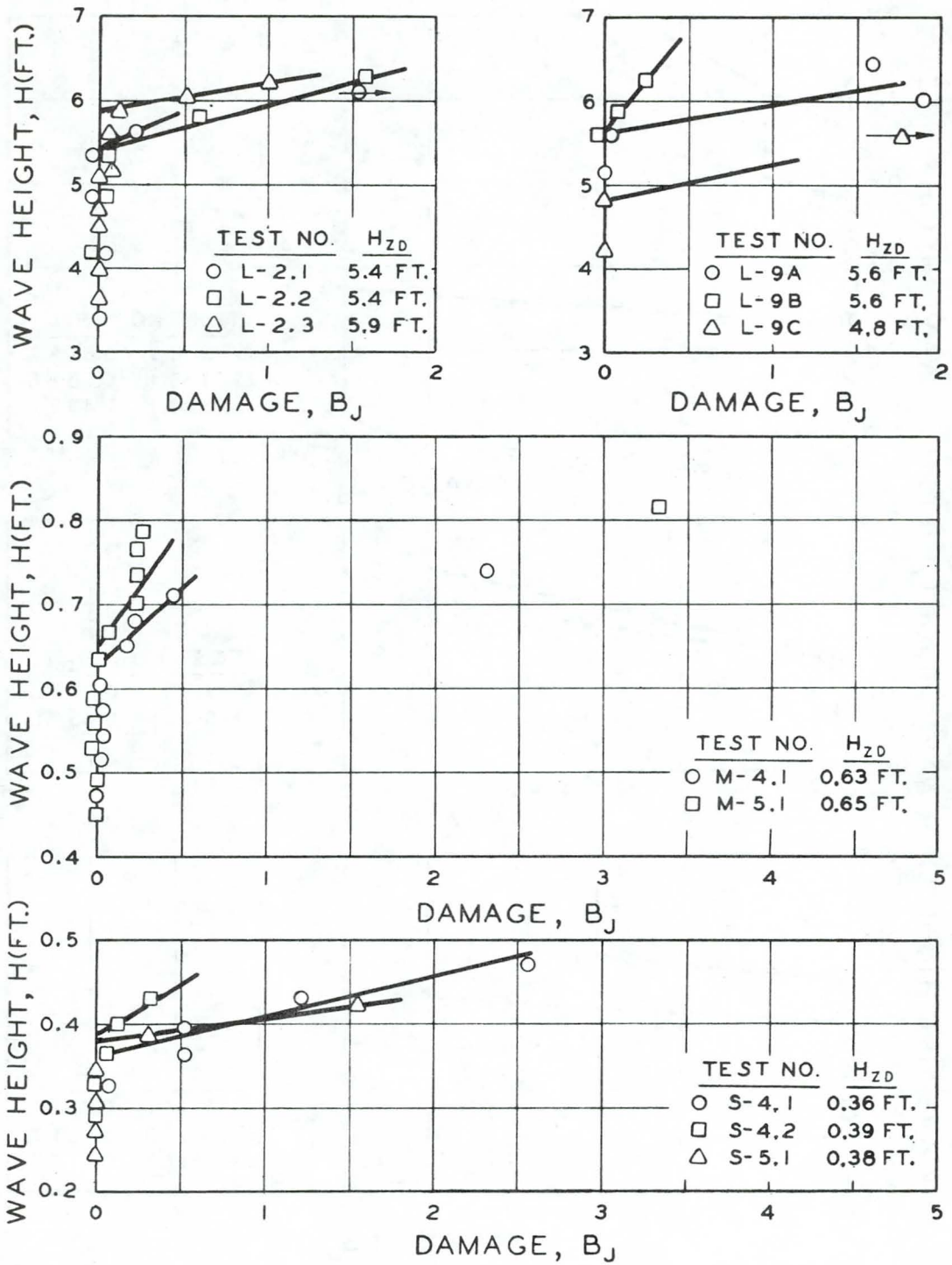


Figure 56. Damage Curves of Placed Tribar Tests, $\cot \alpha = 2$

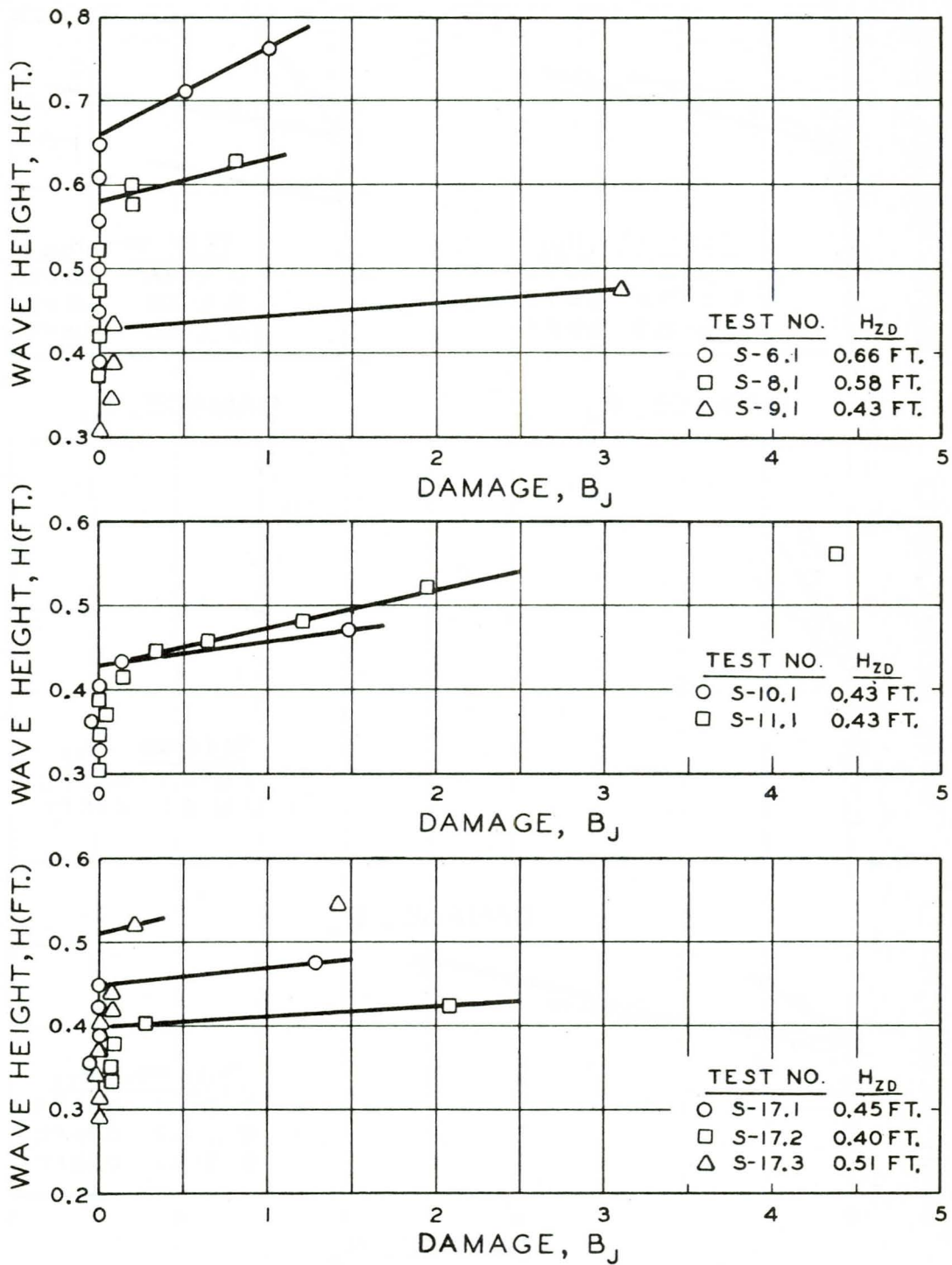


Figure 57. Damage Curves of Placed Tribar Tests, $\cot \alpha = 2$

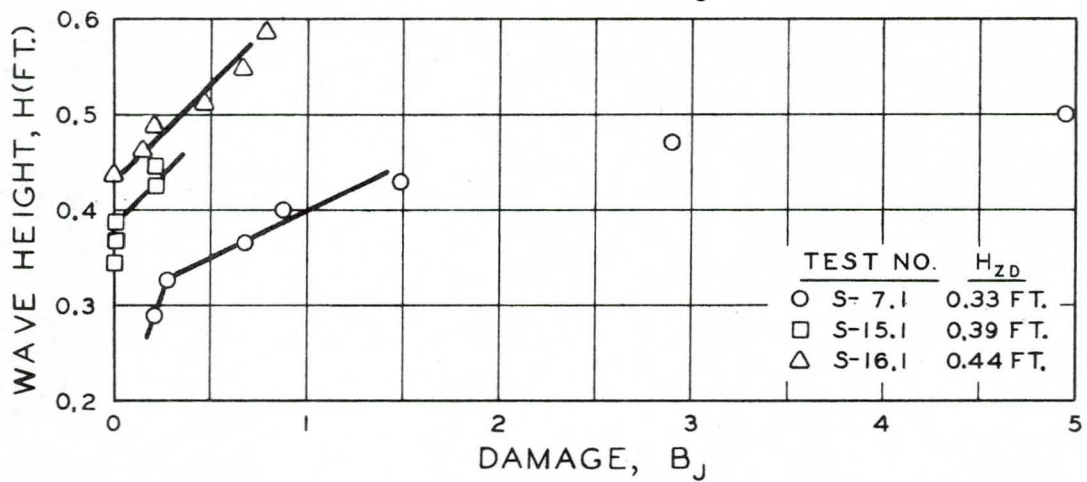
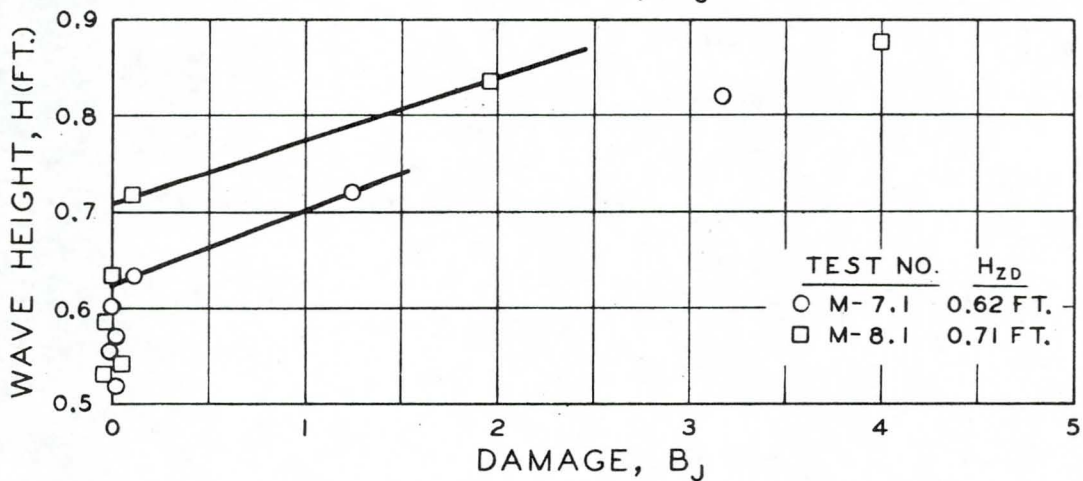
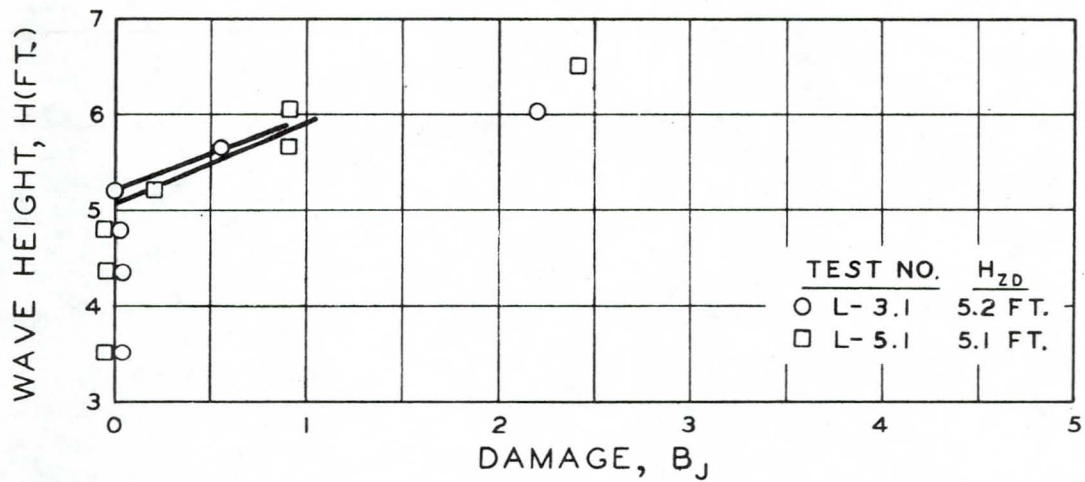


Figure 58. Damage Curves of Dumped Tribar Tests, $\cot \alpha = 2$

APPENDIX D

MODEL TEST CONDITIONS

TABLE 9

Model Test Conditions and Results

d = Water depth	Th = Thickness of armor layer
T = Wave period	W ₅₀ = Median weight of armor gradation
Unif = $(W_{85}/W_{15})^{1/3}$ = Uniformity of armor gradation	h = Actual zero-damage wave height
n = Porosity of armor layer	H _{ZD} = Zero-damage deepwater wave height

Test Number	d (ft)	T (sec)	Unif	n	Th (in)	W ₅₀ (lbs)	h (ft)	H _{ZD} (ft)
<u>Dumped Kimmswick Limestone, Cot $\alpha = 2$, $\gamma = 165$ lbs/cu.ft.</u>								
L-1.1	15.0	3.67	1.48	0.39	26.0	120.0	4.3	4.6
L-1.2	15.0	3.67	1.48	0.39	26.8	120.0	3.9	4.2
L-10.1	8.0	2.50	1.39	0.27	7.4	5.1	1.03	1.10
L-10.2	9.0	6.00	1.39	0.34	7.0	5.1	1.18	1.15
L-10.3	8.0	2.50	1.39	0.41	7.8	5.1	0.91	0.97
M-1.6A	2.0	1.50	1.52	--	4.0	0.49	0.47	0.51
M-1.6B	2.0	1.50	1.52	--	4.0	0.49	0.44	0.47
M-1.6C	2.0	1.50	1.52	--	4.0	0.49	0.49	0.54
M-1.7A	2.0	1.50	1.52	--	4.8	0.49	0.48	0.52
M-1.7B	2.0	1.50	1.52	--	4.5	0.49	0.48	0.52
M-1.7C	2.0	1.50	1.52	--	4.6	0.49	0.51	0.56
M-2.1A	2.0	2.00	1.52	--	2.5	0.49	0.39	0.39
M-2.1B	2.0	2.00	1.52	--	4.0	0.49	0.44	0.44
M-2.1C	2.0	2.00	1.52	--	5.5	0.49	0.44	0.44
S-1.1	1.5	1.16	1.27	--	2.8	0.108	0.24	0.26
S-1.2	1.5	1.16	1.27	--	3.0	0.108	0.24	0.26
S-25.2	1.5	1.16	1.14	0.36	1.5	0.092	0.22	0.24
S-25.3	1.5	2.30	1.14	0.36	1.5	0.092	0.24	0.24

Dumped Sioux Quartzite, Cot $\alpha = 2$, $\gamma = 165$ lbs/cu. ft.

L-6.1	15	3.67	1.15	0.45	32.5	390.0	7.9	8.6
M-11.1	2	1.50	1.29	0.44	3.8	0.60	0.60	0.66

Dumped Boulders, Cot $\alpha = 2$, $\gamma = 165$ lbs/cu. ft.

L-11.1	12.0	3.67	1.95	0.21	18.6	37.5	2.1	2.3
S-12.1	1.5	1.28	1.80	0.34	2.0	0.60	0.15	0.16

TABLE 9 (Continued)

Test Number	d (ft)	T (sec)	Unif	n	Th (in)	W ₅₀ (lbs)	h (ft)	H _{ZD} (ft)
Placed Sioux Quartzite, Cot $\alpha = 2$, $\gamma = 165$ lbs/cu. ft.								
L-7.1	15.0	3.67	1.17	0.42	14.5	188.0	6.5	7.0
M-6.1	2.0	1.50	1.14	--	2.2	0.39	.56	0.60
M-9.1	2.0	1.50	1.29	--	3.0	0.54	.54	0.58
M-10.1	2.0	1.50	1.29	0.38	2.4	0.60	.71	0.76
S-2.1	1.5	1.28	1.26	0.34	1.5	0.27	.40	0.44
S-3.1	1.5	1.28	1.26	0.34	1.5	0.27	.42	0.46

Dumped Occoquan Granite, Cot $\alpha = 2 \frac{1}{2}$, $\gamma = 165$ lbs/cu.ft.

SPL-1	15.0	2.8	1.70	0.37	22.0	28	3.0	3.1
SPL-2	15.0	5.7	1.70	0.40	17.0	28	2.2	2.3
SPL-3	15.0	4.2	1.70	0.40	18.0	28	2.4	2.6
SPL-4	15.0	8.5	1.70	0.40	18.0	28	2.3	2.6
SPL-5	15.0	11.3	1.70	0.40	19.0	28	2.3	2.5
SPL-6	15.0	8.5	1.70	0.40	11.0	28	1.9	2.2
SPL-7	15.0	5.7	1.70	0.40	14.0	28	2.2	2.3
SPL-8	15.0	4.2	1.70	0.40	12.0	28	1.9	2.1
SPL-9	15.0	2.8	1.70	0.40	12.0	28	3.0	3.1
SPL-10	15.0	4.2	1.70	0.40	12.0	28	1.8	2.0

Dumped Kimmswick Limestone, Cot $\alpha = 3$, $\gamma = 165$ lbs/cu.ft.

L-12.1	12.0	2.50	1.93	0.44	11.1	10.0	1.9	2.1
L-13.1	15.0	3.67	1.70	0.50	23.1	84.0	3.9	4.2
L-14.1	15.0	3.67	1.20	--	12.5	80.0	3.9	4.2
L-15.1	15.0	3.67	1.65	0.49	30.5	195.0	6.7	7.3
M-14.1	2.0	1.50	1.24	0.51	2.0	0.27	0.41	0.44
M-15.1	2.0	1.50	1.97	0.50	2.7	0.42	0.45	0.49
M-16.1	2.0	1.50	8.82	0.54	3.5	0.36	0.45	0.48
S-13.1	1.5	1.55	1.15	0.38	1.4	0.097	0.24	0.26
S-13.2	1.5	0.90	1.15	0.38	1.4	0.097	0.41	0.42
S-13.3	1.5	1.16	1.15	0.38	1.4	0.097	0.26	0.28
S-13.4	1.5	2.30	1.15	0.38	1.4	0.097	0.31	0.29
S-22.2	1.5	1.16	1.14	--	1.6	0.092	0.25	0.27
S-22.3	1.5	1.55	1.14	--	1.6	0.092	0.23	0.25
S-22.4	1.5	2.30	1.14	--	1.6	0.092	0.28	0.26
S-22.5	1.5	1.16	1.14	--	1.5	0.092	0.26	0.28

TABLE 9 (Continued)

Test Number	d (ft)	T (sec)	Unif	n	Th (in)	W ₅₀ (lbs)	h (ft)	H _{ZD} (ft)
<u>Dumped Kimmswick Limestone, Cot $\alpha = 5$, $\gamma = 165$ lbs/cu.ft.</u>								
L-16.1	15.0	3.67	1.55	0.39	21.4	105.0	5.9	6.4
L-17.1	15.0	3.67	1.28	0.40	11.2	27.0	3.1	3.4
L-18.1	15.0	3.67	5.47	0.36	18.4	30.0	3.1	3.4
L-19.1	15.0	3.67	1.54	0.37	16.2	41.0	3.5	3.8
M-17.1	2.0	1.50	5.28	0.52	4.0	0.25	0.48	0.52
M-18.1	2.0	1.50	1.45	0.59	3.0	0.22	0.48	0.52
M-19.1	2.0	1.50	1.24	0.63	3.0	0.27	0.54	0.58
M-20.1	2.0	1.50	1.18	0.37	1.3	0.098	0.32	0.35
M-20.2	2.0	1.50	1.18	0.37	1.5	0.098	0.32	0.35
S-26.2	1.5	2.30	1.14	0.35	1.4	0.092	0.34	0.32
S-26.3	1.5	1.55	1.14	0.35	1.5	0.092	0.37	0.40
<u>Dumped Kimmswick Limestone, Cot $\alpha = 7$, $\gamma = 165$ lbs/cu.ft.</u>								
S-19.1	1.5	2.30	1.14	0.41	1.3	0.033	0.27	0.27
S-19.3	1.5	1.55	1.14	0.41	1.3	0.033	0.25	0.27
S-19.4	1.5	1.16	1.14	0.41	1.3	0.033	0.46	0.50
<u>Dumped Kimmswick Limestone, Cot $\alpha = 10$, $\gamma = 165$ lbs/cu.ft.</u>								
S-18.2	1.5	2.30	1.14	0.42	1.0	0.033	0.35	0.35
S-18.4	1.5	1.55	1.14	0.42	1.0	0.033	0.50	0.54
<u>Placed Tribars, cot $\alpha = 2$, $\gamma = 143$ lbs/cu.ft. $\gamma = 140$ lbs/cu.ft.*</u>								
L-2.1	15.0	3.67	0.53	1.00	12.3	81.3	5.0	5.4
L-2.2	15.0	3.67	0.48	1.00	11.2	81.3	5.0	5.4
L-2.3	15.0	4.90	0.54	1.00	12.6	81.3	5.4	5.9
L-9A	15.0	3.75	0.45	1.00	10.4	81.3	5.2	5.6
L-9B	15.0	5.60	0.45	1.00	10.4	81.3	5.3	5.6
L-9C	14.5	11.30	0.45	1.00	10.4	81.3	5.8	4.8
M-4.1*	2.0	1.50	0.52	1.00	2.0	0.30	0.58	0.63
M-5.1*	2.0	1.50	0.57	1.00	2.0	0.43	0.60	0.65
S-4.1*	1.5	1.28	0.32	1.00	1.5	0.12	0.33	0.36
S-4.2*	1.5	1.28	0.32	1.00	1.5	0.12	0.36	0.39
S-5.1*	1.5	1.69	0.32	1.00	1.5	0.12	0.35	0.38
S-6.1*	1.5	0.84	0.32	1.00	1.5	0.12	0.65	0.66
S-8.1*	1.5	0.90	0.54	1.00	1.5	0.12	0.56	0.58
S-9.1*	1.5	1.00	0.54	1.00	1.5	0.12	0.41	0.43
S-10.1*	1.5	1.28	0.54	1.00	1.5	0.12	0.39	0.43
S-11.1*	1.5	1.00	0.54	1.00	1.5	0.12	0.40	0.43
S-17.1*	1.5	1.16	--	1.00	1.5	0.12	0.42	0.45
S-17.2*	1.5	1.69	--	1.00	1.5	0.12	0.37	0.40
S-17.3*	1.5	2.30	--	1.00	1.5	0.12	0.55	0.51

TABLE 9 (Continued)

<u>Test Number</u>	<u>d (ft)</u>	<u>T (sec)</u>	<u>Unif</u>	<u>n</u>	<u>Th (in)</u>	<u>W₅₀ (lbs)</u>	<u>h (ft)</u>	<u>H_{ZD} (ft)</u>
<u>Dumped Tribars, Cot $\alpha = 2$, $\gamma = 143$ lbs/cu.ft. $\gamma = 140$ lbs/cu.ft.*</u>								
L-3.1	15.0	3.67	1.00	--	--	81.3	4.8	5.2
L-5.1	15.0	3.67	1.00	0.61	20.4	81.3	4.7	5.1
M-7.1*	2.0	1.50	1.00	0.58	3.5	0.30	0.57	0.62
M-8.1*	2.0	1.50	1.00	0.55	3.6	0.43	0.66	0.71
S-7.1*	1.5	1.28	1.00	0.62	2.5	0.12	0.30	0.33
S-15.1*	1.5	2.30	1.00	--	--	0.12	0.42	0.39
S-16.1*	1.5	1.16	1.00	--	--	0.12	0.41	0.44

APPENDIX E

TABLE OF MODEL TEST CONDITIONS AND
RESULTS IN DIMENSIONLESS FORM

TABLE 10

Model Test Conditions and Results in Dimensionless Form

- W_{50} = Median weight of armor gradation
 $(W_{85}/W_{15})^{1/3}$ = Uniformity of armor gradation
 $c/(W_{50}/\gamma)^{1/3}\gamma$ = Dimensionless armor coverage (c = pounds of armor per square foot of embankment surface area)
 $d/(W_{50}/\gamma)^{1/3}$ = Dimensionless depth
 $gT^2/(W_{50}/\gamma)^{1/3}$ = Dimensionless wave period
 H_{ZD} = Zero-damage deepwater wave height
 $N_{ZD} = \frac{H_{ZD}^{1/3}}{(W_{50})^{1/3}(S-1)}$ = Zero-damage stability number
 $R_N = \frac{\gamma f}{\mu} \left(\frac{W_{50}}{\gamma}\right)^{1/3} \left(\frac{H_{ZD}}{g}\right)^{1/2}$ = Reynolds number

Test Number	W_{50} (lbs)	Uniformity	Coverage	Depth	Period	H_{ZD} (ft)	N_{ZD}	R_N
<u>Dumped Kimmswick Limestone, Cot $\alpha = 2$, $\gamma = 165$ lbs/cu.ft.</u>								
L-1.1	120.0	1.48	1.47	16.7	481	4.6	3.11	624000
L-1.2	120.0	1.48	1.52	16.7	481	4.2	2.84	633000
L-10.1	5.1	1.39	1.43	25.5	640	1.10	2.13	113000
L-10.2	5.1	1.39	1.23	28.7	3690	1.15	2.23	115000
L-10.3	5.1	1.39	1.23	25.5	640	0.97	1.88	100000
M-1.6A	0.49	1.52	--	13.9	503	0.51	2.16	51300
M-1.6B	0.49	1.52	--	13.9	503	0.47	1.99	49200
M-1.6C	0.49	1.52	--	13.9	503	0.54	2.29	52800
M-1.7A	0.49	1.52	--	13.9	503	0.52	2.20	51800
M-1.7B	0.49	1.52	--	13.9	503	0.52	2.20	51800
M-1.7C	0.49	1.52	--	13.9	503	0.56	2.37	53800
M-2.1A	0.49	1.52	--	13.9	895	0.39	1.65	44900
M-2.1B	0.49	1.52	--	13.9	895	0.44	1.86	47700
M-2.1C	0.49	1.52	--	13.9	895	0.44	1.86	47700
S-1.1	0.108	1.27	--	17.3	498	0.26	1.82	22100
S-1.2	0.108	1.27	--	17.3	498	0.26	1.82	22100
S-25.2	0.092	1.14	0.97	18.2	525	0.24	1.77	20200
S-25.3	0.092	1.14	0.97	18.2	2067	0.24	1.77	20200

TABLE 10 (Continued)

Test Number	W_{50} (lbs)	Uniformity	Coverage	Depth	Period	H_{ZD} (ft)	N_{ZD}	R_N
<u>Dumped Sioux Quartzite, Cot $\alpha = 2$, $\gamma = 165$ lbs/cu.ft.</u>								
L-6.1	390.0	1.15	1.10	11.3	325	8.6	3.93	2040000
M-11.1	0.60	1.29	1.14	13.0	470	0.66	2.61	62000
<u>Dumped Boulders, Cot $\alpha = 2$, $\gamma = 165$ lbs/cu. ft.</u>								
L-11.1	37.5	1.95	1.96	19.7	710	2.3	2.29	308000
S-12.1	0.06	1.80	1.53	21.0	738	0.16	1.36	14300
<u>Placed Sioux Quartzite, Cot $\alpha = 2$, $\gamma = 165$ lbs/cu.ft.</u>								
L-7.1	188.0	1.17	0.67	14.4	414	7.0	4.08	1600000
M-6.1	0.39	1.14	--	15.0	543	0.60	2.74	51600
M-9.1	0.54	1.29	--	13.5	487	0.58	2.38	56500
M-10.1	0.60	1.29	0.85	13.0	470	0.76	3.01	67000
S-2.1	0.27	1.26	0.72	12.7	447	0.44	2.27	39100
S-3.1	0.27	1.26	0.72	12.7	447	0.46	2.37	40000
<u>Dumped Occoquan Granite, Cot $\alpha = 2 \frac{1}{2}$, $\gamma = 165$ lbs/cu.ft.</u>								
SPL-1	28	1.70	1.96	27.3	459	3.1	3.30	484000
SPL-2	28	1.70	1.53	27.3	1903	2.3	2.45	417000
SPL-3	28	1.70	1.62	27.3	1033	2.6	2.77	443000
SPL-4	28	1.70	1.62	27.3	4232	2.6	2.77	443000
SPL-5	28	1.70	1.71	27.3	7480	2.5	2.66	434000
SPL-6	28	1.70	0.99	27.3	4232	2.2	2.35	407000
SPL-7	28	1.70	1.26	27.3	1903	2.3	2.45	417000
SPL-8	28	1.70	1.08	27.3	1033	2.1	2.24	398000
SPL-9	28	1.70	1.08	27.3	459	3.1	3.30	484000
SPL-10	28	1.70	1.08	27.3	1033	2.0	2.13	388000
<u>Dumped Kimmswick Limestone, Cot $\alpha = 3$, $\gamma = 165$ lbs/cu.ft.</u>								
L-12.1	10.0	1.93	1.31	30.6	511	2.1	3.25	272000
L-13.1	84.0	1.70	1.20	18.8	542	4.2	3.20	783000
L-14.1	80.0	1.20	--	19.1	551	4.2	3.25	932000
L-15.1	195.0	1.65	1.22	14.2	409	7.3	4.20	1660000
M-14.1	0.27	1.24	0.73	17.0	614	0.44	2.27	39100
M-15.1	0.42	1.97	0.82	14.7	530	0.49	2.18	47800
M-16.1	0.36	8.82	1.04	15.4	558	0.48	2.25	44900
S-13.1	0.097	1.15	1.11	17.9	922	0.26	1.89	21400
S-13.2	0.097	1.15	1.11	17.9	311	0.42	3.05	27100
S-13.3	0.097	1.15	1.11	17.9	516	0.28	2.03	22200
S-13.4	0.097	1.15	1.11	17.9	2031	0.29	2.11	22600
S-22.2	0.092	1.14	--	18.2	525	0.27	2.00	21400
S-22.3	0.092	1.14	--	18.2	939	0.25	1.85	20600
S-22.4	0.092	1.14	--	18.2	2067	0.26	1.92	21000
S-22.5	0.092	1.14	--	18.2	525	0.28	2.07	21800

TABLE 10 (Continued)

Test Number	W_{50} (lbs)	Uniformity	Coverage	Depth	Period	H_{ZD} (ft)	N_{ZD}	R_N
<u>Dumped Kimmswick Limestone, Cot $\alpha = 5$, $\gamma = 165$ lbs/cu.ft.</u>								
L-16.1	105.0	1.55	1.27	17.4	503	6.4	4.53	1260000
L-17.1	27.0	1.28	1.02	27.4	792	3.4	3.78	555000
L-18.1	30.0	5.47	1.72	26.5	764	3.6	3.76	555000
L-19.1	41.0	1.54	1.35	23.9	689	3.8	3.68	465000
M-17.1	0.25	5.28	1.4	17.4	630	0.52	2.75	41400
M-18.1	0.22	1.45	0.93	18.2	657	0.52	2.87	39700
M-19.1	0.27	1.24	0.80	17.0	614	0.58	2.99	44900
M-20.1	0.098	1.18	0.81	23.8	861	0.35	2.53	24900
M-20.2	0.098	1.18	0.81	23.8	861	0.35	2.53	24900
S-26.2	0.092	1.14	1.25	18.2	2067	0.32	2.37	23300
S-26.3	0.092	1.14	1.34	18.2	939	0.40	2.96	26000
<u>Dumped Kimmswick Limestone, Cot $\alpha = 7$, $\gamma = 165$ lbs/cu.ft.</u>								
S-19.1	0.033	1.14	1.14	25.7	2910	0.27	2.81	15200
S-19.3	0.033	1.14	1.14	25.7	1321	0.27	2.81	15200
S-19.4	0.033	1.14	1.14	25.7	740	0.50	5.20	20700
<u>Dumped Kimmswick Limestone, Cot $\alpha = 10$, $\gamma = 165$ lbs/cu.ft.</u>								
S-18.2	0.033	1.14	0.85	25.7	2910	0.35	3.64	17300
S-18.4	0.033	1.14	0.85	25.7	1321	0.54	5.62	21500
<u>Placed Tribars, Cot $\alpha = 2$, $\gamma = 143$ lbs/cu. ft.</u> <u>$\gamma = 140$ lbs/cu. ft.*</u>								
L-2.1	81.3	1.00	0.59	18.1	523	5.4	5.05	756000
L-2.2	81.3	1.00	0.59	18.1	523	5.4	5.05	756000
L-2.3	81.3	1.00	0.58	18.1	932	5.9	5.51	851000
L-9A	81.3	1.00	0.58	18.1	546	5.6	5.23	1200000
L-9B	81.3	1.00	0.58	18.1	1217	5.6	5.23	1030000
L-9C	81.3	1.00	0.58	17.5	4959	4.8	4.49	908000
M-4.1*	0.30	1.00	0.63	15.5	561	0.63	3.93	51400
M-5.1*	0.43	1.00	0.56	13.8	498	0.65	3.60	59000
S-4.1*	0.12	1.00	0.75	15.8	554	0.36	3.22	29300
S-4.2*	0.12	1.00	0.75	15.8	554	0.39	3.30	29700
S-5.1*	0.12	1.00	0.75	15.8	967	0.38	3.22	29300
S-6.1*	0.12	1.00	0.75	15.8	238	0.66	5.59	38600
S-8.1*	0.12	1.00	0.60	15.8	274	0.58	4.91	36200
S-9.1*	0.12	1.00	0.60	15.8	338	0.43	3.64	31100
S-10.1*	0.12	1.00	0.60	15.8	554	0.43	3.64	31100
S-11.1*	0.12	1.00	0.60	15.8	338	0.43	3.64	31100
S-17.1*	0.12	1.00	--	15.8	455	0.45	3.81	31900
S-17.2*	0.12	1.00	--	15.8	967	0.40	3.39	30000
S-17.3*	0.12	1.00	--	15.8	1791	0.51	4.32	33900

TABLE 10 (Continued)

<u>Test Number</u>	<u>W₅₀</u> <u>(lbs)</u>	<u>Uniformity</u>	<u>Coverage</u>	<u>Depth</u>	<u>Period</u>	<u>H_{ZD}</u> <u>(ft)</u>	<u>N_{ZD}</u>	<u>R_N</u>
<u>Dumped Tribars, Cot $\alpha = 2$, $\gamma = 143$ lbs/cu. ft.</u> $\gamma = 140$ lbs/cu. ft.*								
L-3.1	81.3	1.00	0.65	18.1	523	5.2	4.86	866000
L-5.1	81.3	1.00	0.80	18.1	523	5.1	4.77	935000
M-7.1*	0.30	1.00	0.95	15.5	561	0.62	3.87	50800
M-8.1*	0.43	1.00	0.93	13.8	498	0.71	3.93	61200
S-7.1*	0.12	1.00	0.83	15.8	554	0.33	2.79	27300
S-15.1*	0.12	1.00	0.83	15.8	1791	0.39	3.30	29700
S-16.1*	0.12	1.00	0.78	15.8	455	0.44	3.73	31500

DOCUMENT CONTROL DATA - R & D

(Security classification of title, body of abstract and indexing annotation must be entered when the overall report is classified)

1. ORIGINATING ACTIVITY (Corporate author) U. S. Army Coastal Engineering Research Center 5201 Little Falls Road, N.W. Washington, D.C. 20016		2a. REPORT SECURITY CLASSIFICATION UNCLASSIFIED	
		2b. GROUP	
3. REPORT TITLE RIPRAP STABILITY ON EARTH EMBANKMENTS TESTED IN LARGE- AND SMALL-SCALE WAVE TANKS			
4. DESCRIPTIVE NOTES (Type of report and inclusive dates)			
5. AUTHOR(S) (First name, middle initial, last name) Arvid L. Thomsen Paul E. Wohlt Alfred S. Harrison			
6. REPORT DATE June 1972		7a. TOTAL NO. OF PAGES 127	7b. NO. OF REFS 22
8a. CONTRACT OR GRANT NO.		9a. ORIGINATOR'S REPORT NUMBER(S) Technical Memorandum No. 37	
b. PROJECT NO.			
c.		9b. OTHER REPORT NO(S) (Any other numbers that may be assigned this report)	
d.			
10. DISTRIBUTION STATEMENT Approved for public release; distribution unlimited.			
11. SUPPLEMENTARY NOTES		12. SPONSORING MILITARY ACTIVITY	
13. ABSTRACT Tests of models in wave tanks were made to determine the effectiveness of several riprap designs in protecting embankment slopes from wave action. Models ranging from about 1:20 scale to almost full scale were tested with waves up to about 6 feet high. A range of wave periods were tested, embankment slopes varied from 1 on 2 to 1 on 5, and armor layers were composed of quarried stone, glacial boulders and tribars. Relationships that define the effect of wave height, wave period, embankment slopes and Reynolds number on size of stable armor units were experimentally determined and are given in graphs and tables. Significant conclusions are: 1. The median weight of graded armor material is a satisfactory "effective size" with respect to stability. 2. Small-scale models are less stable than larger scale models. The difference in stability is a function of Reynolds number apparently caused by viscous effects. Consequently, there is a "scale effect" that produces conservative results when the stability determined in a small model is scaled up to prototype size on the basis of Froude number alone when equivalent viscous fluids exist in both prototype and model. 3. Stability is a function of wave period. For longer periods that produced wave steepness less than 0.03, stability is little affected by period. For wave steepness greater than 0.03, stability increases with shorter period. Section VI of this report presents a detailed summary and conclusions.			

14. KEY WORDS	LINK A		LINK B		LINK C	
	ROLE	WT	ROLE	WT	ROLE	WT
Shore Protection						
Riprap						
Hydraulic Models						
Wave Tanks						
Stone Levees						

U. S. Army Coastal Engrg Research Center, CE
WASHINGTON, D. C. 20016

RIPRAP STABILITY ON EARTH EMBANKMENTS
TESTED IN LARGE- AND SMALL-SCALE WAVE
TANKS by Arvid L. Thomsen, Paul E. Wohlt
and Alfred S. Harrison 127 pp. including
68 Illus. and 5 App. June 1972

TECHNICAL MEMORANDUM NO. 37 UNCLASSIFIED

1. Shore Protection
2. Riprap
3. Hydraulic Models
4. Wave Tanks
5. Stone Levees

- I. Title
- II. Thomsen, A. L.
Wohlt, P. E.
Harrison, A. S.

Tests of models in wave tanks were made to determine the effectiveness of several riprap designs in protecting embankment slopes from wave action. Models ranging from about 1:20 scale to almost full scale were tested with waves up to about 6 feet high. A range of wave periods were tested; embankment slopes varied from 1 on 2 to 1 on 5; armor layers were composed of quarried stone, glacial boulders and tribars. Relationships that define the effect of wave height, wave period, embankment slopes and Reynolds number on size of stable armor units were experimentally determined, and are given in graphs and tables.

U. S. Army Coastal Engrg Research Center, CE
WASHINGTON, D. C. 20016

RIPRAP STABILITY ON EARTH EMBANKMENTS
TESTED IN LARGE- AND SMALL-SCALE WAVE
TANKS by Arvid L. Thomsen, Paul E. Wohlt
and Alfred S. Harrison 127 pp. including
68 Illus. and 5 App. June 1972

TECHNICAL MEMORANDUM NO. 37 UNCLASSIFIED

1. Shore Protection
2. Riprap
3. Hydraulic Models
4. Wave Tanks
5. Stone Levees

- I. Title
- II. Thomsen, A. L.
Wohlt, P. E.
Harrison, A. S.

Tests of models in wave tanks were made to determine the effectiveness of several riprap designs in protecting embankment slopes from wave action. Models ranging from about 1:20 scale to almost full scale were tested with waves up to about 6 feet high. A range of wave periods were tested; embankment slopes varied from 1 on 2 to 1 on 5; armor layers were composed of quarried stone, glacial boulders and tribars. Relationships that define the effect of wave height, wave period, embankment slopes and Reynolds number on size of stable armor units were experimentally determined, and are given in graphs and tables.

U. S. Army Coastal Engrg Research Center, CE
WASHINGTON, D. C. 20016

RIPRAP STABILITY ON EARTH EMBANKMENTS
TESTED IN LARGE- AND SMALL-SCALE WAVE
TANKS by Arvid L. Thomsen, Paul E. Wohlt
and Alfred S. Harrison 127 pp. including
68 Illus. and 5 App. June 1972

TECHNICAL MEMORANDUM NO. 37 UNCLASSIFIED

1. Shore Protection
2. Riprap
3. Hydraulic Models
4. Wave Tanks
5. Stone Levees

- I. Title
- II. Thomsen, A. L.
Wohlt, P. E.
Harrison, A. S.

Tests of models in wave tanks were made to determine the effectiveness of several riprap designs in protecting embankment slopes from wave action. Models ranging from about 1:20 scale to almost full scale were tested with waves up to about 6 feet high. A range of wave periods were tested; embankment slopes varied from 1 on 2 to 1 on 5; armor layers were composed of quarried stone, glacial boulders and tribars. Relationships that define the effect of wave height, wave period, embankment slopes and Reynolds number on size of stable armor units were experimentally determined, and are given in graphs and tables.

U. S. Army Coastal Engrg Research Center, CE
WASHINGTON, D. C. 20016

RIPRAP STABILITY ON EARTH EMBANKMENTS
TESTED IN LARGE- AND SMALL-SCALE WAVE
TANKS by Arvid L. Thomsen, Paul E. Wohlt
and Alfred S. Harrison 127 pp. including
68 Illus. and 5 App. June 1972

TECHNICAL MEMORANDUM NO. 37 UNCLASSIFIED

1. Shore Protection
2. Riprap
3. Hydraulic Models
4. Wave Tanks
5. Stone Levees

- I. Title
- II. Thomsen, A. L.
Wohlt, P. E.
Harrison, A. S.

Tests of models in wave tanks were made to determine the effectiveness of several riprap designs in protecting embankment slopes from wave action. Models ranging from about 1:20 scale to almost full scale were tested with waves up to about 6 feet high. A range of wave periods were tested; embankment slopes varied from 1 on 2 to 1 on 5; armor layers were composed of quarried stone, glacial boulders and tribars. Relationships that define the effect of wave height, wave period, embankment slopes and Reynolds number on size of stable armor units were experimentally determined, and are given in graphs and tables.

U. S. Army Coastal Engrg Research Center, CE 1. Shore Protection
WASHINGTON, D. C. 20016 2. Riprap

RIPRAP STABILITY ON EARTH EMBANKMENTS
TESTED IN LARGE- AND SMALL-SCALE WAVE

TANKS by Arvid L. Thomsen, Paul E. Wohlt
and Alfred S. Harrison 127 pp. including
68 Illus. and 5 App. June 1972

TECHNICAL MEMORANDUM NO. 37 UNCLASSIFIED

3. Hydraulic Models
4. Wave Tanks
5. Stone Levees

- I. Title
- II. Thomsen, A. L.
Wohlt, P. E.
Harrison, A. S.

Tests of models in wave tanks were made to determine the effectiveness of several riprap designs in protecting embankment slopes from wave action. Models ranging from about 1:20 scale to almost full scale were tested with waves up to about 6 feet high. A range of wave periods were tested; embankment slopes varied from 1 on 2 to 1 on 5; armor layers were composed of quarried stone, glacial boulders and tribars. Relationships that define the effect of wave height, wave period, embankment slopes and Reynolds number on size of stable armor units were experimentally determined, and are given in graphs and tables.

U. S. Army Coastal Engrg Research Center, CE 1. Shore Protection
WASHINGTON, D. C. 20016 2. Riprap

RIPRAP STABILITY ON EARTH EMBANKMENTS
TESTED IN LARGE- AND SMALL-SCALE WAVE

TANKS by Arvid L. Thomsen, Paul E. Wohlt
and Alfred S. Harrison 127 pp. including
68 Illus. and 5 App. June 1972

TECHNICAL MEMORANDUM NO. 37 UNCLASSIFIED

3. Hydraulic Models
4. Wave Tanks
5. Stone Levees

- I. Title
- II. Thomsen, A. L.
Wohlt, P. E.
Harrison, A. S.

Tests of models in wave tanks were made to determine the effectiveness of several riprap designs in protecting embankment slopes from wave action. Models ranging from about 1:20 scale to almost full scale were tested with waves up to about 6 feet high. A range of wave periods were tested; embankment slopes varied from 1 on 2 to 1 on 5; armor layers were composed of quarried stone, glacial boulders and tribars. Relationships that define the effect of wave height, wave period, embankment slopes and Reynolds number on size of stable armor units were experimentally determined, and are given in graphs and tables.

U. S. Army Coastal Engrg Research Center, CE 1. Shore Protection
WASHINGTON, D. C. 20016 2. Riprap

RIPRAP STABILITY ON EARTH EMBANKMENTS
TESTED IN LARGE- AND SMALL-SCALE WAVE

TANKS by Arvid L. Thomsen, Paul E. Wohlt
and Alfred S. Harrison 127 pp. including
68 Illus. and 5 App. June 1972

TECHNICAL MEMORANDUM NO. 37 UNCLASSIFIED

3. Hydraulic Models
4. Wave Tanks
5. Stone Levees

- I. Title
- II. Thomsen, A. L.
Wohlt, P. E.
Harrison, A. S.

Tests of models in wave tanks were made to determine the effectiveness of several riprap designs in protecting embankment slopes from wave action. Models ranging from about 1:20 scale to almost full scale were tested with waves up to about 6 feet high. A range of wave periods were tested; embankment slopes varied from 1 on 2 to 1 on 5; armor layers were composed of quarried stone, glacial boulders and tribars. Relationships that define the effect of wave height, wave period, embankment slopes and Reynolds number on size of stable armor units were experimentally determined, and are given in graphs and tables.

U. S. Army Coastal Engrg Research Center, CE 1. Shore Protection
WASHINGTON, D. C. 20016 2. Riprap

RIPRAP STABILITY ON EARTH EMBANKMENTS
TESTED IN LARGE- AND SMALL-SCALE WAVE

TANKS by Arvid L. Thomsen, Paul E. Wohlt
and Alfred S. Harrison 127 pp. including
68 Illus. and 5 App. June 1972

TECHNICAL MEMORANDUM NO. 37 UNCLASSIFIED

3. Hydraulic Models
4. Wave Tanks
5. Stone Levees

- I. Title
- II. Thomsen, A. L.
Wohlt, P. E.
Harrison, A. S.

Tests of models in wave tanks were made to determine the effectiveness of several riprap designs in protecting embankment slopes from wave action. Models ranging from about 1:20 scale to almost full scale were tested with waves up to about 6 feet high. A range of wave periods were tested; embankment slopes varied from 1 on 2 to 1 on 5; armor layers were composed of quarried stone, glacial boulders and tribars. Relationships that define the effect of wave height, wave period, embankment slopes and Reynolds number on size of stable armor units were experimentally determined, and are given in graphs and tables.